INFLUENCE OF FLAME RETARDANT STRUCTURES AND COMBINATIONS ON THE FIRE PROPERTIES OF BISPHENOL A POLYCARBONATE /ACRYLONITRILE-BUTADIENE-STYRENE

Inaugural-Dissertation
to obtain the academic degree
Doctor rerum naturalium (Dr. rer. nat.)

submitted to the Department of Biology, Chemistry and Pharmacy
of Freie Universität Berlin

by

MARIE-CLAIRE DESPINASSE

from Saint Chamond

Berlin, 2016

This doctorate studies have been carried out from January 2010 to March 2013 at the BAM Federal Institute for Materials Research and Testing in Berlin, Germany, under the supervision of Priv.-Doz. Dr. habil. Bernhard Schartel.

1st Reviewer: Priv.-Doz. Dr. habil. Bernhard Schartel

2nd Reviewer: Prof. Dr. Rainer Haag

Date of defence: 14.07.2016

ACKNOWLEDGMENTS

First I thank P.D. Dr. habil. Bernhard Schartel and Prof. Dr. Rainer Haag for the supervision and the evaluation of this work. Thanks for the academic support given during these years. I would like to especially thank Dr. Bernhard Schartel for the endorsement during my PhD in his group. Thanks for the support, the enthusiasm, the availability for fruitful discussions, the constructive criticisms and the confidence he gave me till the end.

I wish here to thank my colleagues and friends for the wonderful atmosphere, and for the scientific as non- scientific discussions. Dr. Henrik Seefeldt and Karoline Taüber are specially thanked for the endless support and friendship they gave me. Aleksandra Sut, Dr. Bettina Dittrich, Andreas Hörold, Michael Morys, Dr. Emanuela Gallo, Daniele Frasca, Dr. Eliza Wawrzyn, Dr. Sven Brehme, Sebastian Rabe, Dr. Guang Mei Wu, Melissa Matzen, Dr. Birgit Perret, Dr. Florian Kempel, Dr. Kirsten Langfeld, Dr. Antje Wilke, Sebastian Timme, Nora Konnertz, Dr. Huajie Yin, Marie-Bernadette Watolla, Analice Turski Silva, Julie Ledru and Serhat Ciftci, thank you all for the excellent team working and international ambiance.

Patrick Klack, Horst Bahr, Michael Schneider, Carsten Vogt and Tobias Kukofka are thanked for the helpfulness and the technical and practical support. Thank you to Dr. Simone Krüger, Tina Raspe and Benjamin Klaffke for the great cooperation. My thanks go to further colleagues from the BAM that I met during my PhD time, especially Christian Huth for the rheology measurements, Dietmar Neubert and Tina Garchow for the DSC measurements.

I gratefully thank Dr. Mathieu Jung, Dr. Thomas Eckel, Dr. Uwe Peuckert, Dr. Dieter Wittmann and Dr. Vera Taschner from Bayer MaterialScience AG, for the financial support, the fruitful discussions and the preparation of the different materials.

Of course I want to thank my lovely family and friends, who helped me, by their support, their comprehension or just their love, during all my PhD time. Spécialement pour toi ma Choupinette et ton Juju, merci pour tout!! Vous m'avez vraiment aidé, et je vous en suis reconnaissante. Pour toi ma Naty, pour vous Papa et Maman, pour toi Nico, merci pour votre aide et votre support. Pour toi aussi mémé. Merci aussi à vous mes ami(e)s: Delphine Eyraud, Mickael Agach, Violaine Martin-Tournillon, Claire Chalencon-Chirat, Gaelle Guichard-Fayard, Aurélie Balley, Lorène Richer… Danke an dir auch meine liebe Ellis Brenner und meine liebe Anke Todtermuschke. And most of all I wish to thank my love for his patience, his trust and his confident support.

In the memory of M. J. D.

"Et hop, raclette!!"

KURZFASSUNG

Die Verwendung der Kunststoffmischung PC/ABS für Anwendungen in der Elektro- und Elektronikindustrie, wie z.B für dünnwandige Gehäuse (Laptops, Fernsehgeräte…), erforderte den Zusatz von halogenfreien Flammschutzmittelsystemen zu PC/ABS. Phosphorhaltige Flammschutzmittel stellen eine adäquate Alternative dar. In Wissenschaft und Entwicklung wird weiterhin an diesen Flammschutzmitteln gearbeitet. Ziel dabei ist ein besseres Verständnis der Wirkungsmechanismen und eine weitere Verbesserung des Flammschutzkonzeptes für PC/ABS.

In der vorliegenden Arbeit wurden die Flammschutzmechanismen von verschiedenen neuen, kommerziellen, phosphorbasierten Oligomer-Flammschutzmitteln aufgeklärt. Zur Charakterisierung des Flammschutzeffekts wurden die chemischen Strukturen der Flammschutzmittel variiert, vor allem mit verbrückten Aryldisphosphaten. Dabei wurde die Struktur-Eigenschafts-Beziehung zwischen chemischer Struktur und die Effizienz der Flammschutzmittel aufgedeckt. Ein Flammschutzmittel, das Phosphor sowie Stickstoff enthält, wurde hinsichtlich seines Wirkungsmechanismus in der Polymermatrix untersucht und mit den Organophosphaten verglichen. Des Weiteren wurden Einfluss und Interaktion zweier phosphorhaltiger Flammschutzmittel in Kombination und mit verschiedenen Verhältnissen untersucht und ein möglicher synergistischer Effekt wurde quantifiziert.

Das thermische Abbauverhalten der Materialien wurde mittels Thermogravimetrie (TG) analysiert. Um die flüchtigen, gasförmigen Produkte des thermischen Abbaus zu bestimmen, wurde die TG mit Fourier-transformierter Infrarotspektroskopie (IR) und Massenspektrometrie gekoppelt. Abbaureaktionen, die in der kondensierten Phase des Materials stattfanden, wurden mittels Transmissions-IR durch eine beheizbare Probenzelle online verfolgt. Für die Reaktion der Materialien auf eine kleine Flamme wurden der Sauerstoffindex (OI) und der UL94 Test herangezogen. Das Brandverhalten der Materialien wurde im Cone Kalorimeter untersucht die daraus resultierenden Brandrückstände mit Hilfe von abgeschwächter Totalreflexion (ATR)-FTIR und Elementaranalyse bestimmt.

Eingesetzt in PC/ABS, wirken die einzelnen Flammschutzmittel sowie die untersuchten Kombinationen hauptsächlich in der Gasphase; einige von ihnen zeigen auch Aktivität in der kondensierten Phase. Der Flammschutzmechanismus beruht hier auf der Freisetzung von phosphorhaltigen Verbindungen, die durch Flammenvergiftung wirken. Die

Flammschutzmittel unterscheiden sich vor allem in ihrer Effektivität Brandrisiken zu reduzieren Die dafür verantwortlichen Faktoren sind: die Abbautemperatur der Kunststoffmatrix – besonders von PC -, die hydrolytische Stabilität und die chemische Umgebung der Phosphorgruppen. Diese Parameter kontrollieren die Bildung reaktiver Gruppen während des Abbauprozesses von PC und Flammschutzmitteln und sind verantwortlich für Verkohlung und Vernetzung in der kondensierten Phase. Den effektivsten einzelnen Aryl phosphaten in PC/ABS zeigen Mechanismen in der Gasphase wie auch in der kondensierten Phase. Diese Flammschutzmittel sind in der Lage mit den Abbauprodukten von PC - das für sich selbst schon Verkohlung zeigt - zu reagieren.

Die Kombination von zwei phosphorbasierten Flammschutzmitteln in verschiedenen Verhältnissen zeigte eine Überlagerung der Effekte im Fall eines Arylphosphates mit dem phosphor- und stickstoffhaltigen Flammschutzmittel. Ein synergistischer Effekt des Flammschutzmechanismus in der kondensierten Phase konnte für eine Mischung von zwei Arylphosphaten beobachtet werden. Die Flammschutzwirkung war hier höher als bei den einzelnen Arylphosphaten. Die Abbautemperatur der neugebildeten Verbindung aus der Reaktion zwischen zwei Flammschutzmitteln spielt dabei eine bedeutende Rolle in der Effizienz der Flammschutzmittelkombination.

Im Zuge der vorliegenden Arbeit wurden neue Erkenntnisse über die Flammschutzkonzepte für PC/ABS gewonnen. Das Verständnis der Struktur-Eigenschafts-Beziehungen der einzelnen Flammschutzmittel ist ein Schlüsselfaktor für die weitere Optimierung flammgeschützter PC/ABS Systeme. Der Einsatz von Flammschutzmittelkombinationen ist ein weitere Ansatz, die Brandeigenschaften von PC/ABS zu verbessern.

ABSTRACT

The use of PC/ABS polymer for electrics and electronics applications such as thin wall housings requires the addition of bromine- and chlorine- free flame retardant additives. Phosphorus-containing systems are an adequate alternative. Understand their mode of action in the polymer matrix is a key to improve the flame retardancy concepts of PC/ABS.

In this study the flame retarding mechanisms of different newly commercialized oligomeric flame retardants based on phosphorus were elucidated. The flame retardancy effect was characterized by varying the flame retardant structures of bridged aryl bisphosphates. The structure-property relationship between the chemical structure and the efficiency of the flame retardant was revealed. A phosphorus-nitrogen containing flame retardant was investigated in terms of its mode of action in the polymer matrix, and compared with organophosphates. Furthermore the influence of combinations of two phosphorus-containing flame retardants were investigated at different ratios in the PC/ABS matrix and a possible synergy quantified.

The thermal decomposition behaviour of the materials was analysed by thermogravimetry (TG). Volatile decomposition products were identified by coupling the TG with Fourier transformed infrared spectroscopy (IR) and-Mass Spectrometry. Interactions in the condensed phase were monitored online by transmission-IR coupled with a hot-stage cell. The flammability was characterized by limiting oxygen index (OI) and UL94 tests. The burning behaviour was evaluated in the cone calorimeter under different fire scenarios, and the resulting fire residues were analysed by Attenuated Total Reflectance (ATR)- FTIR and by elemental analysis.

In PC/ABS all of the single flame retardants or combinations of two of them work mainly in the gas phase and for some of them in the condensed phase. They release phosphorus species in the gas phase and act by flame inhibition. The single flame retardants mainly differ in their efficiency in reducing the fire risks due to different factors: the decomposition temperature of the polymer matrix, and especially the one of PC, the hydrolytic stability of the phosphorous groups and the chemical environment of the phosphorous groups. These parameters control the formation of reactive groups from the decomposing PC and the flame retardant that induce cross-links in the condensed phase.

The combination of two phosphorus-based flame retardants at different ratios indicated a superposition of the effect in the case of an aryl phosphate with a phosphorus-nitrogen

containing flame retardant. A synergistic effect on the condensed phase mechanisms was achieved in the case of two aryl phosphates. The efficiency was then higher than with the single aryl phosphates. The temperature of decomposition of the formed species by the reaction of the two flame retardants is a criterion controlling the efficiency of the flame retardant combination.

New insights into the flame retardancy concepts of PC/ABS were gained in this work. Understanding the structure-property relationship of single flame retardant is a key parameter for further optimization of the flame retardant materials. Moreover the use of combinations of flame retardants in PC/ABS is an additional approach to improve the fire properties.

ABBREVIATIONS

List of abbreviations used in this work

Abbreviation	Signification
ATR	attenuated total reflection
DSC	dynamic scanning calorimetry
DTG	differential thermogravimetry
E&E	electrics and electronics
FR	flame retardancy
FTIR	Fourier-transformed infrared spectroscopy
HB	horizontal burning
HRR	heat release rate
LN-MCT	liquid nitrogen cooled mercury-cadmium tellurium
LOI	limiting oxygen index
MS	mass spectrometry
PHRR	peak heat release rate
$SE_{(A)}$	(absolute) synergistic effect
$T_{2\%}$	temperature of 2% of mass loss
TCOP/ML	effective CO release
TG	thermogravimetry
THE	total heat evolved
THE/ML	effective heat of combustion (THE divided by mass loss)
THR	total heat release
t_{ig}	time to ignition
T_{Max}	temperature of maximum mass loss rate
TSR/ML	effective smoke release
UL	Underwriter Laboratory
wt%	Weight percent

List of the material names abbreviated in this work

Abbreviation	**Full denomination**
ABS	Acrylonitrile-butadiene-styrene
BBDP	Biphenyl bis (diphenyl phosphate)
BBXP	Biphenyl bis(2,6-xylyl) phosphate
BDP	Bisphenol A bis(diphenyl phosphate)
CO	Carbon monoxide
CO_2	Carbon dioxide
DPZ	Diphenyl phenoxyphosphazene
DPZ-m	Diphenyl phenoxyphosphazene mixture
HDP	Hydroquinone bis(diphenyl phosphate)
KBr	Kalium bromide
PC	Bisphenol A polycarbonate
PE	Polyethylene
PP	Polypropylene
PTFE	Poly(tetrafluoroethylene)
RDP	Resorcinol bis (diphenyl phosphate)
TCP	Tricresyl phosphate
TPP	Triphenyl phosphate
TXP	Trixylyl phosphate

CONTENT

Chapter 1 INTRODUCTION AND PURPOSE OF THE STUDY

Bisphenol A polycarbonate/acrylonitrile-butadiene-styrene (PC/ABS) blends are engineering thermoplastic alloys that proved well-balanced material and processing properties for a wide range of applications. The mechanical, electrical, and thermal properties of polycarbonate and ABS are advantageously combined in PC/ABS [1, 2]. Especially its high impact toughness (even by low temperatures thanks to the addition of ABS [3]), its stiffness, its dimension stability, its high heat deflection temperature, its low moisture uptake and a good aspect such as gloss and reduced price compared to PC are the right combination for engineering applications such as medical hardware, automotive components (consoles, door handles, wheel covers) and portable electronic devices (notebooks, cell phones, TV) [2, 4, 5]. Moreover the addition of ABS increases the flowability and thus enhances the processability of PC/ABS, which is a key property for the moulding of thin walls for housing applications. Housing applications require high mechanical properties such as high stiffness and high impact resistance to compensate a lower thickness [6].

High flame retardancy properties are additionally needed for housing of electrical and electronical devices, as strong legislations control the market [6]. The electronic device should not start a fire. PC itself is not easily flammable due to its high heat resistance [7]. However adding the high flammable ABS into PC increases the flammability of the PC/ABS blends [1]. Typically PC/ABS blends containing 10 to 20 weight percent (wt.%) of ABS are too flammable to meet the requirements for most of the applications in the electronics sector [5]. That is the reason why flame retardancy is needed to reduce the fire risk.

One of the best approaches in terms of cost and ease of handling for flame retardancy of PC/ABS is to mix flame retardant additives into the polymer matrix [5, 8]. In the past, halogen-containing flame retardants were the most common strategy to protect PC/ABS products [9, 10]. However new regulations in Europe for environmental and ecological issues have increased the demand towards bromine and chlorine-free alternatives. [6] Organic or inorganic phosphorus-containing flame retardants are a promising alternative to replace the effective halogen-containing flame retardants in different plastics [11-14].

Organophosphate esters play among them a major role for the protection of PC/ABS especially aryl phosphates [3, 15, 16]. Understanding the mode of action of the flame retardant in the polymer is the main key for possible improvement in the flame retardancy

concept. The mode of action of the flame retardant is not only depending on its chemical structure but also on the surrounding polymer matrix and other additives. Other additives could be inorganic filler, stabilizers or inorganic and organic flame retardant species. Studies with systematic investigations of structure-properties relationships on newly commercialised bridged aryl phosphates in PC/ABS are missing until now, especially on the deeper understanding of the flame retardancy mechanisms. The influence of phosphorus-nitrogen-containing flame retardants in PC/ABS has been likewise little understood. Moreover combinations of two organic flame retardants based on phosphorus have been only sporadically investigated for this polymer and not fully characterized. Even if phosphorus-phosphorus synergy or phosphorus-nitrogen synergy have been sometimes claimed, no detailed investigation on the reason for the synergy was given.

In this work, oligomeric organic phosphorus-containing flame retardants were evaluated in PC/ABS as single component in term of their chemical structure, or by combination of two of them in term of their synergistic effect. The flame retardancy mechanisms and modes of action in PC/ABS were investigated and the fire behaviour was characterized.

First the influence of the chemical structure of newly commercialized bridged aryl phosphates on the properties of the flame retardant was investigated. Through selective variation of bridging and side unit groups of the bridged aryl phosphates, a deeper understanding in the structure-property relationship on the mechanisms of action of the flame retardants was gained.

Secondly a phosphorus-nitrogen containing flame retardant was added in PC/ABS and the fire properties explained thanks to the stepwise addition of the phosphazene in PC or in ABS to clarify the mechanisms in PC/ABS.

Combinations of two organic phosphorus-containing flame retardants were tested in PC/ABS, to evaluate any synergy resulting from the presence of both additives on the fire properties. In this regard, different ratios of the flame retardant combinations were investigated. First a phosphorus-phosphorus synergy was attempted between two bridged aryl phosphates: bisphenol A bis (diphenyl phosphate) (BDP) and hydroquinone bis(diphenyl phosphate) (HDP). Finally a possible phosphorus-nitrogen synergy was evaluated between an aryl phosphate: BDP and a phenoxy phosphazene.

The elucidation of the fire retardancy mechanisms is a major key for the further design of the flame retardant concepts for specific applications.

Chapter 2 NOVEL PHOSPHOROUS-CONTAINING FLAME RETARDANTS IN PC/ABS

When a plastic like PC/ABS is subjected to an external heat source (candle, electrical shortcut...), it starts first to undergo different physical changes, (softening…) or chemical changes (dehydration). Then if the temperature is high enough, the polymer chains start to decompose into small fragments: the pyrolysis. Various pathways of decomposition occur depending on the polymer, such as depolymerisation, chain-stripping, unzipping or rearrangements [17, 18]. The thermal decomposition is mostly an endothermic process [19]. The schematic representation of the products and the processes evolved during combustion is given in *Figure 2.1*.

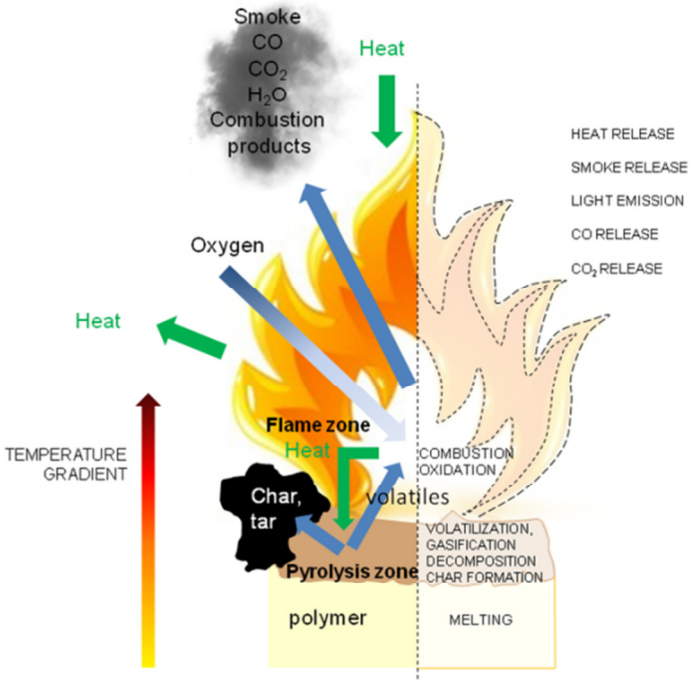

Figure. 2.1 Scheme of the main processes (left) and chemical and physical phenomena (right) during the burning of a polymer

The small fragments that are produced gather thanks to their volatility above the pyrolysis zone. They are oxidized by the oxygen of the air, and ignite if the right proportion between oxygen and combustible is reached [10, 19, 20]. After the ignition, a flame covers the burning material. The concentration in oxygen shows a gradient from the outside of the flame (more concentrated) to the inside of the flame (poorer in oxygen), as oxygen is

consumed in radical reactions in the gas phase. Only little oxygen amount penetrates the flame to reach the decomposing material [21, 22] It was proven by Van Krevelen [7] that the amount of residue in the case of a developing fire is similar to the amount of residue obtained by thermal decomposition under inert atmosphere .The pyrolysis of the polymer is principally an anaerobic process.

The oxidation reactions (combustion) occurring in the flame are numerous and complex, and are dependent on various criteria such as composition of the polymer, concentration in oxygen, ventilation, pressure, temperature, carbon monoxide CO and carbon dioxide CO_2 ratios [21]. The reactions are energetic radical chain reactions, principally propagated by the high reactive H and OH radicals [20, 21, 23, 24]. Some of the main radical reactions are given in *Figure 2.2*.

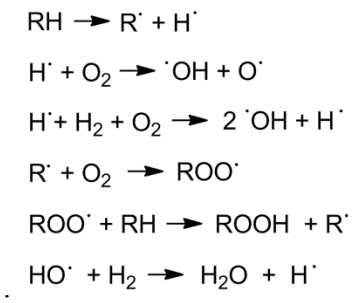

Figure 2.2 Some main exothermic radical reactions in the gas phase during the combustion of a polymer, R = organic rest

Besides the production of fire gases like CO, CO_2, water and smoke, the exothermic combustion processes release energy in the form of heat, responsible for the high temperatures during a fire, and light emissions [25]. Moreover, residues can be formed in the condensed phase, which is the liquid/solid phase. Polymers like ABS decompose completely and burn without residue formation [26-29]. Other polymers like PC carbonize partly to a polyaromatic carbonaceous structure, which stay in the condensed phase of the sample and constitutes the char [30]. The char, during a fire, will acts as a protective layer above the sample [31-34]. This layer protects the underlying polymer against the heat coming from the flame. Moreover the carbonized residue layer diminishes the release of gaseous pyrolysis products, the fuel, from the polymer into the flame zone, which in turns reduces the heat emitted. Non-volatile decomposition products, liquid or solid, collect also in the condensed phase and form the tar.

The heat generated by the oxidation of the volatiles gases (exothermic process) in the flame is transmitted back to the polymer. If the heat received by the polymer from the flame and the external source is high enough, the pyrolysis of the polymer will be a self-sustained process. The combustion will cease only if one of the three components for a fire is depleted: fuel, oxygen or heat.

2.1 Single flame retardant containing phosphorus for PC/ABS: state of the art

Different strategies can be applied to flame retard Bisphenol A polycarbonate/ acrylonitrile-butadiene-styrene (PC/ABS) polymer blend presented in *Figure 2.3*.

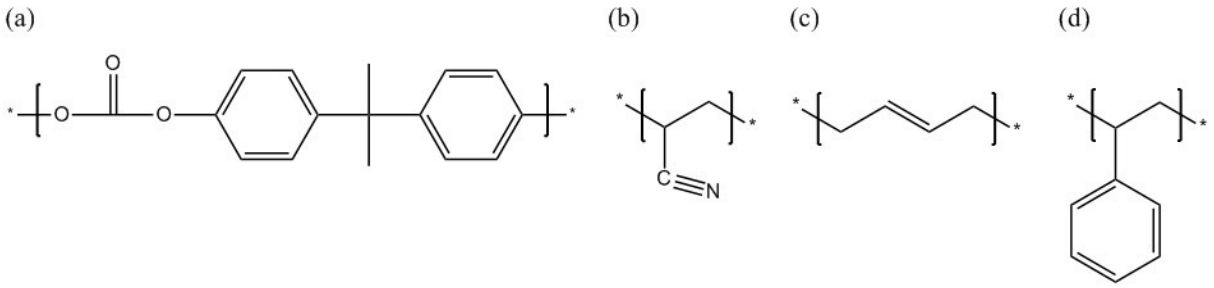

Figure 2.3 Chemical structure of the investigated polymer matrix (a) polycarbonate of Bisphenol A (PC), and the (b) acrylonitrile (c) butadiene and (d) styrene terpolymer (ABS)

Since PC/ABS is not inherently flame retarded, flame retarding species are added in the polymer matrix. Using polymeric flame retardant moiety inside the polycarbonate chains have been tested in the 80's with halogen, mainly brominated units [4, 8, 35]. However the synthesis process is complicated, expensive and compatibility problems with ABS occurred. The easiest, flexible in design, application oriented and cost effective solution are flame retardant additives that will be mix into the PC/ABS blend.

PC/ABS possesses a high processing temperature (between 250 and 280°C [2]), for this reason only flame retardant with a higher decomposition temperature can be used. Moreover PC is sensible to hydrolysis [1], which induces lower molecular mass fragments and in turn could drastically impart the mechanical properties. Flame retardants inducing hydrolysis at room temperature such as acids or bases, should be avoided [36]. For this reason only a few flame retardants are adequate to protect PC/ABS.

Organic phosphate esters, and especially aromatic phosphate esters plays a major role as alternative to halogen-containing additives in PC/ABS [3, 12, 37- 40]. Monophosphate esters such as triphenyl phosphate (TPP), tricresyl phosphate (TCP) and trixylyl phosphate (TXP), are commercial flame retardants for thermoplastics [3, 16, 41, 42]. They are effective flame retardants for PC/ABS. However the low molecular mass of the additives induced high volatilization of the flame retardant and the migration to the surface of the polymer during the injection moulding process that changed the appearance of the finished part, as long as some environmental concern were drawbacks [43].

They were lately replaced by new aryl phosphates with higher molecular mass, mostly oligomers. For example oligomeric bridged aryl phosphates, like resorcinol bis (diphenyl phosphate) (RDP) and bisphenol A bis(diphenyl phosphate) (BDP) are effective in PC/ABS [44-46] (*Figure 2.4*). RDP is less volatile than TPP, but more expensive. RDP suffers from hydrolytic instability, which leads to deterioration of the aging performances of PC/ABS, because of the sensitivity of PC to acids [5, 6, 47]. BDP is thermally and hydrolytically more stable than RDP and shows better performances in PC/ABS [48].

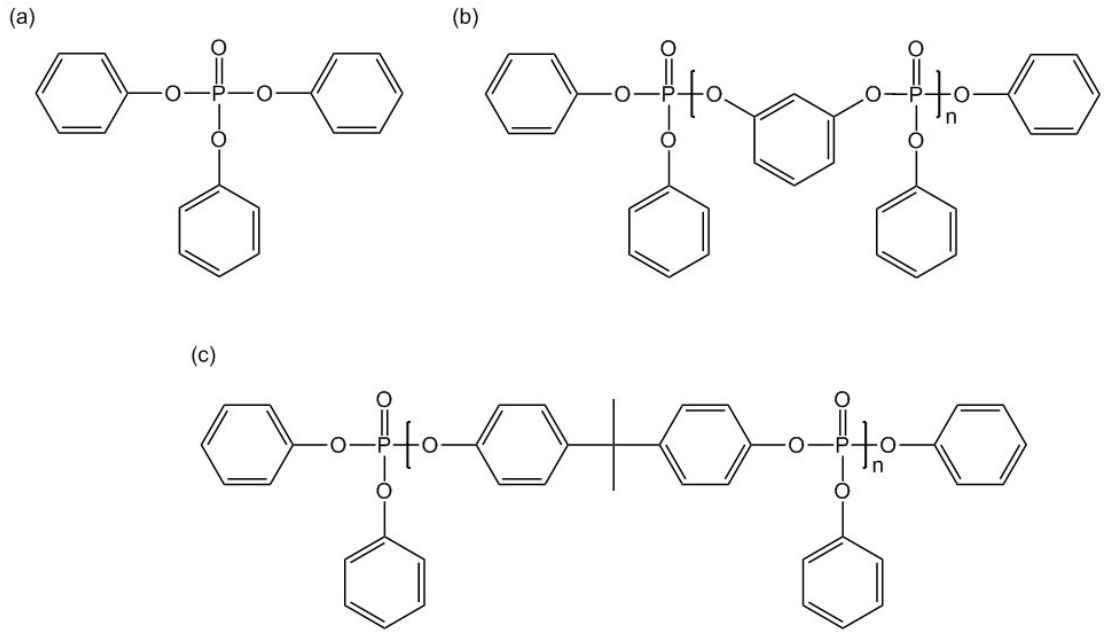

Figure 2.4 Aryl phosphate flame retardant (a) triphenyl phosphate (TPP), (b) Resorcinol bis (diphenyl phosphate) (RDP) and (c) bisphenol A bis(diphenyl phosphate) (BDP)

Aryl phosphate flame retardants have different fire retardancy modes of action. Condensed phase as well as gas phase modes of action are proposed for aryl phosphates [20, 49, 50]. In the gas phase they act in a similar way as for the halogen containing flame retardants but in this case the reactive species are believed to be mostly the PO radicals [50]. These radicals react by radical recombinations with the high reactive H and OH radicals coming from the decomposition of the polymer [20, 23, 24, 51]. Less reactive species or inert species are formed in the flame. The radical reactions of oxidation are slowed down, and the production of heat by the flame decreases. It is called flame inhibition. In *Figure 2.5* some possible reaction between PO and H or OH radicals are represented.

$$PO^{\bullet} + H^{\bullet} \rightarrow HPO$$
$$PO^{\bullet} + HO^{\bullet} \rightarrow HPO_2$$
$$HPO + H^{\bullet} \rightarrow H_2 + PO^{\bullet}$$
$$OH^{\bullet} + H_2 + PO^{\bullet} \rightarrow H_2O + HPO$$
$$HPO_2^{\bullet} + H^{\bullet} \rightarrow H_2O + PO$$
$$HPO_2^{\bullet} + H^{\bullet} \rightarrow H_2 + PO_2$$
$$HPO_2^{\bullet} + HO^{\bullet} \rightarrow H_2O + PO_2$$

Figure 2.5 Scheme of the reaction between PO and H or OH radicals in the gas phase

The conversion of CO to CO_2 in the flame is typically the main exothermic reaction ($HO^{\bullet} + CO \rightarrow CO_2 + H^{\bullet}$) [20], and flame inhibition induces more products of incomplete combustion, especially CO and smoke.

In addition, aryl phosphates or their decomposition products that remains in the condensed phase act with the partly decomposed polymer matrix and initiate or improve cross- linking and aromatization [33, 49, 52]. The formation of the resulting cross-linked structure is made of mostly carbon or carbon linked with phosphorus, and increases the residue. The formation of a layer of the carbonized residue, called char, reduced the quantity of the released combustibles and thereby the heat release. They also act as a physical protective barrier against pyrolysis gas transports from the polymer to the flame, and heat transport from the flame to the pyrolysis zone.

Often the physical and chemical processes are related to each other, for example the chemically formed char layer is also a physical barrier to heat and mass transfer. Especially intumescent layers are here to mention [53-55].

TPP and RDP were studied in polycarbonate by Jang and Wilkie [56], and Murashko and Levchik focused on condensed phase mechanisms of RDP in PC and PC/ABS [45, 57]. More recently Pawlowski et al. [46] investigated TPP, RDP and BDP in PC/ABS blends. It was concluded that TPP acts mainly in the gas phase through flame inhibition, due to its high volatility and low decomposition temperature. RDP and BDP act mainly through flame inhibition, but also through some charring in the condensed phase.

The decomposition temperature of the aryl phosphates compared to that of PC was shown to play a major role regarding their interactions in the condensed phase [58, 59]. A cross-linking mechanism between the decomposing aryl phosphate and the early-stage decomposition products of PC was proposed. The structure of the aryl phosphate is the clue to understanding its decomposition/volatilization temperature, and also the interaction between the flame retardant and decomposing PC/ABS.

2.2 Combinations of flame retardant containing phosphorus for PC/ABS: state of the art

Synergy is a promising approach to reduce the total loading of flame retardants in polymer blends. The addition of flame retardant may deteriorate other properties, such as mechanical properties. Various compounds were claimed to show synergies with aryl phosphates: char-formers such as polyphenylene oxide or novolac phenol in ABS or PC/ABS [60], inorganic additives such as clays or nanoclays in styrenics, polyesters [61] and PC/ABS [62, 63]; alumino-silicates [64], boehmite [65] or zinc borates [66] in PC/ABS; siloxanes [67] or silicone rubber in PC [68, 69]. Phosphorus-phosphorus synergism was sometimes claimed, but it is often hard to differentiate from phosphorus-nitrogen synergy [70] since compounds containing nitrogen were used in most examples. Aryl phosphate mixtures have been addressed previously in a few patents [71, 72], where TPP/RDP mixtures and TPP/BDP were claimed to act synergistically in PC/ABS. But their modes of action have not been explained until now. Weil et al. [73] studied a mixture of TPP and hydroquinone bis (diphenyl phosphate) (HDP) in ABS blended with char formers. TPP and HDP were believed to have synergistic effects in reducing burning times. Nevertheless, no detailed investigations were performed to investigate the reason for this synergy.

Moreover, the combination of phosphorus and nitrogen-containing groups in flame retardant formulations is sometimes claimed to give a phosphorus-nitrogen (P-N) synergy [70, 74, 75]. The P-N synergy is depending on the particular system used [50], on the chemical and on the physical interactions occurring between the different components. Different P- and N- containing flame retardants were developed for plastics. In the case of PC/ABS, the addition of ammonium polyphosphate (APP) a common P-N containing flame retardant, was deleterious to PC/ABS properties [37]. The polycarbonate manufacturing sector raised its interest for the novel class of phosphazene additives [76, 77]. Phosphazenes were first developed as intrinsically fire resistant polymers, but are expensive [30, 78-81]. The tricylophosphazene derivatives are now mostly used as basis for reactive flame retardants in thermosets [82-85], as long as additives in thermoplastics [86, 87] where they proved flame retardancy properties. Additionally, combinations of the phosphazene additives with aryl phosphate are claimed to show improved flame retardancy properties in PC/ABS [88, 89]. Even if the patents applications concerning the used of tricyclophosphazene as single flame retardant or combinations with aryl phosphates in PC/ABS are numerous, the understanding of the decomposition mechanisms in PC/ABS leading to the improved flame retardancy are until now missing. Further detailed investigations are needed.

2.3 Choices of aryl phosphates structures and combinations for PC/ABS

This work was dedicated to investigate alternative phosphorous-containing flame retardant additives to optimize the flame resistance of PC/ABS, and to evaluate in detail the flame retardancy mode of action of them, in term of pyrolysis, fire behaviour and flame retardancy mechanisms. In this study the polymer matrix used was always the same for a better evaluation of the flame retardant properties. The PC:ABS ratio of the polymer matrix was held constant at 4.7:1 for all the blends. The A:B:S ratio was constant at 21:13:66, except if differently indicated. Furthermore small amount of poly(tetrafluoroethylene) (PTFE) was used in flame retarded PC/ABS blends to suppress dripping, acting as an anti-dripping agent [90, 91]. The rest of the composition (0.6 wt%) corresponded to other additives.

The choice of the flame retardants has been made taking into account the actual stand of the research of PC/ABS flame retardancy, following the different points:

- evaluating in detail the influence of the structure of oligomeric aryl phosphate on the flame retardancy performances of the blends.

- evaluating a new phosphorus- and nitrogen-containing flame retardant in PC/ABS blend, and any P/N synergy resulting from it.

- combining different mixtures of the above mentioned flame retardants, to enhance the flame retarding action through phosphorus-phosphorus or phosphorus-nitrogen synergy.

Chapter 3 APPROACHES

In this work, the flame retardancy properties of PC/ABS with different halogen-free flame retardant additives have been investigated in terms of flame retardant mechanisms and fire behaviour. The four different approaches are represented in *Figure 3.1*.

	Aryl phosphates in PC/ABS	**Phosphorus-nitrogen flame retardant: phosphazene in PC/ABS**
Single flame retardant	APPROACH 1 Influence of the aryl phosphate structure on the mechanisms: Core and substitution	APPROACH 3 Halogen-free alternative to aryl phosphates: example with a phosphorus-nitrogen containing flame retardant
Combi--nations	APPROACH 2 Synergy between phosphorus-containing flame retardants combinations	APPROACH 4 Synergy between phosphorus- and phosphorus-nitrogen-containing flame retardants combinations

Figure 3.1 Approaches used in this work in function of the type of flame retardant and the type of mixture studied.

3.1 Approach 1: Influence of the aryl phosphate structure on the flame retardancy mechanisms

Firstly, a deeper understanding of the structure-properties relationship of oligomeric bridged aryl phosphate in PC/ABS has been evaluated. This has been done with single aryl phosphate flame retardants for the Approach 1. To further correlate the structure-properties relationships between the flame retardant and its effect in the PC/ABS matrix, the structure of different oligomeric bridged aryl phosphate have been varied, from the core structure (bridging unit) and the variation of the end group unit. The core unit has been varied from a hydroquinone core to a bisphenol A core.

Variation of the core structure of the FR (bridging unit)

The structure-property relationship in the flame retardancy of PC/ABS blends by oligomeric aryl phosphates was first studied by variation of the core (skeletal structure of the repeating unit) of aryl phosphates. In this purpose three flame retardants were used: bisphenol A bis(diphenyl phosphate) (BDP), already commercially available, biphenyl bis (diphenyl phosphate) (BBDP) and hydroquinone bis(diphenyl phosphate) (HDP) as represented in *Figure 3.2.*

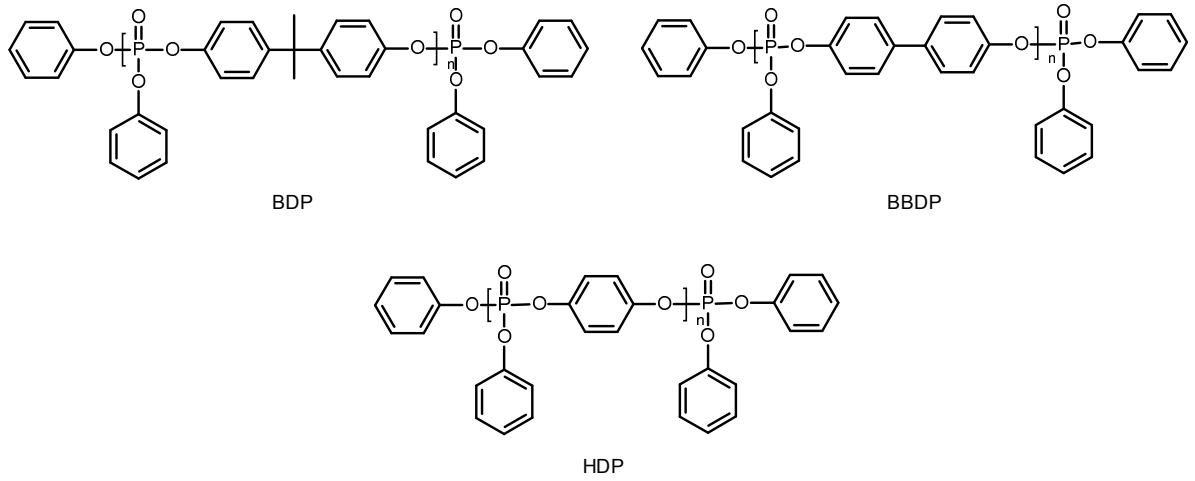

Figure 3.2 Variation of the bridging unit of the aryl phosphate: chemical structure of BDP (bisphenol A bis(diphenyl phosphate)) , HDP (hydroquinone bis(diphenyl phosphate)) and BBDP (biphenyl bis (diphenyl phosphate))

Variation of the end unit: the substitution of phenyl end ring

As oligomers are used, the end substitution of the organophosphate is important (average n=1,1 for BDP). In the literature, the substitution is described to increase the hydrolytic stability. Therefore biphenyl bis(2,6-xylyl) phosphate BBXP was studied, and compared with BBDP (*Figure 3.3)*, to correlate the substitution of the phenyl ring with dimethyl groups in the ortho position on the flame retardancy properties.

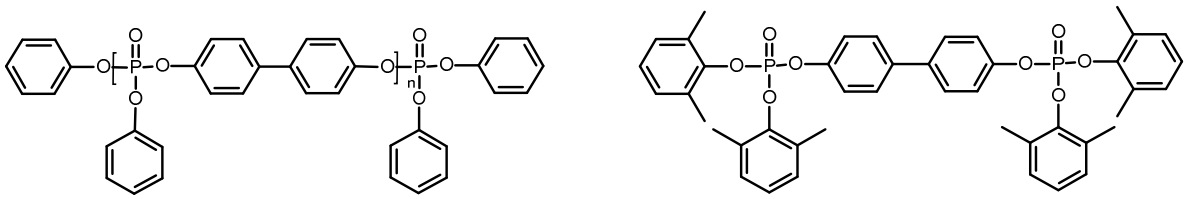

BBDP BBXP

Figure 3.3 Influence of the substituents groups: structure of the flame retardant BBXP (biphenyl bis (di-2,6-xylyl phosphate)) compared with BBDP (biphenyl bis (diphenyl phosphate)

The amount of phosphorus was maintained constant (1.1 wt%) in all the blends investigated with the different aryl phosphates for ease of comparison. The compositions of the blends are given in *Table 3.1*.

Table 3.1 Compositions of PC/ABS$_{PTFE}$ with different aryl phosphates structures (at constant amount of phosphorus: 1.1 wt%)

PC/ABS$_{PTFE}$ +	-	+BDP	+BBDP	+HDP	+BBXP
			Components in wt.%		
PC	81.30	71.00	71.70	72.80	69.90
ABS	17.65	15.45	15.65	15.85	15.25
PTFE	0.45	0.45	0.45	0.45	0.45
BDP		12.50			
BBDP			11.60		
HDP				10.30	
BBXP					13.80

3.2 Approach 2: Synergy between phosphorus-containing flame retardant combinations

The changes in mechanistic effects with a combination of two flame retardant aryl phosphates with various ratios has been the second approach to evaluate alternative flame retardant mixtures in PC/ABS. Since HDP had the higher volatility and thus the highest gas phase activity, and BDP the highest condensed phase activity, a combination of both flame retardants were investigated at different ratios. The improved flame retardancy properties are then not only achieved by changing the structures of single flame retardant, but an optimum is tried by combining different modes of actions.

3.2.1 Series of investigated materials

Seven different materials based on PC/ABS were investigated: PC/ABS_{PTFE} and PC/ABS_{PTFE}+BDP/HDP with different BDP:HDP ratios. The exact compositions of the blends are given in *Table 3.2*. All of the investigated materials contain 12.5 wt.% of the flame retardant mixture. 0.45 wt.% of the anti-dripping agent polytetrafluoroethylene (PTFE) was added to all of the materials.

Table 3.2 Composition of PC/ABS$_{PTFE}$ and PC/ABS$_{PTFE}$ +BDP/HDP blends and amount of phosphorus (%P) in the blend measured by elemental analysis

Composition (wt%)	PC/ABS$_{PTFE}$	PC/ABS$_{PTFE}$+BDP:HDP					
		100:0	80:20	60:40	40:60	20:80	0:100
PC	81.30	71.00	71.00	71.00	71.00	71.00	71.00
ABS	17.65	15.45	15.45	15.45	15.45	15.45	15.45
PTFE	0.45	0.45	0.45	0.45	0.45	0.45	0.45
BDP	-	12.5	10.0	7.5	5.0	2.5	0
HDP	-	0	2.5	5.0	7.5	10.0	12.5
%P measured by elemental analysis	-	1.19	1.25	1.35	1.36	1.37	1.32

3.2.2 Definition of synergy

The synergisms between BDP and HDP were evaluated in PC/ABS$_{PTFE}$ blends. Synergism is defined as an effect of two components which is higher than the superposition of the effect of each component taken separately, and antagonism an effect which is less than the superposition.

Quantitative descriptions of the synergisms are rarely used. However synergisms in flame retardancy effects were quantified in particular by Lewin [92, 93], Weil [70, 94] and lately Schartel [95]. They give a mathematical and quantitative description to define a synergistic effect index (SE) for LOI or PHRR respectively.

For materials with the same amount of additives, and so the same matrix amount, the synergitic effect (SE_A) concerning the absolute reduction in parameter y (such as PHRR, residue %R…) is defined as follow in *equation (1)*:

$$SE_A = \frac{\Delta y_{PC^*ABS+x1A:x2B}}{\frac{x_1}{x_1+x_2}\left(\Delta y_{PC^*ABS+(x1+x2)A}\right)+\frac{x_2}{x_1+x_2}\left(\Delta y_{PC^*ABS+(x1+x2)B}\right)} \quad (1)$$

where x_1 and x_2 relates to the amount, in weight percent, of the flame retardant A and B, respectively, in the PC/ABS_{PTFE}+A:B blend.

A value of $SE_A > 1$ indicates synergy, SE_A close to 1 superposition, and $SE_A < 1$ antagonism. In the case of residue, Δy is the absolute increase in residue, and in the case of THE/ML Δy is the absolute reduction in THE/ML. In *equation (1)* linearity is assumed between flame retardant effect and additive concentration. This is of course an oversimplifying model, since often the flame retardancy effect shows a non-linear increase with flame retardant concentration, especially for a wider range of concentrations.

3.3 Approach 3: Novel phosphorus-nitrogen-containing flame retardant

The phosphorus- and nitrogen-containing flame retardant, phenoxyphosphazene was tested in PC/ABS_{PTFE} but also in the single component PC and ABS to identify its mode of action. The diphenyl phenoxyphosphazene (DPZ) flame retardant contained 99.8% of the cyclic trimer hexaphenoxytricyclophosphazene, and the rest was a mixture of tetramers and linear oligomers. The linear or cyclic structures of DPZ components are represented in *Figure 3.4*.

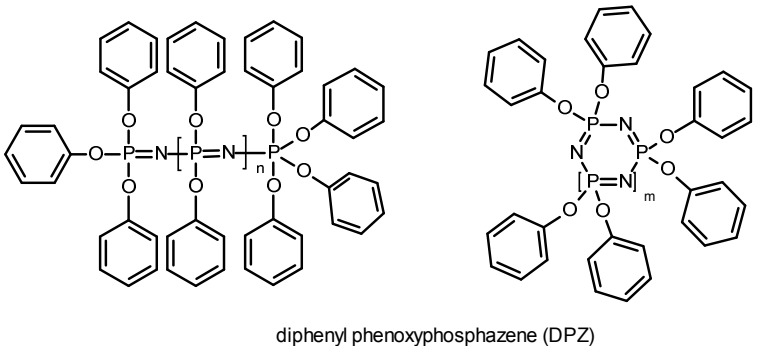

Figure 3.4 Linear or cyclic structure of the phosphorus-nitrogen-containing flame retardant DPZ (hexaphenoxytricyclophosphazene with m=1, octaphenoxytetra-cyclophosphazene m=2)

A mixture of 70% of the cyclic trimers, 20% of the cyclic tetramers and 10% of linear oligomers was also investigated, and is denominated DPZ-m.

The effect of the phosphorus and the nitrogen atoms for the flame retardancy of PC/ABS_{PTFE} is of great interest, in terms of flame retardancy mechanisms and the resulting fire behavior of the blends. The compositions of the blends investigated are given in *Table 3.3*.

Table 3.3 Compositions of the blends based on PC, ABS, and PC/ABS_{PTFE} containing DPZ

Composition (wt%)	PC/ DPZ	PC/DPZ $_{PTFE}$	ABS/DPZ $_{PTFE}$	PC/ABS $_{PTFE}$	PC/ABS/ DPZ_{PTFE}
PC	91.4	90.5	-	81.3	74.7
ABS (21:13:66)	-	SAN 0.45	90.95	17.65	16.25
PTFE	-	0.45	0.45	0.45	0.45
DPZ (trimer 99.8%)	8	8	8	-	8

3.4 Approach 4: Combination between phosphorus- and phosphorus-nitrogen-containing flame retardants

In Approach 4, an aryl phosphate flame retardant (here BDP) and a phosphorous-nitrogen based flame retardant (here DPZ) were combined. The possibility to combine the positive effect of the flame retardant mechanisms of both additives to reach an additive effect or even a synergistic effect on the flame retardancy properties was evaluated by the use of different ratios between BDP and DPZ (*Table 3.4*). The ratios are related to the percentage of phosphorus originating from BDP or DPZ.

Table 3.4 Composition of the PC/ABS$_{PTFE}$ + BDP/DPZ blends, with a constant concentrations in phosphorus in the blend (1.1 wt%).

Composition (wt%)	PC/ABS$_{PTFE}$	PC/ABS$_{PTFE}$+BDP/DPZ					
		100:0	80:20	60:40	40:60	20:80	0:100
PC	81.3	71.0	71.7	72.5	73.2	74.0	74.7
ABS	17.65	15.45	15.65	15.75	15.95	16.05	16.25
PTFE	0.45	0.45	0.45	0.45	0.45	0.45	0.45
BDP	-	12.5	10.0	7.5	5.0	2.5	-
DPZ	-	-	1.6	3.2	4.8	6.4	8.0
%P	-	1.1	1.1	1.1	1.1	1.1	1.1

3.5 Experimental investigations on the effect of flame retardant in term of polymer properties, pyrolysis and fire behaviour

A flame retardant is added to the polymer matrix, in order to increase the self-extinguishing properties of the material, to shift its ignition or to reduce the heat produced during its burning, depending on the fire scenarios. Different properties of the material play a role in dependency of the fire scenario, and so the fire test. That is why different tests are needed to characterized the effect of the flame retardant in the blend.

The different techniques used in this study are schematically illustrated in *Figure 3.5*, in term of the characterization of the polymer properties, the pyrolysis and the fire behaviour.

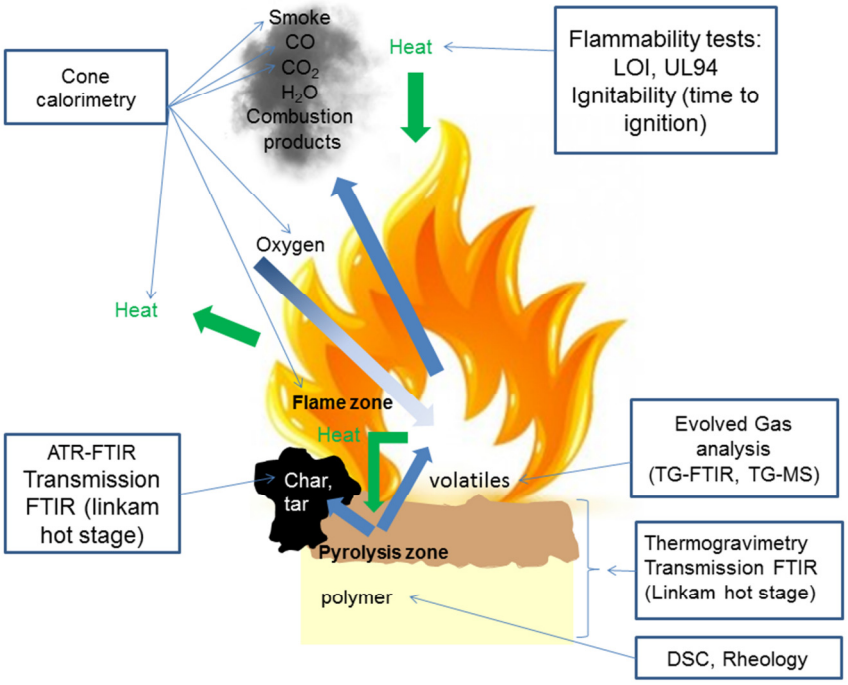

Figure 3.5 Schematic representation of the different experimental methods used to characterize the phenomena during the combustion of the polymer blends

3.5.1 Physical properties of the polymer

Changes in the physical properties of the polymer by the addition of the flame retardant were evaluated in terms of glass transition temperature and rheological properties such as viscosity. For this purpose dynamic scanning calorimetry (DSC) [96] and rheological measurements were carried out on the polymer blends, to clear any difference that will modify the behaviour of the polymer blend with increasing temperature before decomposition.

3.5.2 Thermal stability and thermal decomposition of the polymer blends

The thermal decomposition of a flame retarded polymer is strongly depending on the chemical structure of the flame retardant, on the chemical structure of the polymer matrix and the possible interactions that result from it. That is why the thermal decomposition of the polymer needs to be investigated with and without flame retardant, in the condensed and in the gas phase.

Thermogravimetry (TG) was used to investigate the decomposition temperature of the flame retarded blends. In this technique, the change in the mass of a sample (mass loss) is

monitored in function of the temperature or the time. The DTG curve (differential thermogravimetry curve) corresponds to the first derivative of the TG curve and gives indication on the mass loss rate of the polymer [97, 98]. The decomposition during a fire in the pyrolysis zone is mostly anaerobic, that is why an inert atmosphere was used for the TG measurements (nitrogen or argon gas carrier).

Fourier-transformed infrared spectroscopy coupled with TG (TG-FTIR) is an efficient tool to investigate the gas evolved during the pyrolysis of a polymer, in dependency of the decomposition steps [99]. The chemical nature of the pyrolysis products, as long as their product decomposition rates in function of the time were evaluated. Additionally thermogravimetry coupled with mass spectrometry (MS) was used as a complementary tool in evolved gas analysis to confirm the presence of some products whose could not be unambiguously identified in FTIR [100].

The pyrolysis in the condensed phase was evaluated with transmission FTIR. For this purpose, a heatable cell (Linkam hot stage) was used in a transmission configuration. The FTIR spectra of a thin film of the investigated material were recorded online with the increasing temperature or time. Chemical changes during the thermal decomposition of the polymer and interactions between matrix and flame retardants additives can then be characterised.

The combined investigations of the decomposition in the gas and condensed phase enable the understanding of the chemical reactions occurring between the flame retardant and the polymer matrix. The decomposition mechanisms and the modes of action of the flame retardants were proposed based on these results.

3.5.3 Flammability

The efficiency of flame retardant in a polymer has been investigated in term of the reduction of the fire hazards during the start of a fire: ignition and developing fire. Reduction in flammability (when in contact with a small flame) and ignitability (self-ignition or ignition in the presence of a spark) and flame spread are critical parameters.

It is the region where a fire can be stopped or retarded that allow people to escape the room or to extinguish the fire. Especially in the case of electronical equipment, which are in

contact with high intensities or currents, a high fire resistance is required. The items should not be the start of a fire.

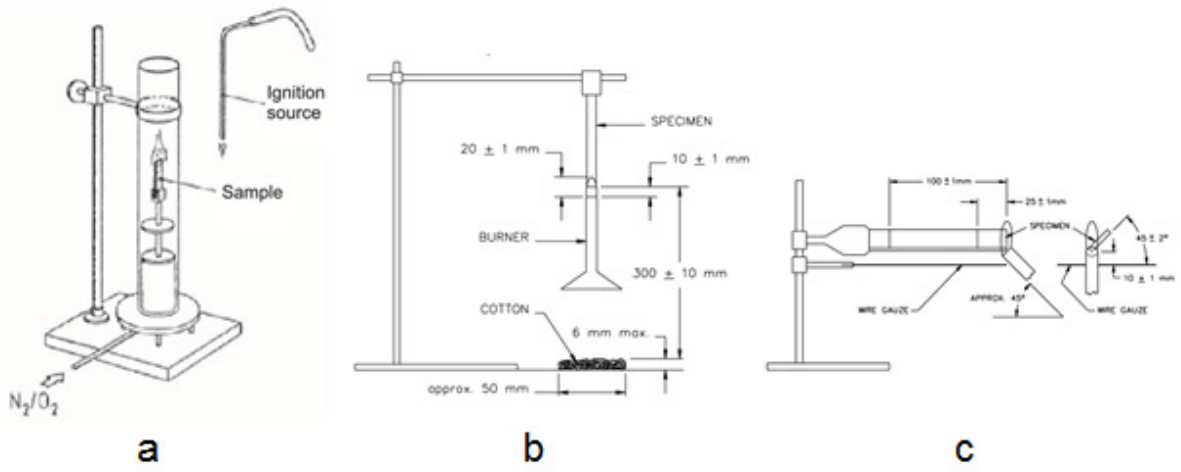

Figure 3.6 Schematic representation of the flammability test setups (a) LOI, (b) UL94 V-test and (c) UL94-HB test

The flammability (reaction to a small flame) of the blends was evaluated through the UL94 and limiting oxygen index tests (LOI). UL94 is characterized by an upward burning when a flame is brought to the bottom end of a polymer stab [101-103]. After 10 seconds application, the flame is removed and the time of burning of the material until self-extinction is registered. If the material extinguishes, the flame is applied to another 10 seconds. The time of burning after the first and the second application time are then measured. If the single burning time are under 10 sec, the material is classified V-0, it is the best classification from this standard. Between 10 and 30 seconds, the material is classified V-1, and if the material drips and ignites a cotton placed under the sample, the material is then classified V-2. If the material burns longer than 30 seconds or burns completely, the material is then non rating in vertical test, and has to be tested horizontally (classification horizontal burning HB or non-rating n.R, in dependence of the burning rate of the material).

Another flammability test is the limiting oxygen index (LOI). The LOI gives the minimum concentration of oxygen in an N_2/O_2 atmosphere necessary to sustain the burning of the material (burning more than 3 min or more than 50 mm) [104]. The flame is here applied on the top of a polymer stab. Characteristic values of LOI are between 17-21% O_2 for easy flammable materials (PE, PP,…), between 21-25% for non-easy flammable materials (PC, …), and above 30 to 50 for fire resistant materials (polyimide,…).

3.5.4 Fire behaviour under forced flaming combustion

Cone calorimetry is the most used fire bench-scale tests to characterize the fire behaviour under forced flaming combustion in well-ventilated conditions [105-108]. Irradiations of 35 kWm^{-2} (developing fire, burning paper basket), 50 kW m^{-2} (developing fire) and 70 kW m^{-2} (fully developed fire) [25] permits to evaluate the fire behaviour of the different blends in different fire scenarios, as it occurred for example during a room fire (*Figure 3.7*).

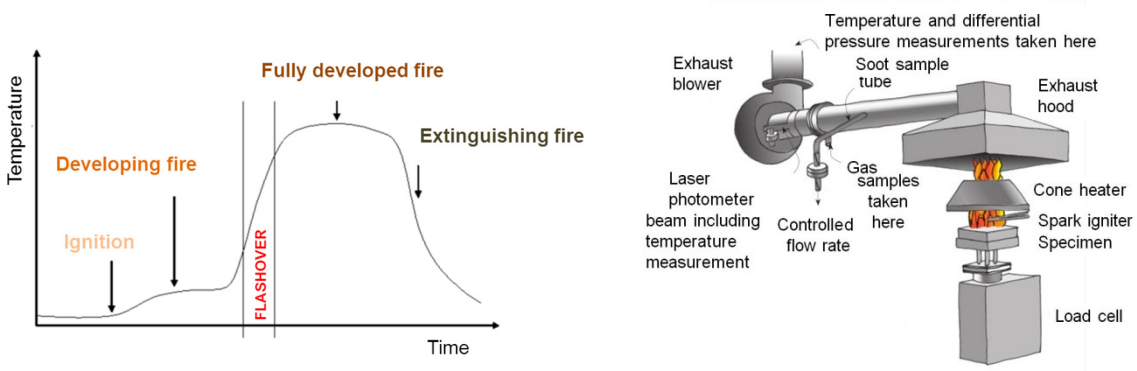

Figure 3.7 The different stages during a typical room fire (left) and schematic representation of the cone calorimeter apparatus (right)

In cone calorimetry, a material is submitted horizontally to an external heat flux by a cone heater. The polymer warms up and decomposes. A spark igniter ignites the volatile gases as soon as a flammable gas mixture is formed (*Figure 3.7*). The main criteria evaluated are the time to ignition of the material t_{ig}, the heat release rate (HRR) and the total heat release (THR) over the combustion until extinction of the flame. The peak heat release rate (PHRR) is the maximum of the HRR curve, and correlates with the risk of a fast flame spread of the fire by the material [109, 110]. The total heat evolved (THE) features the fire load, so the risk caused by a long burning fire. CO and CO_2 production, smoke density and mass loss of the sample are evaluated over the test. Deformation, formation of char and glowing are observed visually during the fire and give hints on the mode of action of the flame retardant. The effect of the flame retardant is then characterized by a possible reduction in the main fire risks.The residues obtained in cone calorimetry were then analysed by attenuated Total Reflectance infrared spectroscopy (ATR-FTIR) as a powder, and elemental analysis was used to characterise the residue compositions at flame out or at the end of the cone calorimeter tests.

Chapter 4 ALTERNATIVE ARYL BISPHOSPHATE FLAME RETARDANTS IN POLYCARBONATE/ACRYLONITRILE-BUTADIENE-STYRENE

4.1 PC/ABS$_{PTFE}$

The non-flame retarded polymer matrix used in this study is a blend of polycarbonate (PC) and of acrylonitrile-butadiene-styrene terpolymer (ABS), with low amount polytetrafluoroethylene (PTFE). To understand the influence of the flame retardant on the pyrolysis of PC/ABS$_{PTFE}$, it is essential to understand the pyrolysis of the polymer matrix.

PC/ABS$_{PTFE}$ is characterized by a two-step decomposition under nitrogen, corresponding to the decomposition of its two main components, see *Figure 4.4.1*. The first maximum mass loss at around 700 K corresponds to the decomposition of ABS. ABS decomposes between 650 and 750 K, with the temperature of maximum mass loss rate (T_{Max}) of 681 K. ABS decomposes almost completely without letting char (0.6 wt%). The mass loss of PC/ABS$_{PTFE}$ during the first step is of 20.3 wt%, a little bit above the amount of ABS in the blend (17.8 wt%) indicating the overlapping start of PC decomposition.

The second maximum mass loss at 785 K corresponds to the decomposition of PC (see *Figure 4.1.1*). PC decomposes in one step between ca. 725 and 850 K, with a T_{Max} of 799 K. PC is a naturally charring material [111] and so 24 wt% residue is obtained at the end of the decomposition of the PC/ABS$_{PTFE}$ blend.

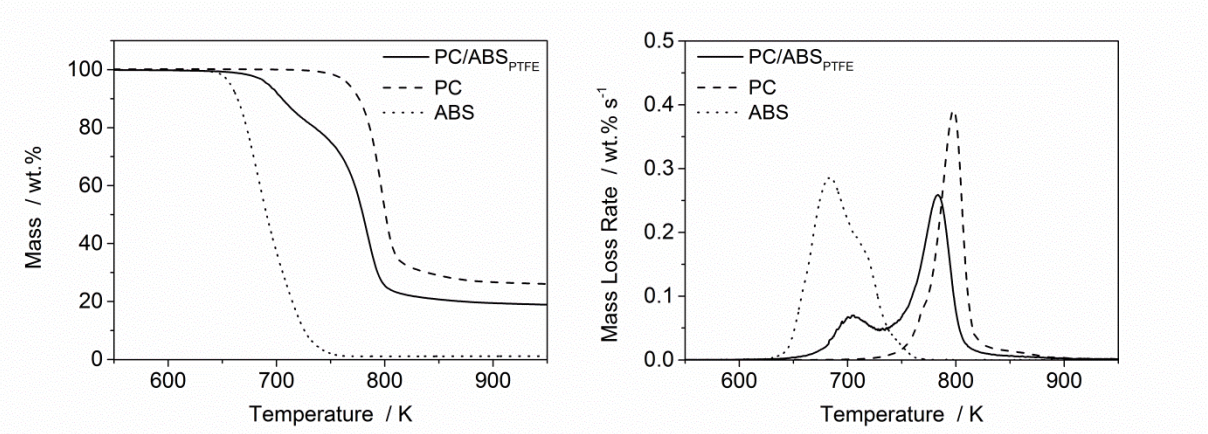

Figure 4.1.1 TG (left) and DTG (right) signals of PC, ABS and PC/ABS$_{PTFE}$ under nitrogen, with a heating rate of 10 K/min

The evolved gas analysis of the decomposition products of PC/ABS_{PTFE} by FTIR confirms the results of the TGA, see *Figure 4.1.2a*. During the first decomposition step, mainly products from the decomposition of ABS are observed, and the two FTIR spectra of PC/ABS_{PTFE} for the first mass loss step and ABS at the maximum of decomposition are similar. The in-situ FTIR gas phase spectra are dominated by the absorption bands of styrene and its derivatives: C_{Ar}-H stretching at 3077 and 3036 cm^{-1}, CH_2=CH- stretching at 1628 cm^{-1}, C_{Ar}=C_{Ar} stretching of the aromatic ring at 1600 and 1491 cm^{-1}, and deformation vibrations of C_{Ar}-H of the aromatic ring at 989, 910, 773 and 694 cm^{-1}. Aliphatic components with -CH_2 or -CH_3 groups are also detected under 3000 cm^{-1} (2969, 2935 and 2876 cm^{-1}) from styrene and butadiene derivatives. Evolution of acrylonitrile or its derivatives is also observed at 954 cm^{-1}. These decomposition products correlated well with the ABS decomposition products proposed in the literature [27, 29, 112], where it is reported that ABS mainly decomposes into aliphatic products, resulting from butadiene, styrene monomers and its derivatives, such as dimers, trimers, methyl styrene and toluene. A minor evolution of phenol derivatives is also observed in FTIR, with C_{Ar}O-H vibration at 3650 cm^{-1} and C_{Ar}-O stretching at 1259 and 1175 cm^{-1} in the case of PC/ABS_{PTFE}, indicating the start of decomposition of PC.

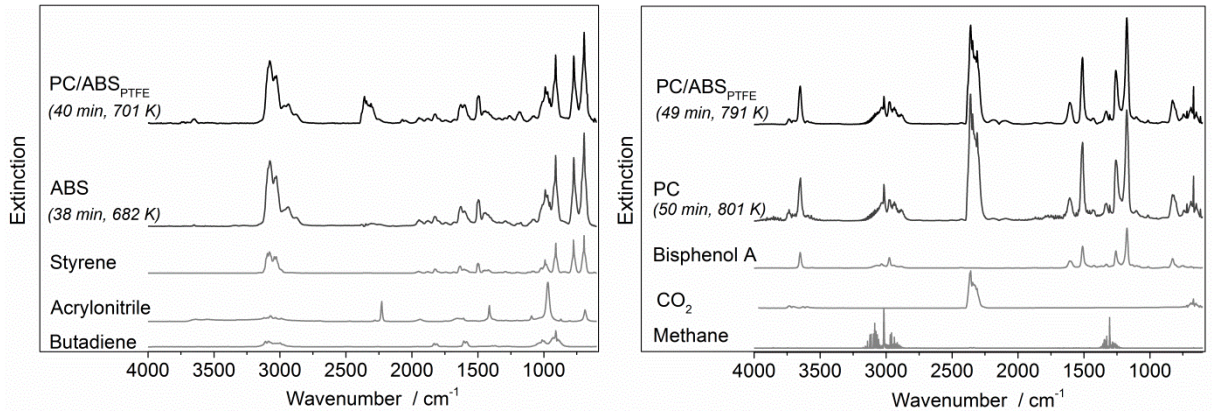

Figure 4.1.2 TG-FTIR spectra (TG under nitrogen, 10 K min^{-1}) of left: PC/ABS_{PTFE} first decomposition step at 40 min, ABS main decomposition step (38 min) and reference spectra of styrene, acrylonitrile and butadiene, and right: PC/ABS_{PTFE} during second decomposition step at 49 min, PC main decomposition step and reference spectra of bisphenol A, CO_2 and methane

During the second mass loss of PC/ABS_{PTFE} similar decomposition products than PC evolved in the gas phase (*Figure 4.1.2*). CO_2 with characteristic bands at 2360 cm^{-1} and 669 cm^{-1}, phenol derivatives such as bisphenol A, phenol,4-methylphenol or 4-ethylphenol with characteristic bands of free Ph-OH at 3650 cm^{-1}, and deformation bands at 1603, 1509, 1259, 1175 and 829 cm^{-1}, methane (3016 and 1305 cm^{-1}) and CO (2185 and 2091 cm^{-1}) are the main volatile decomposition products.

The products decomposition rates of main decomposition products of PC/ ABS_{PTFE}, obtained in mass spectrometry coupled to the TG, are illustrated in *Figure 4.1.3*. They confirm the observations from FTIR with the release of decomposition products from ABS during the first mass loss step (with styrene for example at m/z=104) and the decomposition of the PC part during the second decomposition step. Moreover the release of some CO_2 already during the first step indicates the overlapping of the two decompositions, as suggested by the higher mass loss in step 1 in the TGA than the amount of ABS, and the presence of CO_2 and CO in the FTIR spectrum of the first decomposition step.

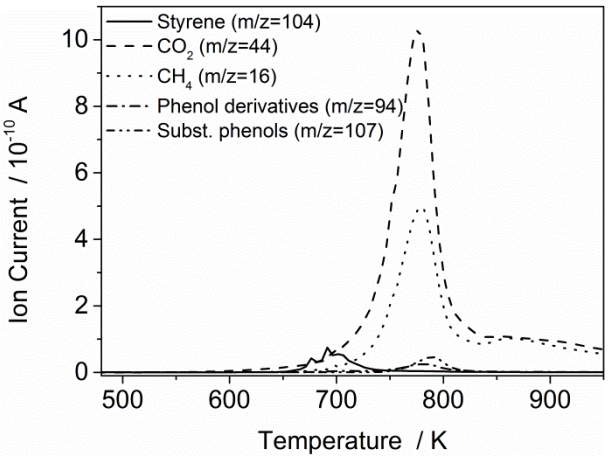

Figure 4.1.3 Product decomposition rates (TG-MS under nitrogen 10 K/min) of styrene at m/z =104 a.m.u, CO_2 at m/z =44 a.m.u., methane at m/z =16 a.m.u, phenol derivatives at m/z =94 a.m.u. and alkyl substituted phenols at m/z =107 a.m.u. from PC/ABS_{PTFE} decomposition.

The condensed phase of PC/ABS_{PTFE} has been monitored under nitrogen at a constant heating rate in *Figure 4.1.4*. At 300 K the FTIR spectra is dominated by the absorption bands of polycarbonate, with the characteristic carbonate stretching bands (C=O 1775 cm^{-1} and C_{Ar}-

O at 1227 cm^{-1}; and the –OCOO- asymmetric stretch at 1192 and 1162 cm^{-1}; and symmetric stretch at 887 cm^{-1}), the isopropyl group (C-H_3 stretching at 2969, 2934 and 2874 cm^{-1}, C-$(CH_3)_2$ deformation at 1465 and 1364 cm^{-1} asymmetric and symmetric respectively), and the aromatic rings (C_{Ar} -H stretching at 3060 and 3040 cm^{-1}, C_{Ar}-C_{Ar} ring stretch at 1600 and 1504 cm^{-1}; C_{Ar}-C_{Ar} deformation at 1015 cm^{-1} and C_{Ar}-H deformation for para substituted rings at 829 cm^{-1}). [113]. The peaks of ABS are mainly overlapped by the one of PC, except the -C≡N stretching of acrylonitrile at 2237 cm^{-1} and C_{Ar}-C_{Ar} ring deformation from the styrene ring at 700 cm^{-1}.

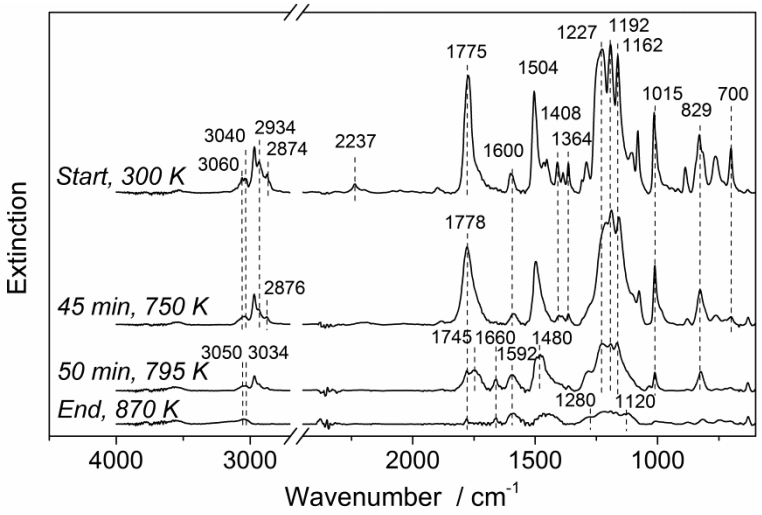

Figure 4.1.4 FTIR spectra of PC/ABS_{PTFE} in the condensed phase at different temperatures (under nitrogen, 10 K min^{-1}) a) at start, at end step 1 ca 750 K, at 795 K, Max step 2, and residue after storage 10 min at 870K

At 750 K, corresponding to the end of the first mass loss step, the characteristic peaks of ABS have disappeared, and the intensities of the aliphatic C-H stretching under 3000 cm^{-1} reduce and the peaks position widen and shifts, corresponding to the decomposition of ABS. Moreover, aromatic alcohol groups formed during the first step with the appearance of a new broad band around 3550 cm^{-1}. The environment of the carbonate linkage changed, with the broadening and shift of the bands at 1778 cm^{-1} and 1227 cm^{-1}, indicating that the group reacts. Phenol groups are formed at the carbonate group either by rearrangement of PC or by hydrolysis or alcoholysis at the carbonate linkage. PC decomposition and rearrangements result in the release of CO_2 and small amount of phenol derivatives observed in the gas phase during the first step [114, 115].

At 795 K, corresponding to the maximum mass loss temperature of the second decomposition step, the carbonate group has nearly completely disappeared, and new esters groups (C=O str at 1745 cm^{-1}) and xanthone groups (C=O str at 1660 cm^{-1}) are formed. At the same time the C-O bands around 1200 cm^{-1} broaden, corresponding to the formation of aromatic ethers, esters and xanthone. The increase of the broad band at 3580 cm^{-1} indicates the presence of H-bonded phenol-OH groups. The aromatics absorption bands, C_{Ar}-H stretch and C_{Ar}-C_{Ar} ring stretch strongly broadened and partly shifted to lower wavenumbers (3050 and 3034 cm^{-1} or 1592 and 1480 cm^{-1}, respectively). It indicated the polyaromatisation of the residue, the char, mainly through cross-linking reactions between the phenyl rings due to the decomposition of PC. Mostly all aliphatics, especially from the isopropyl groups from PC, had decomposed, with the corresponding release of methane and aliphatic substituted phenols in the gas phase seen in TG-FTIR over the second decomposition step.

After storage of the residue 10 min at 870 K, mainly polyaromatics and C-O groups and C_{Ar}-OH groups are present in the PC char, with very broad bands. Esters groups decomposed completely, to give ethers and release of carbon monoxide, or by the release of CO_2 and further aromatisation.

Even if blended together, PC and ABS decomposes separately, without chemical changes, as observed in TGA, TG-FTIR-MS and transmission–FTIR of the condensed phase. Every constituent of ABS (*Figure 4.1.5*) decomposed mainly by homolytic radical scission, to give mainly styrene or styrene derivatives for polystyrene, acrylonitrile for polyacrylonitrile and butadiene and butadiene derivatives for polybutadiene.

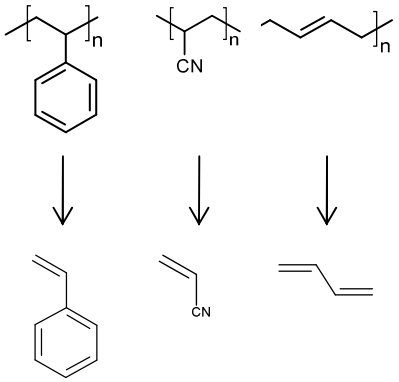

Figure 4.1.5 Schematic representation of the decomposition of ABS in the PC/ABS_{PTFE}

PC decomposed mainly by alcoholysis/hydrolysis reactions due to the small amount of water or phenols present inside the blend before decomposition. PC hydrolysis released phenolic derivatives such as bisphenol A and CO_2 as main decomposition products. Due to the formation of phenols by this reaction, the decomposition by alcoholysis is self-sustained [114, 116].

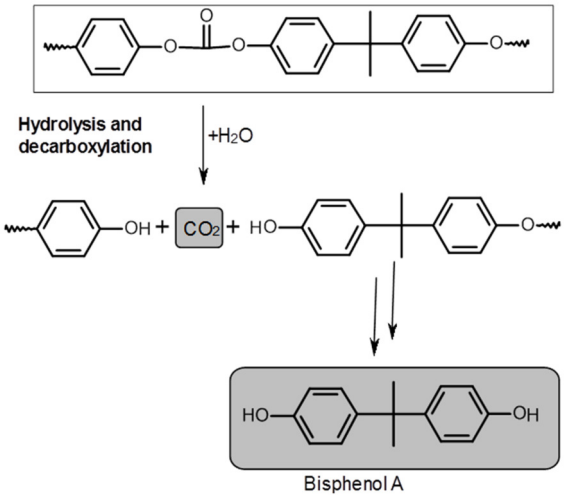

Figure 4.1.6 Main decomposition of PC by hydrolysis/alcoholysis at the carbonate linkage

Other decomposition pathways occurred simultaneously. The isopropylidene groups decomposed by radical scission explaining the release of CH_4, and substituted phenols such as ethyl phenols and methyl phenols.

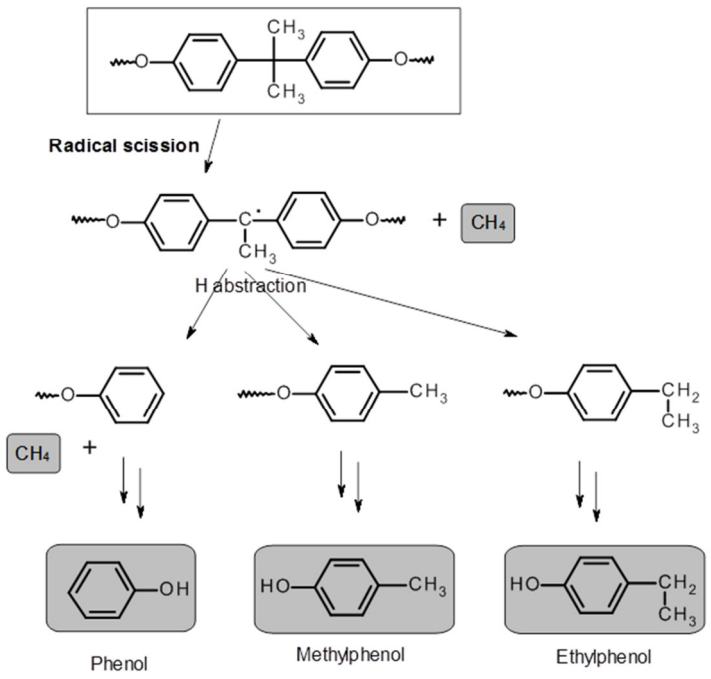

Figure 4.1.7 Decomposition of PC in the PC/ABS$_{PTFE}$ by radical scission at the isopropylidene linkage

The decomposition of PC is in competition to condensation and rearrangement reaction leading to cross linking and gelation in the condensed phase [111]. Rearrangements reactions are major thermal decomposition pathways of PC, such as Fries rearrangement or Kolbe-Schmitt rearrangement [117]. The former leads to the formation of ether and carboxylic end groups (*Figure 4.1.8*), while the second one yields phenol and phenol ester end groups (*Figure 4.1.9*).

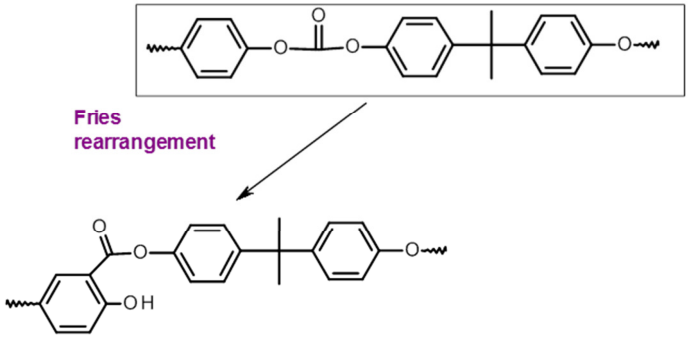

Figure 4.1.8 Possible rearrangements of PC by Fries rearrangement

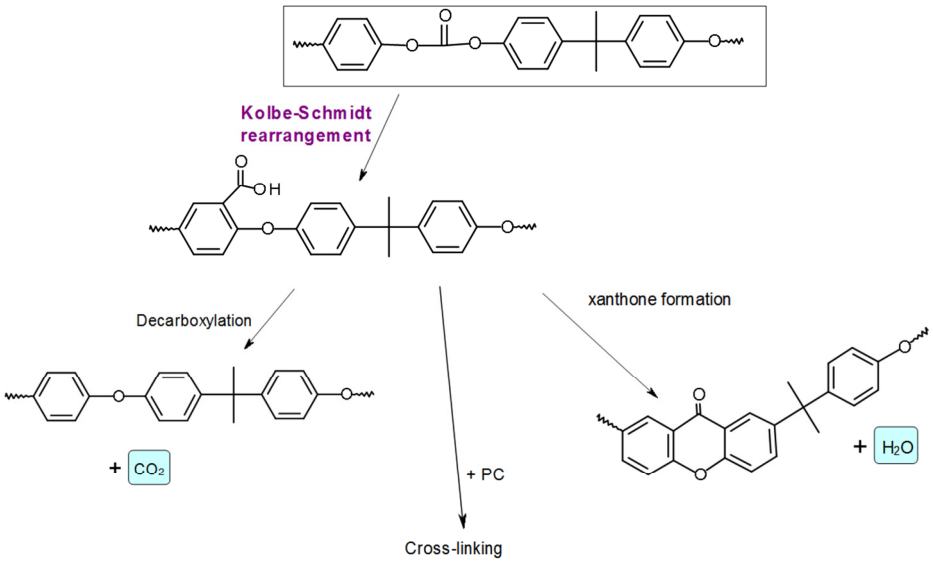

Figure 4.1.9 Kolbe Schmitt rearrangement of PC leading to the formation of ether groups or xanthone groups.

4.2 Aryl phosphate flame retardants with different bridging unit structures: BDP, BBDP, HDP

4.2.1 Pyrolysis

The pyrolysis of BBDP, BDP and HDP under nitrogen is represented in *Figure 4.2.1*. The flame retardants decompose in one main step. HDP decomposes at a lower temperature than BDP or BBDP. HDP decompose mainly between 550 K and 700 K, with a maximum mass loss temperature T_{Max} at 684 K. BDP and BBDP decompose later, mainly between 600 and 800 K, with a T_{Max} of 748 K for both. BBDP decomposition presents a shoulder around 800 K, probably due to oligomers presence. The three flame retardants leave only 3 to 5 wt.% of residue. The core structure has an influence on the thermal stability of the flame retardant, following the order of the molecular weight HDP<BBDP≈BDP. BDP, BBDP, and to a lesser extent HDP, decompose in the same decomposition range as the PC and the ABS components, enabling interaction with their decomposition products.

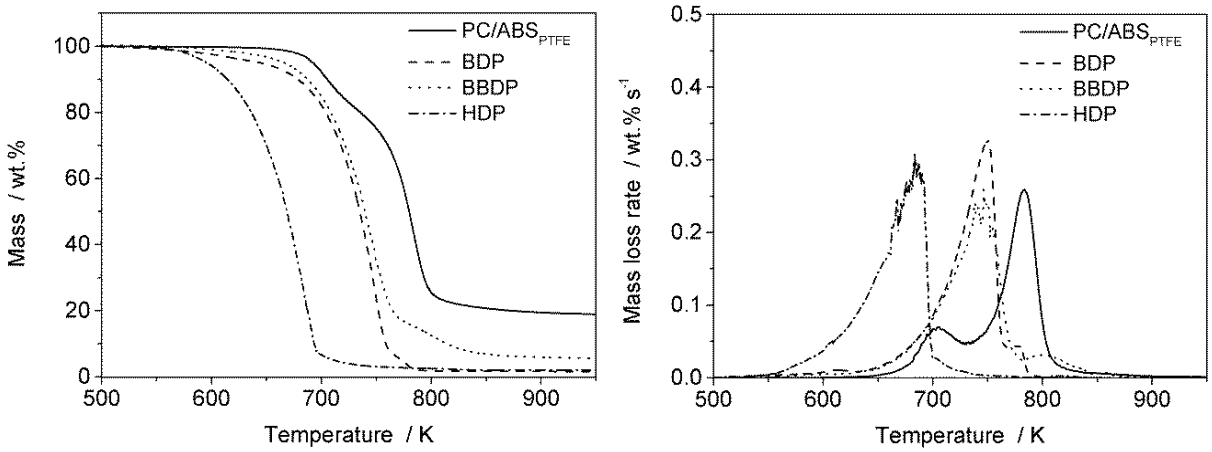

Figure 4.2.1 TG and DTG of PC/ABS$_{PTFE}$ and the single flame retardants BDP, BBDP and HDP

The thermal decompositions under nitrogen of the blends of HDP, BDP and BBDP with PC/ABS$_{PTFE}$ are illustrated in *Figure 4.2.2*. The additions of the flame retardants do not change the two-step decomposition of PC/ABS$_{PTFE}$. But the decomposition temperatures are shifted compared to non-flame retarded PC/ABS$_{PFTE}$ indicating interaction with the decomposing matrix. Minimal destabilization is seen for PC/ABS$_{PTFE}$+BDP and PC/ABS$_{PTFE}$+BBDP with respect to the beginning of decomposition ($T_{2\%}$, *Table 4.2.1*). But the T_{Max} of the first decomposition step is shifted downward, from 8 K for BBDP to 13K for BDP. This is due to the overlapping decomposition of the flame retardant in this temperature range. The mass loss for the first step is between 24 to 28 wt.%, correlating roughly to the amount of ABS and flame retardant. Due to the lower thermal stability of HDP, PC/ABS$_{PTFE}$+HDP starts to decompose already 40 K ($T_{2\%}$) before PC/ABS$_{PTFE}$, and T_{Max} of the first decomposition step is shifted 13 K downwards.

The addition of the flame retardants have however a positive effect on the second step, corresponding to PC decomposition. The T_{Max2} are shifted to higher temperatures (+14 to 15 K). Thus the decomposition temperatures of PC in PC/ABS$_{PTFE}$+BDP and in PC/ABS$_{PTFE}$+BBDP approach that of pristine PC (ca. 800 K). The flame retardant stabilizes and delays the start decomposition of PC in the blend. The mass losses between 48-50 wt.% for the second step of the blends agree with charring PC and a possible further decomposition of the flame retardant.

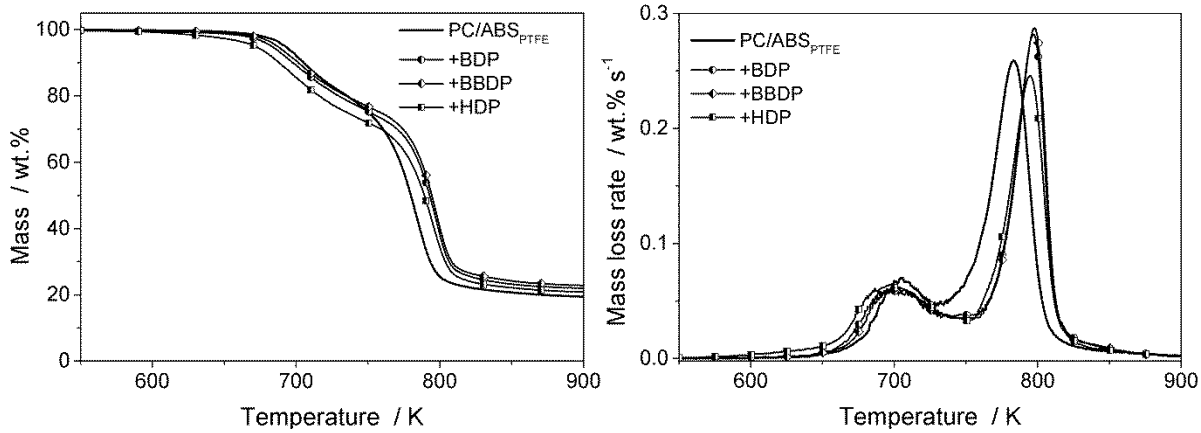

Figure 4.2.2 TG and DTG of PC/ABS$_{PTFE}$ and the blends PC/ABS$_{PTFE}$+BDP, PC/ABS$_{PTFE}$+HDP and PC/ABS$_{PTFE}$+BBDP

The residues increase in the presence of the flame retardants. They lay between 24 and 26 wt.%. An increase of +3% for HDP, to +5-6% for BBDP and BDP is obtained, compared to the expected residue from pristine PC/ABS$_{PTFE}$ and flame retardant. Hence the flame retardant exhibits a condensed phase action in the blend, increasing the formation of char from PC. This interaction is lower for HDP due to its earlier decomposition/volatilization.

Table 4.2.1. TG results of PC/ABS$_{PTFE}$+BDP HDP or BBDP blends (anaerobic pyrolysis, 10K min^{-1})

Material		Mass loss I (ABS)		Mass loss II (PC)			
	$T_{2wt\%}$ K	$T_{Max\ 1}$ K	ML1 wt.%	$T_{Max\ 2}$ K	ML2 wt.%	Residue wt.%	Expected residue wt%
PC/ABS$_{PTFE}$	670	702	20.1	782	57.3	22.6	-
PC/ABS$_{PTFE}$ + BDP	667	703	25.5	797	49.4	25.2	19.9
PC/ABS$_{PTFE}$ +BBDP	669	700	24.7	797	49.1	26.3	20.4
PC/ABS$_{PTFE}$ + HDP	637	701	28.2	796	48.1	23.8	20.7

The evolved gas FTIR spectra at the two main decomposition steps of the blends are illustrated in *Figure 4.2.3*. In the presence of BDP, BBDP or HDP, the PC/ABS$_{PTFE}$ blends show during the first decomposition step an increase in the release of phenol derivatives such as bisphenol A at 3650, 1259, 1175 and 829 cm^{-1}. Aromatic phosphate esters are released

from the flame retardant into the gas phase, as indicated by new sharp bands at 964 and 1192 cm^{-1} (P-O-C_{Ar}) and 1298 cm^{-1} (P=O). In the case of PC/ABS_{PTFE}+HDP, the intensity of the bands corresponding to the organophosphorus compounds at the first maximum mass loss is somewhat lower than for PC/ABS_{PTFE}+BDP or +BBDP. The reason for that is the volatilization/decomposition of HDP in an earlier and broader decomposition temperature range compared to BDP and BBDP. CO_2 evolved in small amounts in this step. A new band appeared at 1233 cm^{-1} for all of the flame retarded blends, and is attributed to the characteristic absorption band of phenyl ether derivatives (-C_{Ar}-O-C_{Ar}). The interaction of phosphorus compounds with decomposition products of PC is a possible explanation for the light destabilization of the flame retarded blends observed in TG.

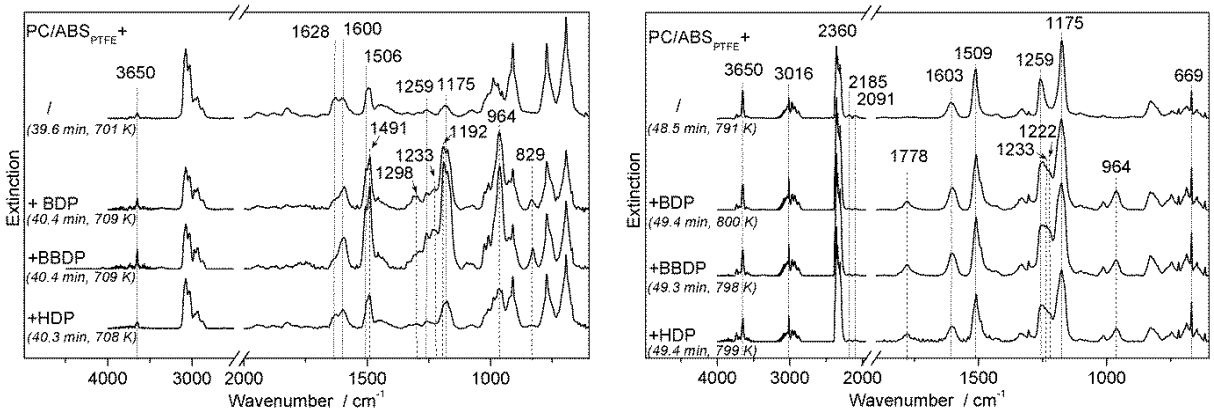

Figure 4.2.3 FTIR gas phase spectra of the evolved products, left: at the maximum of the first mass loss step and right: at the maximum of the second mass loss step for PC/ABS_{PTFE} and PC/ABS_{PTFE}+BDP, PC/ABS_{PTFE}+BBDP and PC/ABS_{PTFE}+HDP

During the second decomposition step, the main decomposition products of the flame retarded blends are similar to those of PC/ABS_{PTFE}, with the release of CO_2 (2360 and 669 cm^{-1}), phenol derivatives (3650, 1259, 1175 and 829 cm^{-1}), CO (2185 and 2091 cm^{-1}) and methane (3016 cm^{-1}). However, the addition of the flame retardant partly modifies the decomposition pathways of PC, inducing the release of aromatic carbonates, such as diphenyl carbonate with visible O-C(=O)-O stretching vibrations at 1778 cm^{-1} and at 1222 cm^{-1}, which were not observed in the case of PC/ABS_{PTFE}. Phenyl ethers derivatives (1233 cm^{-1}) and some phosphate esters were also evolved during the second step as minor products (964 cm^{-1}; the bands at 1176 and 1298 cm^{-1} are not clearly identifiable due to overlapping). Significant

release of volatiles containing phosphorus was observed for all the three aryl bisphosphate blends during the two decomposition steps, indicating potential for flame inhibition in the gas phase.

The product release rates of selected pyrolysis gases from the decomposition of PC/ABS_{PTFE}, PC/ABS_{PTFE}+BDP, PC/ABS_{PTFE}+BBDP and PC/ABS_{PTFE}+HDP monitored by TG-MS and TG-FTIR are presented in *Figure 4.2.4*. No change in ABS decomposition by the presence of the three aryl phosphates is deduced by the release of styrene in a similar way than for PC/ABS_{PTFE}. PC proceeds mainly by the same main hydrolysis/alcoholysis pathways forming phenol derivatives as for PC/ABS_{PTFE}, since phenol derivatives are released for all blends during the second decomposition step, in similar amounts, only shifted in the time (*Figure 4.2.4.a*). However aryl carbonate derivatives evolved during the second decomposition step for all three of the flame retarded blends with BDP, BBDP or HDP with an higher intensity (*Figure 4.2.4.b*). The amount of small gases such as carbon dioxide (*Figure 4.2.4 e*) or methane (*Figure 4.2.4.f*) is higher in the three flame retarded blends than in PC/ABS_{PTFE}. On the contrary, release of carbon monoxide is reduced (*Figure 4.2.4 c*), indicating the changes in some decomposition pathways of PC.

The variation in the core structure of the flame retardants, from bisphenol A, biphenyl or hydroquinone based phosphate esters, has the same influence on the change in the mechanisms of PC. The increase in CO_2 and methane and reduction in CO is related to changes in the decomposition pathways of PC. The presence of the phosphate esters is suggested to favor rearrangements of PC [46] and these rearrangement products are able to cross-link with phosphate esters, but also to release small molecules such as carbon dioxide.

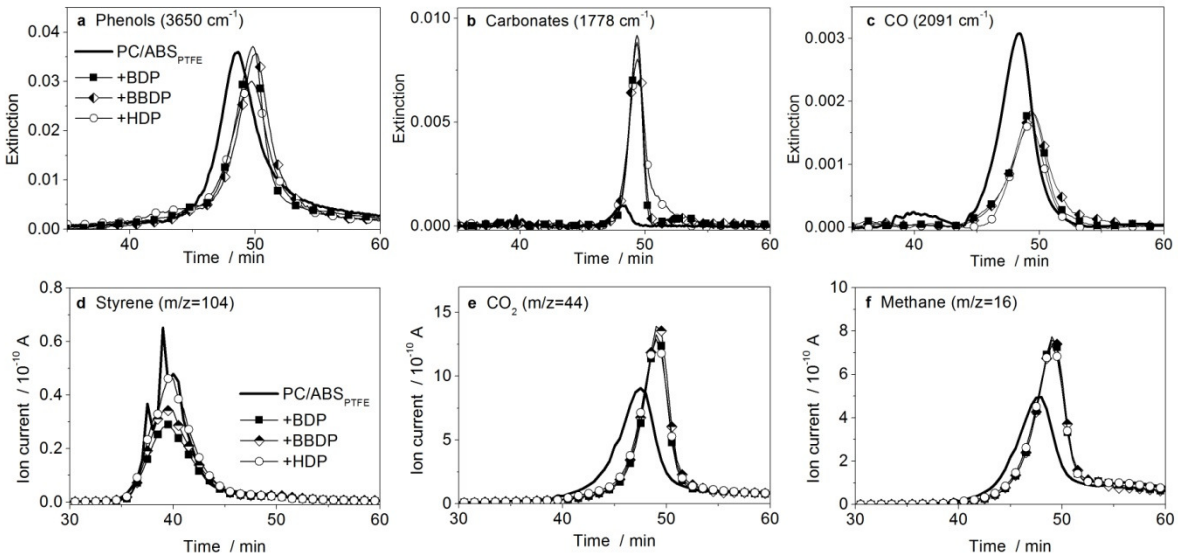

Figure 4.2.4 Product decomposition rates of PC/ABS$_{PTFE}$ blends with BDP, BBDP or HDP monitored by TG-FTIR or TG-MS (under nitrogen, 10 K min^{-1})

In *Figure 4.2.5* are represented the condensed phase spectra of the three flame retarded blends and the original PC/ABS$_{PTFE}$ matrix for comparison. At 300 K, (*Figure 4.2.5.a*) besides the characteristic bands of PC/ABS$_{PTFE}$, the three flame retarded blends show the presence of the aryl phosphates, with characteristic P-O-C_{Ar} stretching band at 962 cm^{-1}, $(C_{Ar}O)_3P{=}O$ stretching as a shoulder at 1308 cm^{-1}; C_{Ar}-C_{Ar} band at 1592 cm^{-1}; monosubstituted phenyl deformation band at 690 cm^{-1} (shoulder); and P-O-C deformation at 510 cm^{-1}. P-O-C stretch at 1160 and 1192 cm^{-1} and other bands, for example from the core structure of the aryl phosphates are overlapped by the bands of the matrix.

At around 750 K, corresponding to the end of step 1 (*Figure 4.2.5 b*), acrylonitrile completely decomposed with the loss of the CN band 2237cm^{-1}, a major part of the styrene components is lost, for example visible by the reduction of the bands at 700 cm^{-1}, and the aliphatics bands reduced, indicating the release of ABS parts for all the flame retarded PC/ABS$_{PTFE}$ blends (+BDP, +BBDP, +HDP). The release of the organophosphorous compounds seen in TG-FTIR corresponded to the decomposition of the aryl phosphate in the condensed phase. The P-O-C band strongly reduced and broadened with a shift to 960 cm^{-1}, which indicated the change in the environment of the phosphorus, principally by the formation of $(C_{Ar}O)_2$-(O=)P-OH groups due to hydrolysis. Another shoulder formed at 989 cm^{-1}, which is assigned to $(C_{Ar}O)$-(O=)P-$(OH)_2$ groups or P-O-P polyphosphate groups. But the phosphate did not completely decomposed, indicating a possible condensed phase action.

Moreover the aromatics bands from the aryl phosphates have broaden (690 and 1592 cm^{-1}) indicating the change in the environment of the aromatics bounded to the phosphate unit, due to a partial interaction (transesterification) between the substituent groups of the flame retardants. With addition of the flame retardant into the PC/ABS_{PTFE} matrix, the carbonate groups of PC is more stable, as seen by the reduced broadening of the –OC=OO- band at 1778 cm^{-1} and the absence of the shoulder at 1745 cm^{-1} corresponding to mainly esters and other carbonyl groups formation. In the case of +BDP and +BBDP, the carbonate linkage only lightly broadened and the intensity is only slightly reduced, compared to +HDP and the non-flame retarded matrix, where the carbonate linkage strongly decomposed or rearranged. An interaction of PC and the flame retardant decomposition products by transesterification forming carbonate groups during the first step is not excluded by the results, as new formed aromatic carbonate groups will have a similar band as the one of PC.

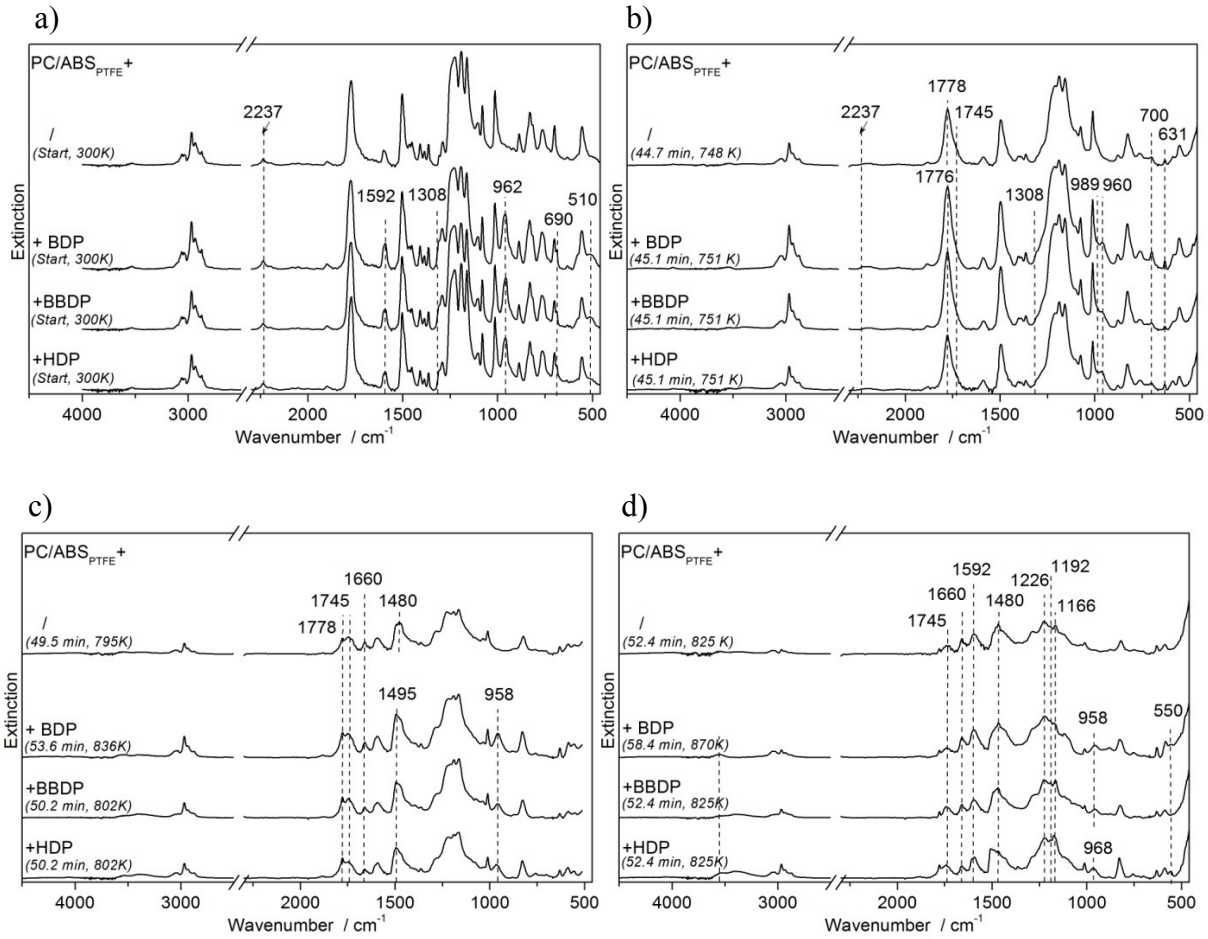

Figure 4.2.5. FTIR spectra of condensed phase of the blends (linkam, heating rate 10K/min, under nitrogen) at (a) Start 300K; (b) End of step 1 at ca. 750 K; (c) Max of Step 2 at ca. 800 K, (d) end of Step 2 at ca. 825 K

At around 800 K, corresponding to the maximum of decomposition of PC (*Figure 4.2.5 c*), mainly all the bands of PC have decreased. Esters, carbonyl groups (C=O stretch at 1745 cm^{-1}), xanthones or aromatic ketones (C=O str at 1660 cm^{-1}) and different O-containing groups such as ether groups (broad C-O stretch around 1200 cm^{-1}) formed from the decomposition of the carbonate groups. OH bands from phenol end groups formed, and P-OH groups are visible with a broad peak between 3600 and 3300 cm^{-1}. Char is forming, indicated by the increase and the shift of the C_{Ar}-C_{Ar} stretch around 1600 cm^{-1}. PO-H band broadened at 958 cm^{-1}, due to the interaction with the phenol end groups of PC decomposition products.

At around 825 K, corresponding to the end of step 2 (*Figure 4.2.5 d*), the carbonyls groups, mainly esters, further decomposed to more stable ethers, phenol or xanthone groups. Phosphorus bands, even partly decomposed until end of the step, still remained in the condensed phase. The broad band by 1480 cm^{-1} are related to the strong formed char with C_{Ar}=C_{Ar} stretch. However the possibility of the formation of P-C_{Ar} bounds by the vibration at around 1460 cm^{-1}, due to the reduction of the phosphate by the carbonaceous char at this temperature, is not excluded [118].

4.2.2 Influence of the structure on the flame retardancy mechanisms

Aryl phosphate flame retardants are more reactive towards hydrolysis than carbonates. Studies on PC blended with aryl phosphates indicates the reduction of the hydrolysis/ alcoholysis in the presence of the phosphates [119], or even the suppression of this pathway in the case of polyphosphates blended with diphenyl carbonate, a low molecular weight model system for PC [120]. In this case the decomposition of the aryl phosphate will stabilise the carbonate linkage and thus retard the decomposition of PC (*Figure 4.2.6*)

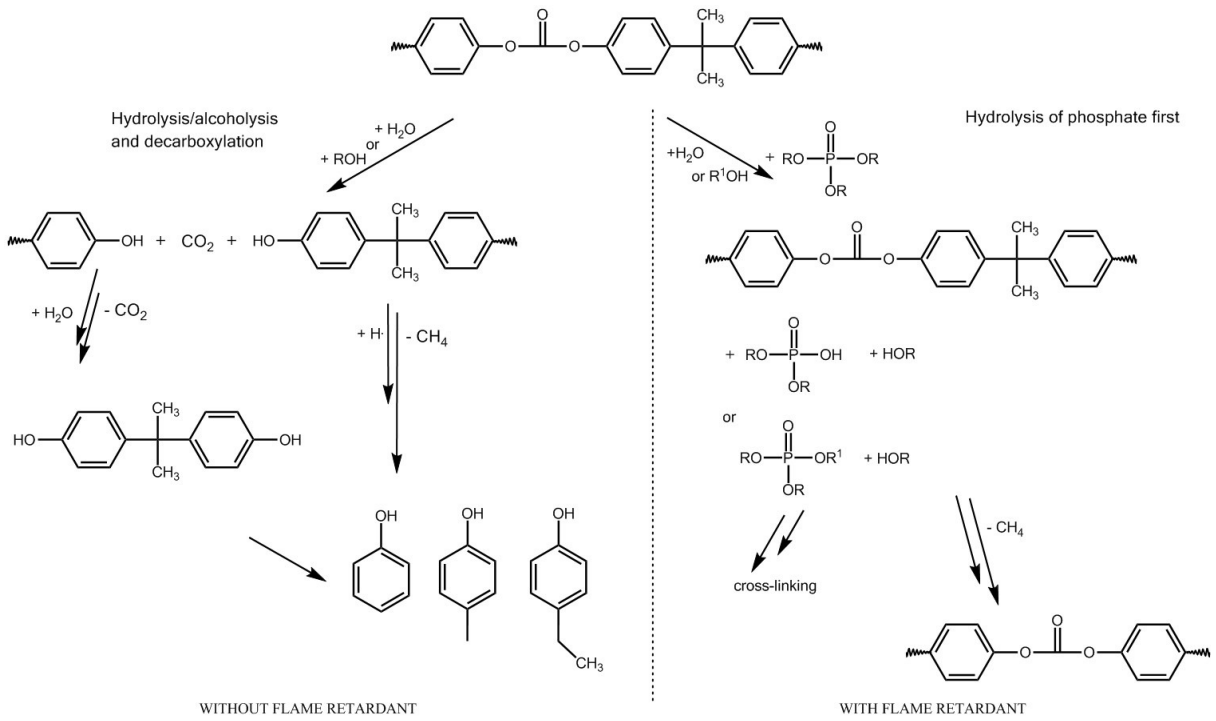

Figure 4.2.6 Action of the phosphate flame retardant on the hydrolysis/alcoholysis decomposition pathway of PC, explaining the stabilisation of the carbonate linkage at the start of decomposition

During the decomposition of PC, the phosphates resulting from the decomposition of the flame retardant will further interact with decomposing PC, for example with phenol end groups of PC by addition elimination. If the reaction occurs at the three position of the phosphate, cross-linking will occur and thus increase the residue.

The phosphate could also react via transesterification with phenol end groups created by rearrangement of the carbonate group, for example through the Fries rearrangement. The chain will thus be cross linked instead of scission and the residue will increase.

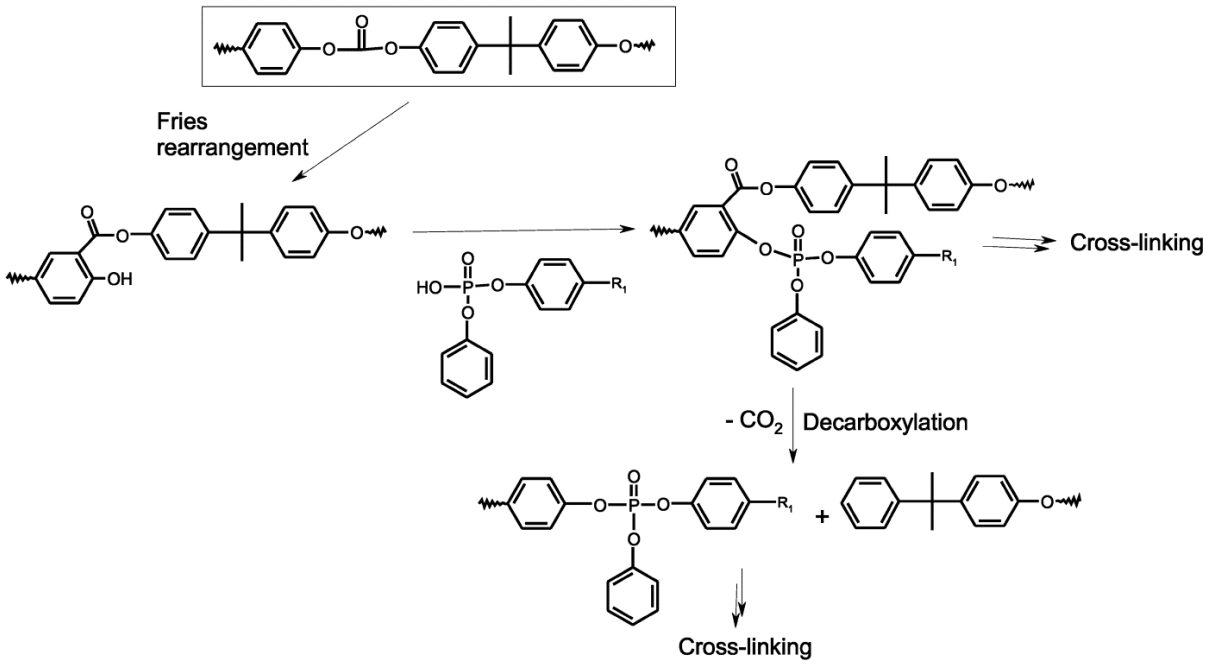

Figure 4.2.7 Fries rearrangements of PC and possible subsequent transesterification with phosphate from the flame retardant

4.2.3 Fire behaviour

PC/ABS_{PTFE} is a quite easily flammable polymer, despites its charring ability. It has a Limiting Oxygen Value (LOI) of 24.2%, and failed the vertical burning test of the UL94 (V) because of an afterflame time longer than 30 seconds, but passed the horizontal burning (HB) classification of the UL94 (*Table 4.2.2*). The blend did not drip due to the presence of 0.45 wt.% of the antidripping agent PTFE, that induced a flow limit in the melt [103]. PTFE acts by a physical mode of action. It is believed that PTFE forms fibrils during the processing of the blends. The particles soften and are elongated due to the shear stress of the extrusion. These fibrils retract and a network that prevents dripping is formed when the polymer burns [90]. The addition of aryl phosphates increased the LOI to a value above 29% and improved the UL94 to the best classification V-0. Two effects occurred: the polymer melt withdraw from the flame thanks to the presence of the PTFE, and the flame self-extinguished within few seconds after removing the burner thanks to the gas phase action of the flame retardants, combined with improved charring ability. In the LOI test, the formation of char is even more pronounced, and is one of the parameters limiting the spread of the flame along the material.

Table 2.2.2 Flammability (reaction to a small flame) and ignitibility results for all the investigated blends; t_{ig} stands for time to ignition in cone calorimeter experiments

PC/ABS_{PTFE}+	/	+ BDP	+ BBDP	+ HDP
LOI (%)	24.2	29.5	29.3	29.2
UL 94	HB	V-0	V-0	V-0
t_{ig} in s at 35 kW m^{-2}	122 ± 29	83 ± 1	93 ± 2	89 ± 3
t_{ig} in s at 50 kW m^{-2}	60 ± 5	38 ± 1	46 ± 6	43 ± 2
t_{ig} in s at 70 kW m^{-2}	25 ± 1	23 ± 2	25 ± 1	24 ± 2

The LOI and UL 94 classification achieved are similar for all blends containing BDP, BBDP or HDP. Analogous to the literature [121], a main flame retardant action in the gas phase is proposed, for which the structure of the flame retardant plays a minor role. The time to ignition in the cone calorimeter at 35 and 50 kW m^{-2} is reduced in the presence of the flame retardants in the blends, supporting the earlier start of decomposition observed in thermal analysis. The time to ignition for all PC/ABS_{PTFE} blends are similar at 70 kW m^{-2} due to fast pyrolysis reactions, and the small differences between the blends are within the error range.

In the cone calorimeter, the combustion of the blends was investigated under forced flaming conditions in well-ventilated atmosphere. Different effects can be observed in this bench scale test, like gas poisoning by the flame retardants because the pyrolysis products are not completely oxidized in the flame. In *Figure 4.2.8* the heat release rate (HRR) and the total heat release (THR) curves are displayed at 70 kW m^{-2}. The complete data from cone are given in *Table A.4.1* in the appendix. The HRR curves are typical for char forming polymers [109], with a main high peak followed by a reduction of the HRR resulting from the formation of char, mostly from PC. PC/ABS_{PTFE} burned with a relative low peak heat release thanks to its naturally char forming properties, when compared to other commodity polymers like PE or PP (PHRR are typically above 1000 kWm^{-2}) [122, 123]. The char formed acts as a protective barrier against heat transport from the flame to the material, and against fuel transport from the pyrolysis zone of the polymer into the flame.

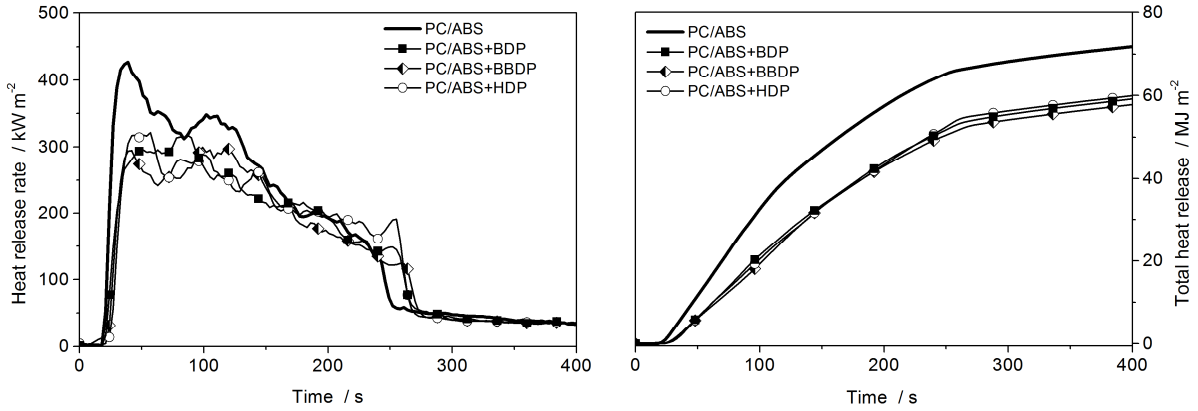

Figure 4.2.8 Heat release rate curves (HRR) and total heat release rate (THR) of the PC/ABS_{PTFE}, PC/ABS_{PTFE}+BDP, PC/ABS_{PTFE}+BBDP, PC/ABS_{PTFE}+HDP in the cone calorimeter at 70 kW m^{-2}

The addition of the aryl phosphates flame retardants BDP, HDP or BBDP induced lower heat release rates during the whole burning time and a lower THR than PC/ABS_{PTFE}. All the flame retarded PC/ABS_{PTFE} blends deformed strongly, and high "towers" of chars are formed during the burning (see *Figure 4.2.9*). The deformations started before ignition from the edges or the corners of the plates, when the polymer was softening, followed by the start of the pyrolysis with the emission of the pyrolysis gases and the formation of small bubbles on the surface. This indicated the start of the pyrolysis, where the sample decomposed and first decomposition products were released in the gas phase. After the sample ignited, the flame covered the whole surface and a char layer formed and increased. When the amount of pyrolysis products diminished, the intensity of the flame reduced until extinction and thermo-oxidation of the char occurred. Since the height of the char varied during a measurement, that means the distance to the cone heater, sometimes until inside the cone heater spiral, the HRR curves were not smooth and the reproducibility was lower. This is due to various factors, but the most influent were the rate and position of char formation, and the shrinking of the polymer melt due to the contraction of the PTFE fibrils (mostly along the axis of the injection moulding).

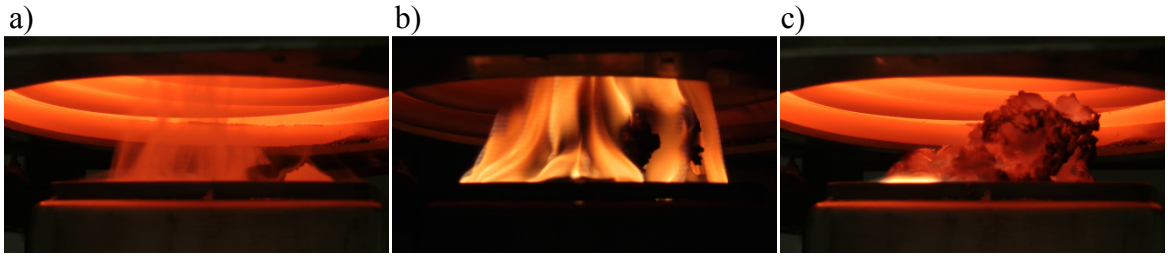

Figure 4.2.9 Fire behaviour of PC/ABS$_{PTFE}$ + HDP under forced flaming combustion in the cone calorimeter: a) before ignition, with the release of pyrolysis products and the shrinkage of the polymer b) during combustion with flame covering the whole sample and formation of a char "tower" c) char residue after extinction

In *Figure 4.2.10* the influence of the external heat fluxes on the fire retardancy mechanisms are investigated. The fire load is represented by the total heat evolved (THE), which is the THR taken at flame out. The fire load is decreased by the presence of the aryl phosphates. The THE of the blends containing BDP, BBDP or HDP is reduced of 10 to 17% in the presence of the flame retardants, and the reduction is quite similar for the three external heat fluxes applied.

The reduction in the fire load correlates well with the reduction of THE/ML (THE divided by the mass loss), which is the combustion efficiency multiplied by the effective heat of combustion of the pyrolysis products. The THE/ML reduction for the flame retarded blends ranged from 9 to 16% at 35 kW m^{-2} until 15 to 22% at 70kWm^{-2}, indicating a significant flame inhibition as the main flame retardancy mechanism which becomes even more predominant with increasing external heat flux.

The reduction in the peak heat release rate (PHRR) is for PC/ABS$_{PTFE}$+BDP, +BBDP and +HDP from around 10-15% at 35kWm^{-2}; 20-23% at 50kW m^{-2} to 28-30% at 70 kW m^{-2} compared to non-flame retarded PC/ABS$_{PTFE}$. The PHRR determines fire propagation. It represents the maximum rate of heat released by the flaming combustion of the material. The addition of the aryl phosphates reduced this fire hazard. The flame poisoning mode of action of the aryl phosphate is partly a reason for the decrease of the PHRR, the rest is explained by the protective barrier formed by the char. The condensed phase action by the formation of residue is the second minor action. The amounts of residue for the flame retarded blends are lower than those for PC/ABS$_{PTFE}$, due to the lower amount of PC in the initial sample. If the ratio of residue per initial mass of PC is calculated, BDP and BBDP show a slight condensed

phase action with higher residue than PC/ABS$_{PTFE}$ (+4wt%), even though the differences are, strictly speaking, within the margin of error for all heat fluxes. Moreover the residues decrease with increasing heat flux, correlating with the higher release of phosphorus in the gas phase, and a decreased cross-linking action in the condensed phase.

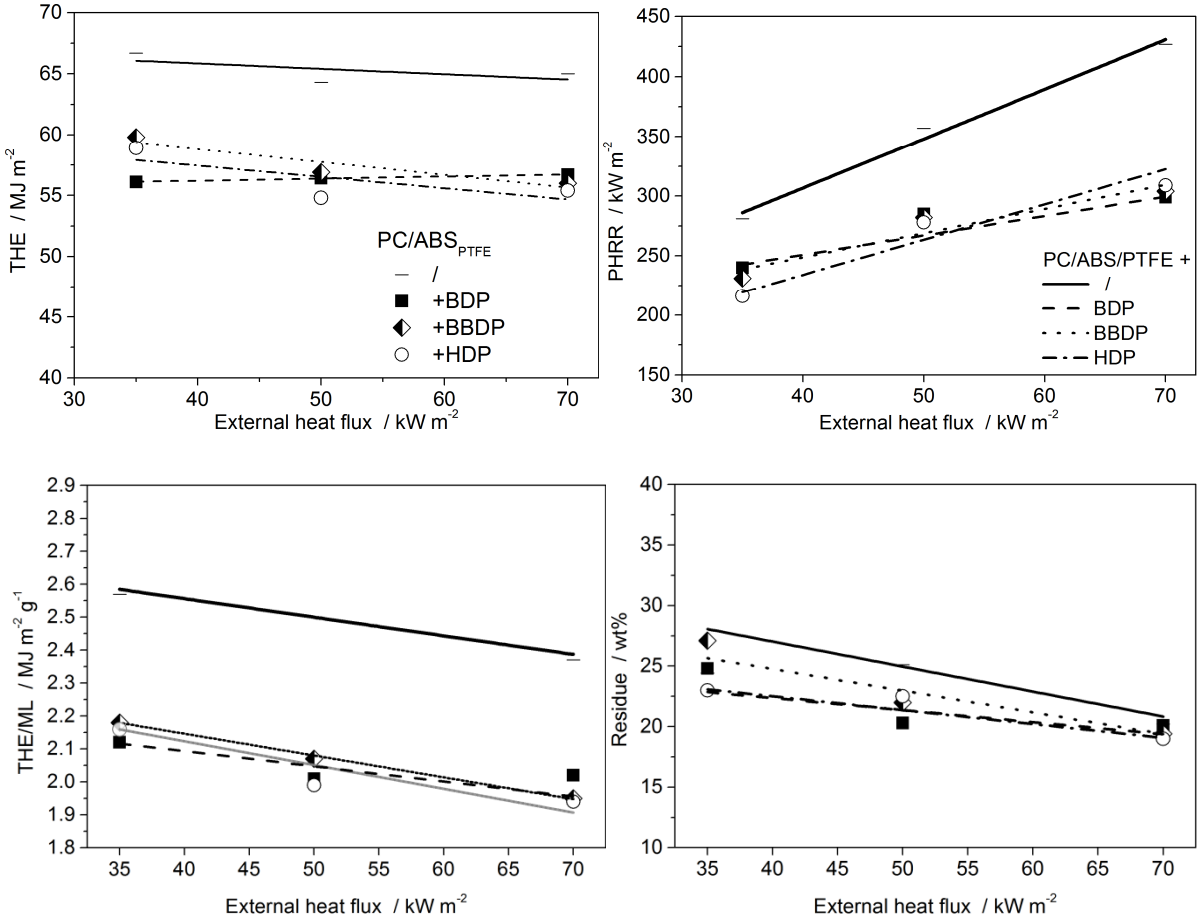

Figure 4.2.10 Total heat evolved (THE), peak heat release rate (PHRR), effective heat of combustion (THE/ML) and residue in the cone calorimeter test at different external heat fluxes for PC/ABS$_{PTFE}$, PC/ABS$_{PTFE}$+BDP, PC/ABS$_{PTFE}$+BBDP and PC/ABS$_{PTFE}$+HDP at different external heat fluxes (35, 50 and 70 kW m^{-2})

The three aryl phosphates BDP, BBDP and HDP have really similar modes of action in PC/ABS$_{PTFE}$, as already concluded from the TG results. The influence of the core structures of the flame retardants plays a minor role, since this part has little influence on the reactivity of the phosphate groups, which is mostly involved in the flame retardancy reactions. The only light differences is related to the higher volatility of HDP compared to BDP or BBDP,

inducing a slightly better performance of HDP in the gas phase than BDP and BBDP, and a reduced condensed phase action. BDP shows higher residue forming ability.

4.3 Aryl phosphate flame retardants with different side chain unit structures

4.3.1 Pyrolysis

The 4,4'-biphenyl bridging unit is the same for both flame retardants, BBDP and BBXP, and only the two freestanding aromatic substituents vary from diphenyl for BBDP to 2,6-dimethyl phenyl for BBXP. BBXP decomposes under nitrogen in a single step, and the pyrolysis is given in *Figure 4.3.1*. BBXP starts to decompose at a higher temperature (T2%) 8K higher than BBDP. The maximum mass loss temperature T_{Max} is 6 K higher than BBDP (754 K). BBXP forms three times more residue than BBDP, with ca.19 wt.% instead of 6 wt.% for BBDP.

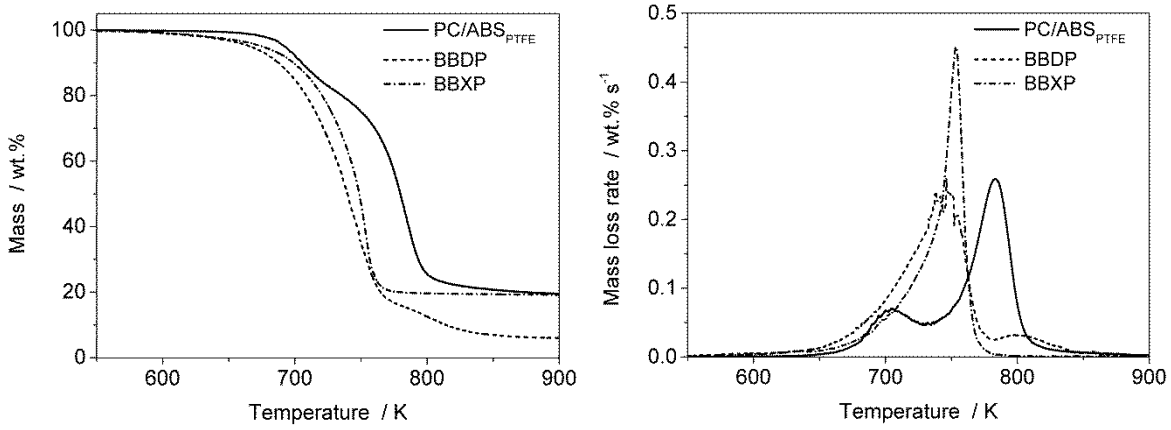

Figure 4.3.1 TG and DTG of the single flame retardant: BBDP, BBXP and PC/ABS$_{PTFE}$

When BBXP is added in PC/ABS$_{PTFE}$, the decomposition of PC/ABS$_{PTFE}$+BBXP differs from the one observed for PC/ABS$_{PTFE}$+BBDP (*Figure 4.3.2*). PC/ABS$_{PTFE}$+BBXP started to decompose at the same temperature as the blend with BBDP. But a third decomposition process appeared at 728 K, between the mass losses of ABS and PC. This third mass loss occurs in the same temperature range than the decomposition of BBXP alone. In *Table 4.3.1*,

the mass loss for each step of PC/ABS_{PTFE}+BBXP decomposition corresponds with the amount of the three main components: ABS, BBXP and PC.

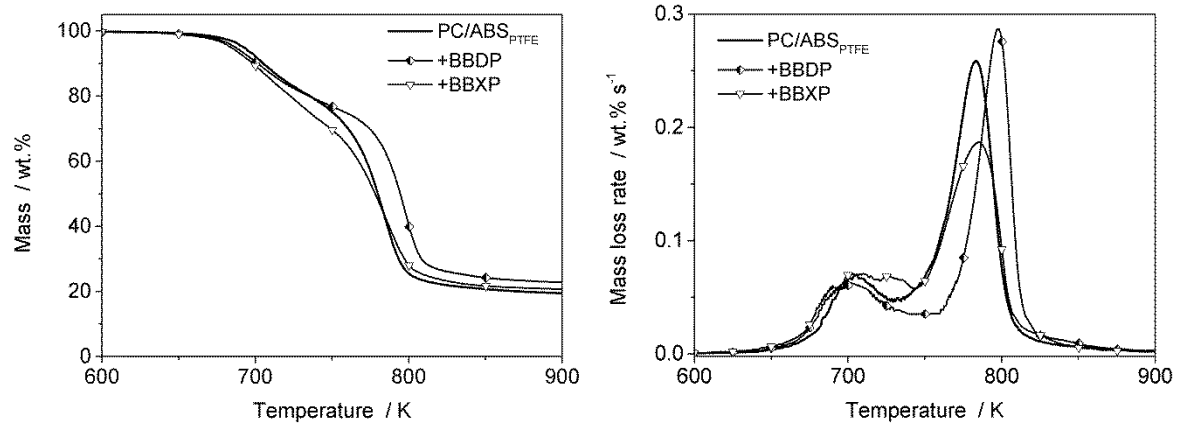

Figure 4.3.2 TG and DTG of PC/ABS_{PTFE}, PC/ABS_{PTFE} + BBDP and PC/ABS_{PTFE} +BBXP (10K min^{-1}, under nitrogen)

Moreover, the temperature shift observed for the decomposition of PC in the presence of BBDP (+15 K) only slightly occurs in the presence of BBXP (+5 K). With BBXP, the mass loss rate is lower and the peak is broader than in the presence of the unsubstituted phenyl-ended flame retardants like BBDP, HDP or BDP. A lower interaction between the BBXP and the decomposition products of PC is thus suggested.

Table 4.3.1 Thermogravimetric analysis of PC/ABS_{PTFE}, PC/ABS_{PTFE}+BBDP and PC/ABS_{PTFE}+BBXP (anaerobic pyrolysis, 10 K min^{-1})

PC/ABS_{PTFE} +	$T_{2wt\%}$	Mass loss I		Mass loss II		Mass loss III (PC)		Residue wt.%
	K	$T_{Max\ 1}$ K	ML1 wt.%	$T_{Max\ 2}$ K	ML2 wt.%	$T_{Max\ 3}$ K	ML3 wt.%	
/	670	702	20.1	-	-	782	57.3	22.6
+BBDP	669	700	24.7	-	-	797	49.1	26.3
+ BBXP	666	706	18.6	728	9.3	787	48.6	23.6

The TG-FTIR gas phase spectra at the three decomposition steps of PC/ABS_{PTFE}+BBXP are given in *Figure 4.3.3*. The first decomposition step, Step 1, shows similar decomposition products as for the decomposition of ABS, in styrenic (3077, 1628, 1600, 910, 773, 694 cm^{-1}) and butadienic (2935 cm^{-1}) derivatives. Additionally, bands at 964, 1192, 1164 (P-O-C_{Ar}) and 1298 cm^{-1} (P=O), already during the first decomposition step, indicate the start of decomposition of BBXP into aromatic phosphate esters. Moreover CO_2 is released during the first decomposition step, indicating the reaction of the carbonate group of PC.

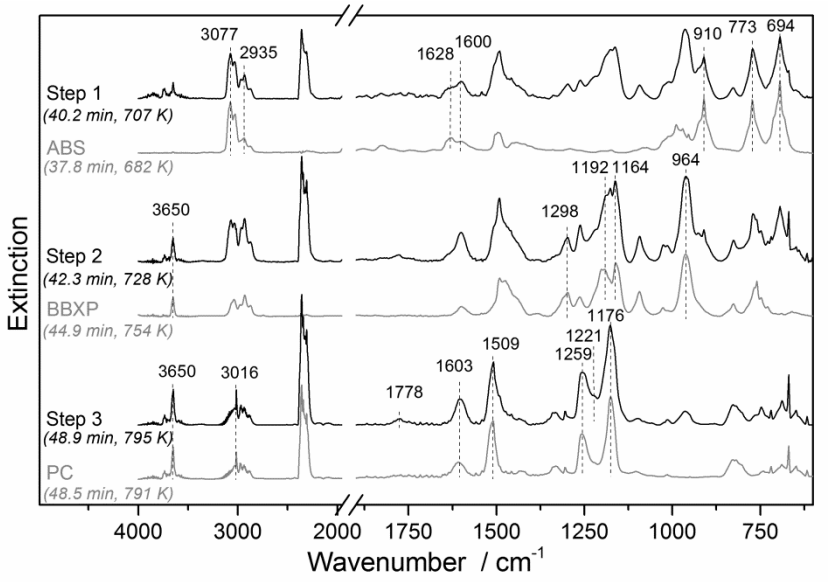

Figure 4.3.3 TG-FTIR gas spectra of PC/ABS_{PTFE}+BBXP at the maximum mass loss for the three decomposition steps 1, 2 and 3, and comparison with the gas phase spectra from main decomposition step of ABS, BBXP and PC.

The FTIR spectrum of Step 2 is characterized by the decomposition products of the BBXP part. This additional mass loss was not observed in the case of PC/ABS_{PTFE}+BBDP. BBXP decomposes mainly into aromatic phosphate esters (964, 1192, 1164 and 1298 cm^{-1}). The release of 2,6-dimethyl phenol (3650 cm^{-1}), indicates that BBXP also decomposes via hydrolysis/alcoholysis, as observed for BBXP main decomposition step. The decomposition overlapped with the end of the decomposition of the ABS part of the PC/ABS_{PTFE}+BBXP blend.

The characteristic decomposition products of PC are observed during the third mass loss step, like CO_2 (2360, 669 cm^{-1}), methane (3016 cm^{-1}) and phenol derivatives (3650, 1603,

1509, 1259, 1176 cm^{-1}). Some phosphate esters also evolved, as seen by the vibration band at 964 cm^{-1}. Small amount of aryl carbonates (1778, 1221 cm^{-1}) and aryl ethers (1233 cm^{-1}) also evolved during the third mass loss. However, the amount of ethers and carbonate derivatives is much lower than in the case of PC/ABS_{PTFE}+BBDP. The amount in CO_2 and methane is also reduced to values closer to that of PC/ABS_{PTFE}, as seen by the product release rates in *Figure 4.3.4*.

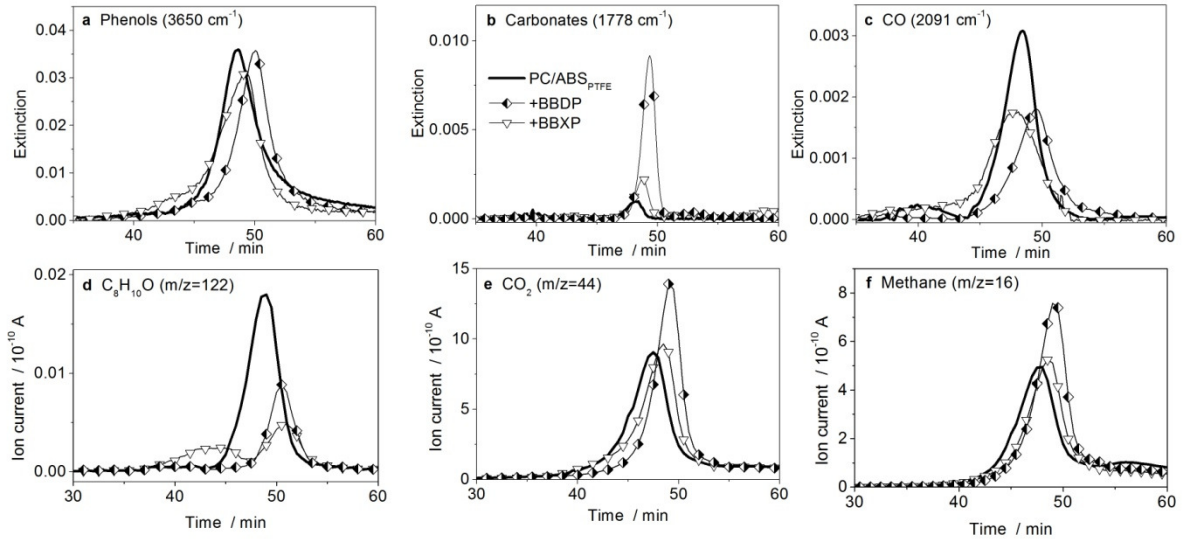

Figure 4.3.4 Products decomposition rates during pyrolysis of PC/ABS_{PTFE}, PC/ABS_{PTFE}+BBDP and PC/ABS_{PTFE}+BBXP, measured in TG-FTIR or TG-MS (under nitrogen, 10 K min^{-1}).

In *Figure 4.3.4.d* the evolution of $C_8H_{10}O$ shows two maxima in the case of PC/ABS_{PTFE}+BBXP, whereas only one maximum was observed for PC/ABS_{PTFE} and PC/ABS_{PTFE}+BBDP. The first maximum occurs at 43 min, which corresponds to the additional mass loss of PC/ABS_{PTFE}+BBXP, and the second maximum corresponds to the decomposition of PC. For all, the second maximum is attributed to the release of ethylphenol, from the decomposition of PC, whereas the first relates the release of 2,6-dimethylphenol from the decomposition of BBXP.

In *Figure 4.3.5* are reported the condensed phases spectra of PC/ABS_{PTFE}+BBXP during the pyrolysis. At 300 K, most of the vibrations of BBXP are overlapped by the one of the matrix. But the P-O-C_{Ar} symmetric stretching band of BBXP is unambiguously present at 957 cm^{-1}. The CH_3 stretch of BBXP is visible only at 1470 cm^{-1}, and the C-H ring deformation

band of the flame retardant is at 1092 cm^{-1}, the tri-substitution of the 2,6-dimethylphenyl group is characterized by the band at 732 cm^{-1}.

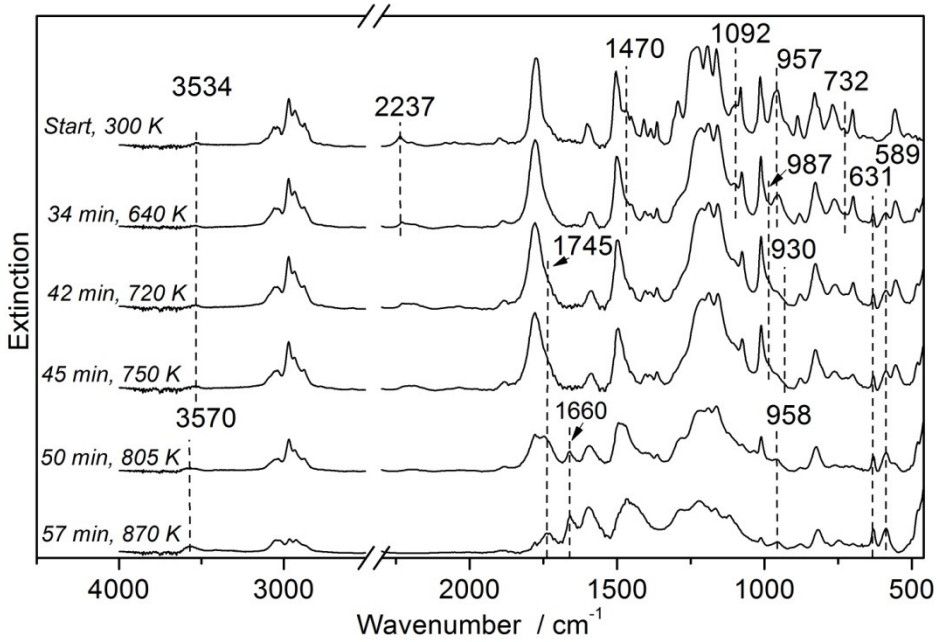

Figure 4.3.5 FTIR spectra of the condensed phase of PC/ABS$_{PTFE}$+BBXP at different decomposition stages (linkam, heating rate 10K/min, under nitrogen) (a) Start 300K; (b) Beginning of step 1 (34 min), (c) End of step 1 at ca. 720 K; (d) End of Step 2 at ca. 750 K, (e) Max of Step 3 at ca. 800 K and (f) End of step 3 at ca. 870 K.

Already at the beginning of the decomposition, at around 34 min, BBXP rearranged and provide new aromatic vibration, as it is observed also in the case of the condensed phase of BBXP alone. New band at 631 and 589 cm^{-1} are arising from BBXP decomposition and rearrangement, and partly also from PC. They are attributed to C_{Ar}-OH deformation and C_{Ar}-H deformation of polysubstituted aromatics, respectively, occurring through the residue forming of BBXP. In the course of the decomposition, these two bands increased. OH groups are present already at the beginning of the decomposition (3534 cm^{-1}), and their amount increased during the main decomposition of PC, due to phenol end groups, but also some other hydroxyl groups from PC hydrolysis. The phosphorus band of BBXP already broadened and reduced, indicating change in the environment of the phosphorus atom.

A new band appeared as a shoulder at 987 cm^{-1} already at 640 K, the beginning of step 1, and was attributed to P-O-P polyphosphate groups or $(C_{Ar}O)$-$(O{=})P$-$(OH)_2$ groups. At ca. 720

K, the P-O-C_{Ar} band of BBXP continued to broaden and to reduce, and the appearance of a new shoulder at 930 cm^{-1} indicates the formation of new P-OH bands. As the decomposition goes further, the P-O-C_{Ar} is completely decomposed and only (RO)(O=)P-OH from poly or pyrophosphates are present in the residue (958 cm^{-1}). The result from the condensed phase analysis indicates that other competing pathways occur during the decomposition of BBXP, such as rearrangements.

4.3.2 Flame retardancy mechanisms

The 2,6-dimethyl substitution on the phenyl group changed the reactivity of the aryl phosphate. In one way, the rate of hydrolysis of the phosphate may be reduced by the substitution. It has been shown in the literature that the kinetic parameters for the hydrolysis of 2,6-dimethyl hindered phosphates (TXP) is more fold lower compared to its unsubstituted equivalent TPP [124]. This approximation is supposed to be valid for BBXP, as the core structure showed to have little influence on the reactivity of the aryl phosphate in the mechanisms of reaction with PC (between BDP, HDP and BBDP).

But BBXP showed some reactions in the condensed phase analyses. At different heating rates (not shown), BBXP showed different amount of residues under nitrogen, with higher residues for higher heating rates. The dependency on the heating rate for the formation of residues indicates that more than two decomposition pathways are occurring, and the pathway leading to the lowest amount of residue is the kinetically slower. It is proposed that this is the hydrolysis of the flame retardant, due to the slow formation of the bipyramidal intermediate which is the kinetically determining step of the hydrolysis reaction (*Figure 4.3.6*).

Char forming reactions are competing pathways. BBXP is able to form char by itself, so reacting with “himself”. The high activation energy for the decomposition of BBXP is a hint that other mechanisms through radical scission or rearrangement may occur. Since the reactions have to be kinetically faster than the hydrolysis, rearrangements reactions, such as intramolecular rearrangements of BBXP are the most probable. It has been suggested that 2-methyl diaryl ethers rearranged almost completely to 2-benzyl phenols above 620 K through intramolecular reactions, and this hypothesis was later extended to poly (2,6-dimethyl-1,4-phenyl ether) resin decomposition [125, 126]

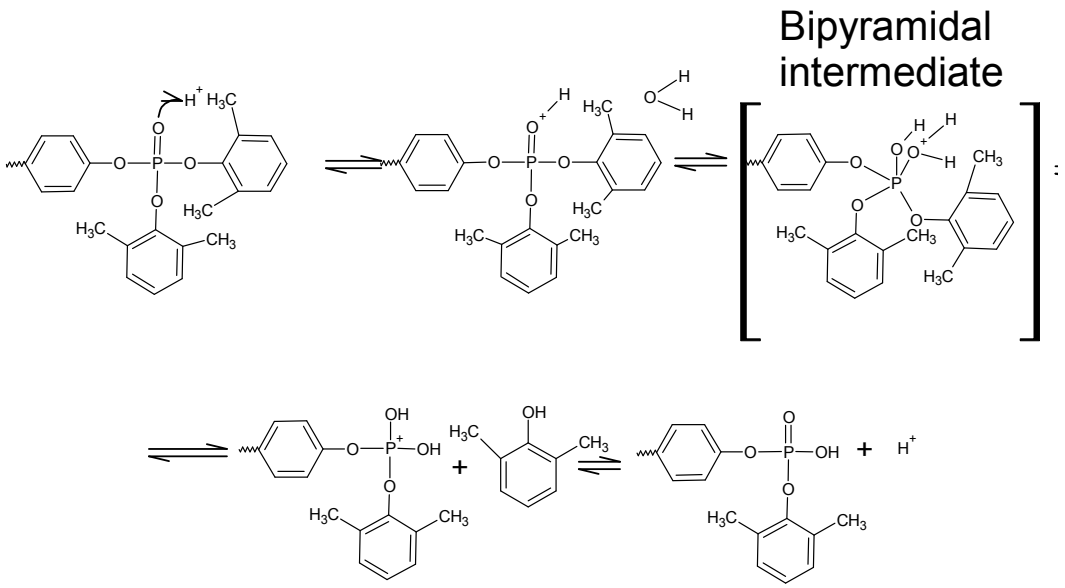

Figure 4.3.6 Scheme of the hydrolysis of BBXP with the slow formation of the bipyramidal intermediate because of steric hindrance

It is here proposed that such a rearrangement may occur in the case of BBXP, explaining the reduction of the CH_3 band in the condensed phase due to rearrangements (*Figure 4. 3.7*). The first proposition resulted in the formation of acid phosphate group and an aliphatic substitution on the aryl group. The second possibility is the formation of a phosphonate group and a phenol groups. Both hydroxyl moieties that are formed could further react by intermolecular reactions forming cross-links.

Moreover some radical reactions due to the CH_3 group on the aryl group may be the reason for the formation of benzyl radical, which further form cross-link and may explain the high formation of the char from BBXP compared to BBDP.

However the products resulting from the rearrangements of BBXP are only intermediate products and they further decomposed during the additional mass loss step between ABS and PC decomposition steps, as see in the TGA part. The instability of the rearrangement products is a further hint that the P-C_{alkyl} or the CH_2-Aryl bonds formed, and then further decomposed at higher temperatures.

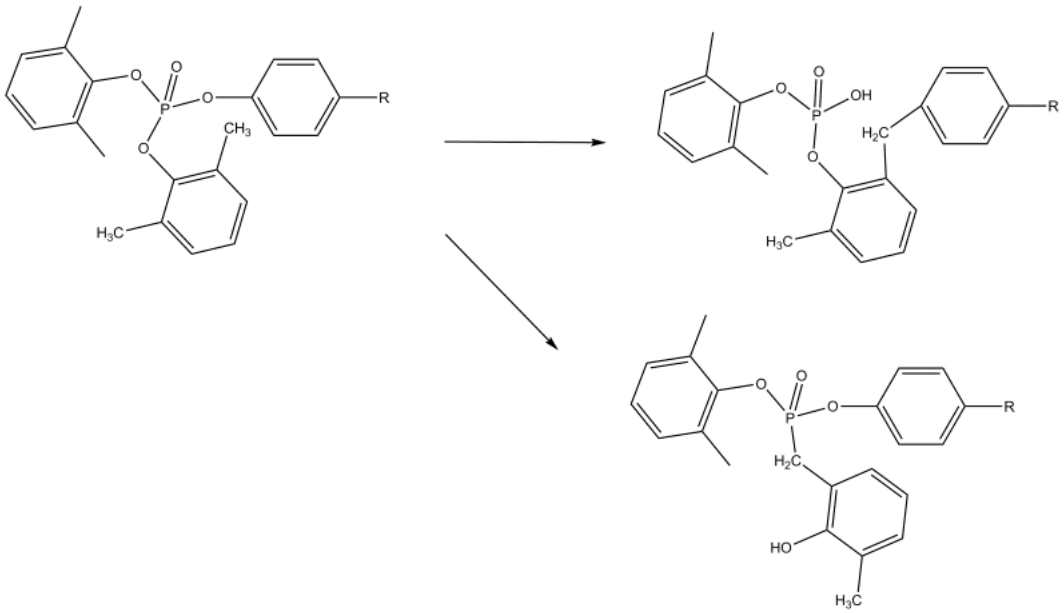

Figure 4.3.7 Possible intramolecular rearrangement reactions of BBXP

Since the aryl phosphates investigated in this study mainly increased the stability of PC due to their hydrolysis properties before the decomposition of PC, and interfering in the hydrolysis/alcoholysis schemes of PC decompositions, and thus cross-linking properties, BBXP decomposition products only from the hydrolysis will be able to stabilise PC. The other pathways will lead to reduced interaction with PC, and thus explain the reduced performances of PC/ABS_{PTFE}+BBXP compared to BBDP.

The reactions of BBXP "with himself" represents competing pathways to the reactions with PC, explaining the reduced interactions with PC leading to higher thermal stability of PC and higher cross linking.

4.3.3 Fire behaviour

In the flammability tests, BBXP added to PC/ABS_{PTFE} showed similar to worsen results in the LOI and UL94 tests than did BBDP (*Table 4.3.2*). The LOI values were similar, and were strongly increased compared to the non-flame retarded blend. In the UL94 test, the blend containing BBXP achieved a V-0 classification at 3.2 mm. The ignition times in the cone calorimeter tests are also very similar or slightly lower than the one of PC/ABS_{PTFE}+BBDP, and are reduced compared to the time of ignition of PC/ABS_{PTFE}. This correlated well with

the results of the TGA, where ABS started to decompose earlier in the case of the flame retarded blends.

Table 4.3.2 Flammability (reaction to a small flame) and ignitibility results for all the investigated blends; t_{ig} stands for time to ignition in cone calorimeter experiments

Material	LOI (%)	UL94 classifi-cation (3.2 mm)	t_{ig} in s		
			at 35 kW m^{-2}	at 50 kW m^{-2}	at 70 kW m^{-2}
PC/ABS_{PTFE}	24.2	HB	122 ± 29	60 ± 5	25 ± 1
PC/ABS_{PTFE} +BBDP	29.3	V-0	93 ± 2	46 ± 6	25 ± 1
PC/ABS_{PTFE} + BBXP	28.9	V-0	90 ± 6	40 ± 2	23 ± 2

The fire behaviour in the cone calorimeter of PC/ABS_{PTFE}, PC/ABS_{PTFE}+BBDP and PC/ABS_{PTFE}+BBXP are represented in *Figure 4.3.8*. The reduced flame retardant activity in the condensed phase and in the gas phase, highlights in the pyrolysis, leads to deteriorated performances in the case of a fire. Even if PC/ABS_{PTFE} +BBXP is forming char, with a typical HRR for char forming polymer, the fire performances in the case of PC/ABS_{PTFE} +BBXP are similar or deteriorated in comparison with PC/ABS_{PTFE}+BBDP. The PHRR is higher than what is observed for BBDP, and the THR is also increased.

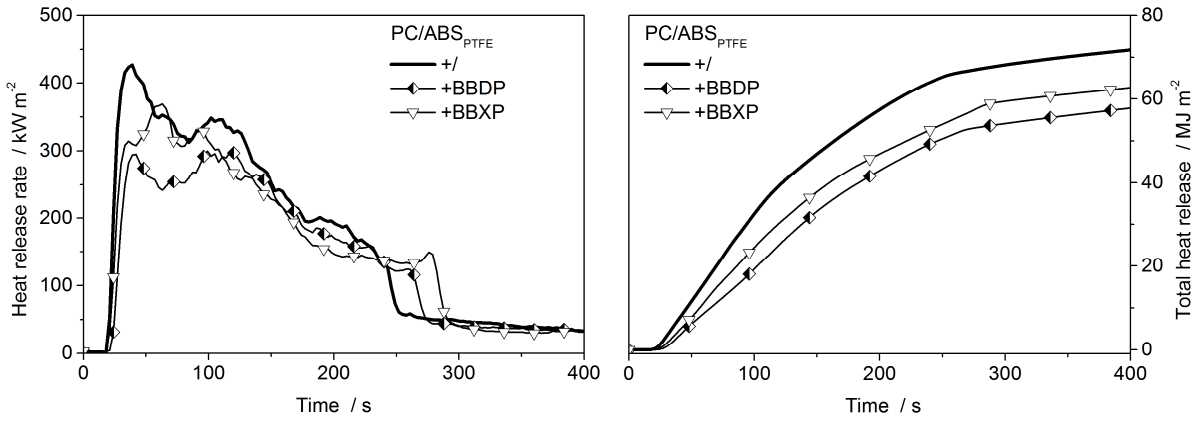

Figure 4.3.8 Heat release rate (HRR) and total heat release rate (THR) of PC/ABS$_{PTFE}$, PC/ABS$_{PTFE}$+BBDP and PC/ABS$_{PTFE}$+BBXP in the cone calorimeter at 70 kW m^{-2}

The complete data from cone are given in *Table A.4.1* in the appendix. In *Figure 4.3.9*, the total heat release over the combustion process (THE) is higher in the case of BBXP. The THE of both the flame retarded systems is diminished compared to the non-flame retarded one, but the reduction is only 7-9% for BBXP additive, at all three of the external heat fluxes, rather than 10-17% for BBDP. The peak of heat release rate for PC/ABS$_{PTFE}$+BBXP is higher than the blend flame retarded with BBDP especially at higher irradiances.

The average effective heat of combustion (THE/ML) is increased compared to BBDP, supporting a reduced flame inhibition action, due to reduced release of phosphorus in the gas phase. The THE/ML is then reduced only by 14%, instead of 17% for PC/ABS$_{PTFE}$+BBDP. Gas phase activity is the main fire retardancy mechanisms for BBXP in the cone calorimeter. The amount of residue is decreased compared to BBDP, due to less interaction in the condensed phase between BBXP and the early decomposition products of PC. Elemental analysis was carried out on cone calorimeter residues at 50 kW m^{-2}, showing that 50% of the initial phosphorus of PC/ABS$_{PTFE}$+BBXP stays in the condensed phase compared to only 30% in the case of PC/ABS$_{PTFE}$+BBDP, suggesting that BBXP reacts with itself, competing with the reaction with PC and the phosphorus release in the gas phase.

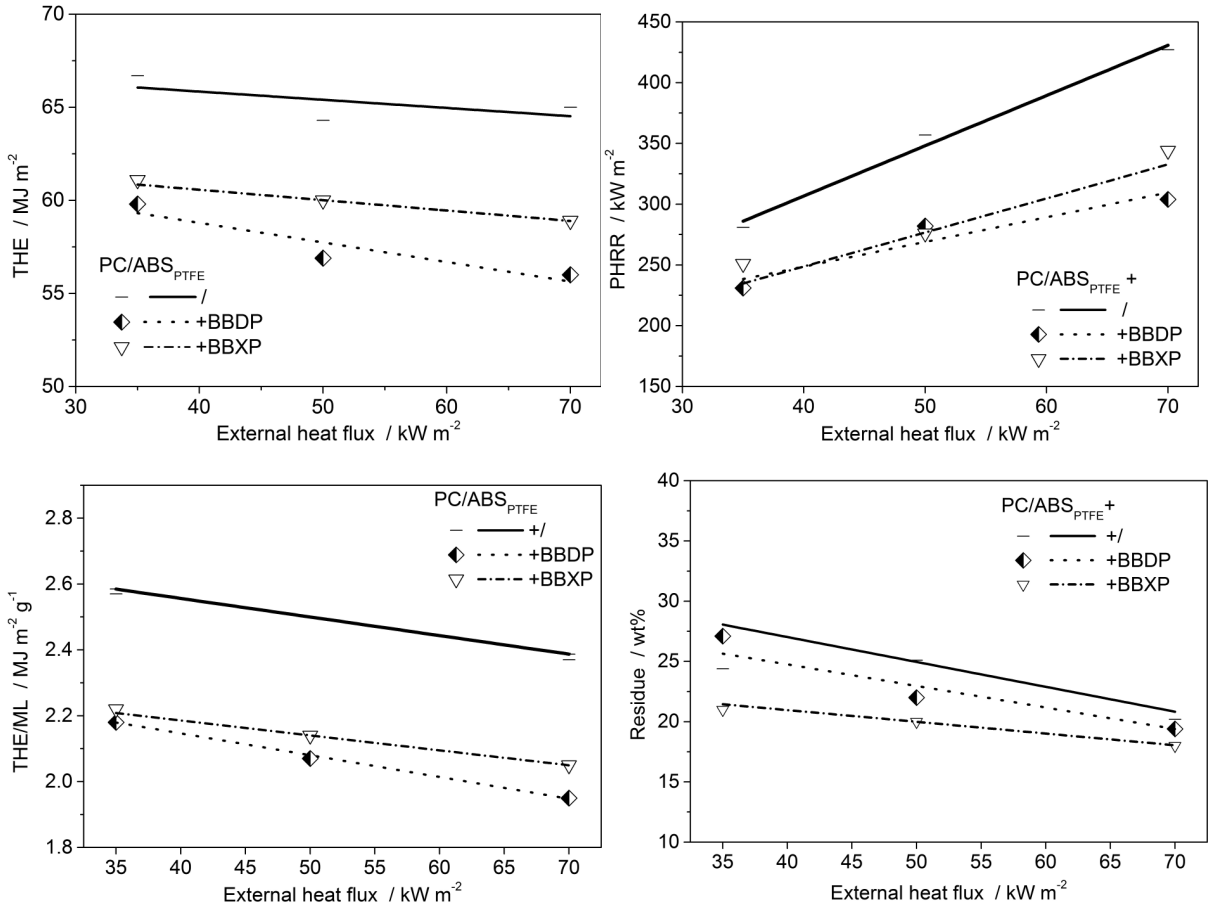

Figure 4.3.9 THE (total heat evolved), peak heat release rate (PHRR), THE/ML (effective heat of combustion) and residue at different external heat fluxes (35, 50 and 70 kW m^{-2}) of PC/ABS$_{PTFE}$, PC/ABS$_{PTFE}$+BBDP and PC/ABS$_{PTFE}$+BBXP in the cone calorimeter

The substitution of the flame retardant with 2,6-dimethyl on the phenyl group modifies the reactivity of the flame retardant, and thus the fire performance. The substitution of the FR highlights an important criterion, additionally to the decomposition temperature range: the reactivity of the flame retardant, to permit the formation of reactive species which will interact with the decomposition products of the polymer matrix.

4.4 Combination of two aryl phosphates as flame retardants for polycarbonate/acrylonitrile-butadiene-styrene

4.4.1 Pyrolysis

A mixture of BDP and HDP was chosen to evaluate the influence of the composition on the flame retardancy mechanisms of PC/ABS_{PTFE}, because BDP showed the highest condensed phase action, and HDP due to its earlier release, the highest gas phase action of the investigated aryl phosphates.

The addition of the BDP/HDP mixture to PC/ABS_{PTFE} at the various BDP:HDP ratio decreases the start of decomposition of the blends see *Figure 4.4.1*.

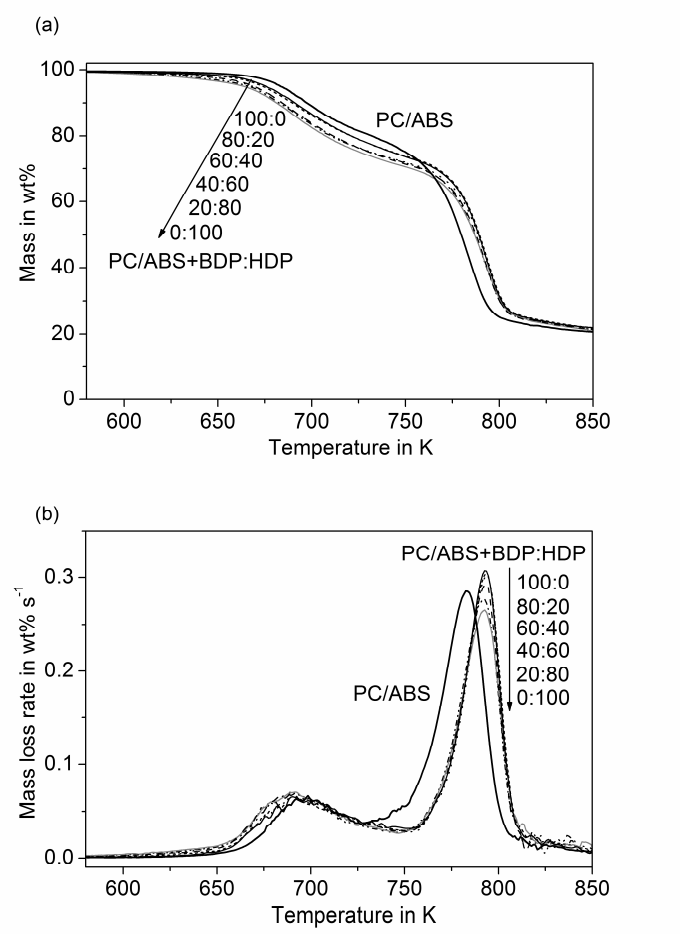

Figure 4.4.1 TG-DTG of PC/ABS_{PTFE}+ BDP:HDP under inert atmosphere (10 K min^{-1}, N_2).

$T_{2\%}$ decreased linearly with increasing amounts of HDP over BDP in the BDP/HDP mixture. The highest decrease (67 K shift) is obtained in the case of BDP/HDP 0:100. The early decomposition of the blends between 601 and 653 K correlated well with the earlier decomposition/volatilisation of HDP compared with BDP.

For the first decomposition step, the temperature of maximum mass loss rate (T_{Max} 1) is shifted to 5-10 K lower for the blends containing the aryl phosphate mixtures BDP/HDP compared to PC/ABS_{PTFE} (*Table 4.4.1*). The first mass loss ML1 for the PC/ABS_{PTFE}+BDP/HDP blends is higher than the initial amount of ABS in the blends. The flame retardants thus partially decompose, dependent on the decomposition temperature. This suggests an early decomposition of PC due to interactions with the flame retardants.

Table 4.4.1 Thermogravimetric results of the PC/ABS_{PTFE}+BDP:HDP blends (N_2, 10 K min^{-1})

PC/ABS_{PTFE} +BDP:HDP	/	100:0	80:20	60:40	40:60	20:80	0:100
T2% in K	668	653	652	646	642	615	601
			Mass Loss I				
ML1 in wt%	18.9	26.5	26.5	27.6	27.3	28.0	28.8
T_{Max} 1 in K	699	691	694	689	692	694	693
			Mass Loss II				
ML2 in wt%	57.2	48.9	48.4	47.7	47.6	47.7	47.7
T_{Max} 2 in K	785	793	793	794	794	793	793
			Residue				
Residue in wt%	24	24.7	25.1	24.8	25.0	24.4	23.6

The mass loss of the first decomposition step (Mass Loss 1) of PC/ABS_{PTFE}+BDP/HDP for the different BDP/HDP mixtures is represented on *Figure 4.4.2a*. Due to the higher volatility of HDP, Mass Loss 1 increased with an increasing amount of HDP over BDP in the blends. The increase in ML1 correlates well with the earlier start of the decomposition $T_{2\%}$.

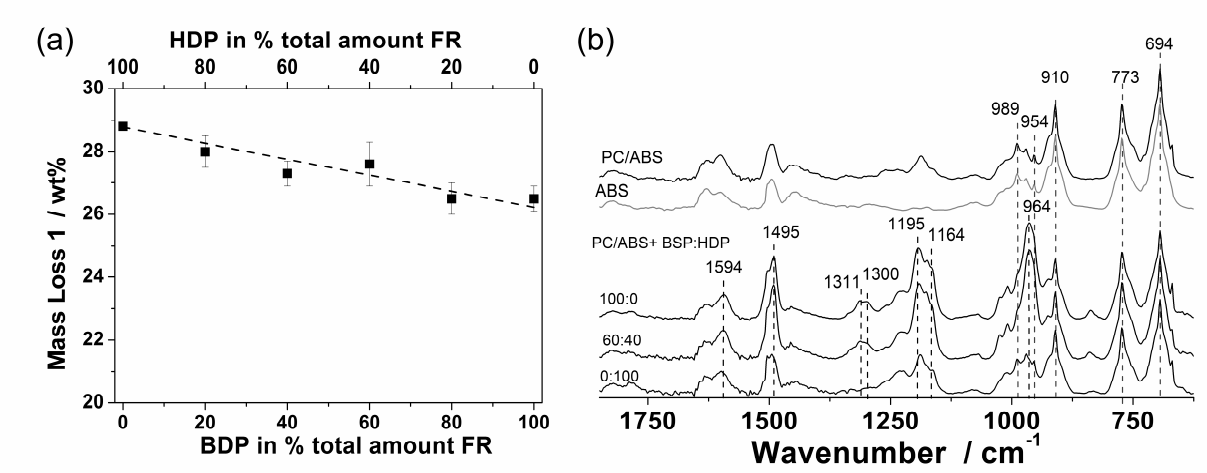

Figure 4.4.2. (a) Mass Loss 1 in dependency of the flame retardant mixtures (the dash is a linear fit) and (b) FTIR spectra of the evolved gases at ML 1 (39 min) for the different PC/ABS$_{PTFE}$+BDP/HDP blends and ABS.

The decomposition products of the blends during ML1 are similar to the evolved gases of PC/ABS$_{PTFE}$ during the first decomposition step and that of ABS *(Figure 4.4.2 b*). The decomposition products of ABS were not changed by the presence of the flame retardant mixtures. An additional release of aromatic phosphate esters in the gas phase occurred for all the BDP/HDP mixtures, as it is already the case for the single flame retardant, HDP or BDP. However the intensities of the P-O-C bands at 964, 1195 and 1164 cm^{-1} were considerably higher in the case of PC/ABS$_{PTFE}$+BDP:HDP 60:40 than for 100:0 or 0:100, even when the decomposition temperature of the blend was lower. Interaction between BDP and HDP are presumed, and could explain that HDP was not completely vaporized, and products of these reactions act longer in the condensed phase. The release of phosphorus species in the gas phase at a later point is then achieved.

The second mass loss step in TGA corresponded to the decomposition of the PC of the PC/ABS$_{PTFE}$ with a maximum mass loss rate temperature T_{Max} 2 of 785 K *(Figure 4.4.3*). The mass loss during the second decomposition step for the blends PC/ABS$_{PTFE}$+BDP/HDP is given in *Figure 4.4.3a* as a function of the BDP/HDP composition. The mass loss during the second decomposition was not constant and did not follow a linear relationship. ML 2 was lower than expected in the case of intermediate mixtures of BDP/HDP 40:60 and 60:40. A stabilising effect of the mixture BDP/HDP on the PC decomposition is presumed.

When BDP or HDP or the BDP/HDP mixture was added to PC/ABS, the decomposition of PC was shifted to decomposition temperatures 8-9 K higher. The flame retardant BDP and HDP stabilises PC, as shown in *Part 4.1*. Within the different BDP/HDP compositions, the increase in temperature was marginal, with an increase of 1 K in the case of the intermediate mixtures 40:60 and 60:40 compared to BDP (100:0) or HDP (0:100) (*Table 4.4.1*)

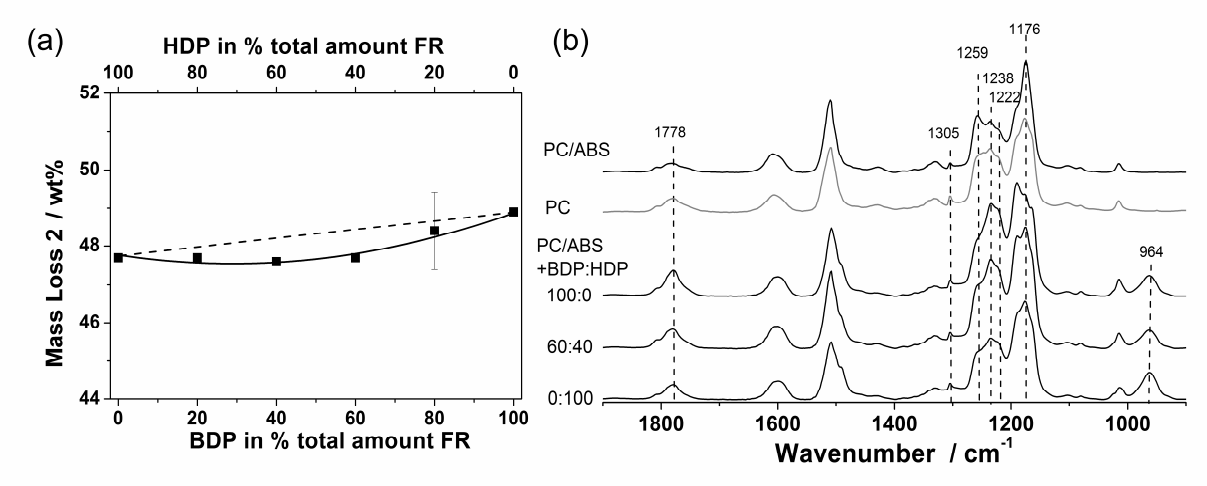

Figure 4.4.3 (a) Mass Loss 2 in dependency of the flame retardant mixtures (the dash is a linear fit) and (b) FTIR spectra of the evolved gases at ML 2 (ca. 50 min) for the different PC/ABS$_{PTFE}$+BDP/HDP blends and PC.

The results from TG-MS (*Figure 4.4.4*) confirmed the results of the TG-FTIR. The mixtures of BDP and HDP induced the shift of the maximum decomposition temperature of ABS, characterized by the release of its major product styrene (m/z=104) at an earlier time. The MID of styrene also confirms that the increase in Mass Loss 1 is due to the additional release of HDP during the first decomposition step, since the quantity of styrene is almost the same for all the blends, flame retarded or non-flame retarded. During the second decomposition step, the MS confirmed the shift to higher temperature of the decomposition of PC, characterized by one of its main decomposition products, CO_2. The little trend of the increase in residue, and especially the increase in the stability of the residue for the intermediate blends, is reflected in the light reduction of the CO_2 and methane emission at the end of the second mass loss step.

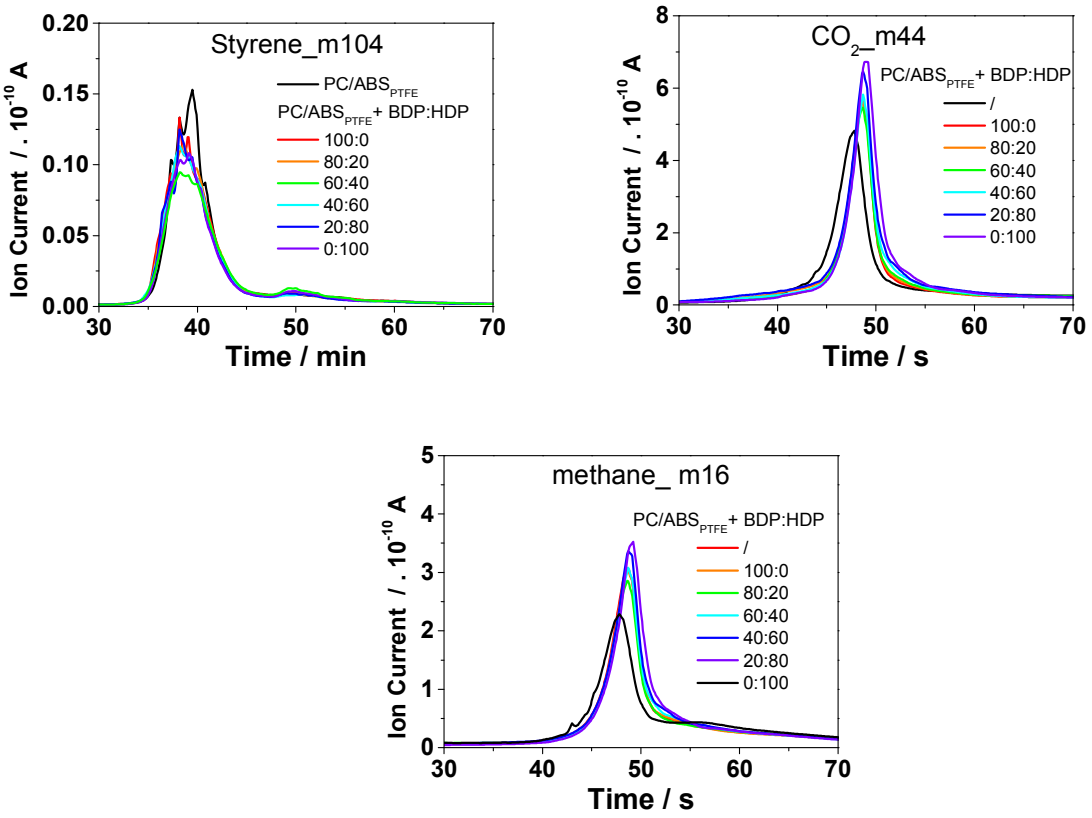

Figure 4.4.4 Products decomposition rates during pyrolysis of PC/ABS$_{PTFE}$, PC/ABS$_{PTFE}$+BDP:HDP blends measured in TG-MS (under nitrogen, 10 K min^{-1}).

The main products evolved during the second decomposition step of the blends were similar as the one of PC. Some oligomeric carbonates were also released during PC decomposition [127, 128] as well as some ethers [56]. The addition of the BDP/HDP mixture induced changes in the composition of the decomposition products of PC as well as the apparition of new species. The release of aromatic carbonates and of aromatic ethers increased (*Figure 4.4.3b*). The presence of the aryl phosphates induced changes and new pathways in the PC decomposition mechanisms. The increase in aromatic carbonates results from complex mechanisms. It is mainly due to a reduction of the hydrolysis/alcoholysis of the carbonate group thanks to the presence of the aryl phosphates, as proposed for BDP and HDP alone in *Chap. 4.1*. The amounts of aromatic carbonates were slightly higher in the case of blends with intermediate BDP/HDP mixtures (60:40) and with a high amount of BDP. This increase supported not only a stronger action by BDP in the condensed phase compared to HDP, as expected by the previous results, but also a possible interaction between HDP and BDP in interacting with PC in the appropriate BDP:HDP ratio.

Under pyrolytic conditions, residues for PC/ABS_{PTFE}+BDP/HDP were between 2 and 4 wt% higher than the amount of residue expected from the superposition of the char yields of each component: PC/ABS_{PTFE}, HDP and BDP. The increase in residue, calculated as the difference between the experimental residue and the calculated residue from the superposition, is plotted as a function of the flame retardant compositions in *Figure 4.4.5*.

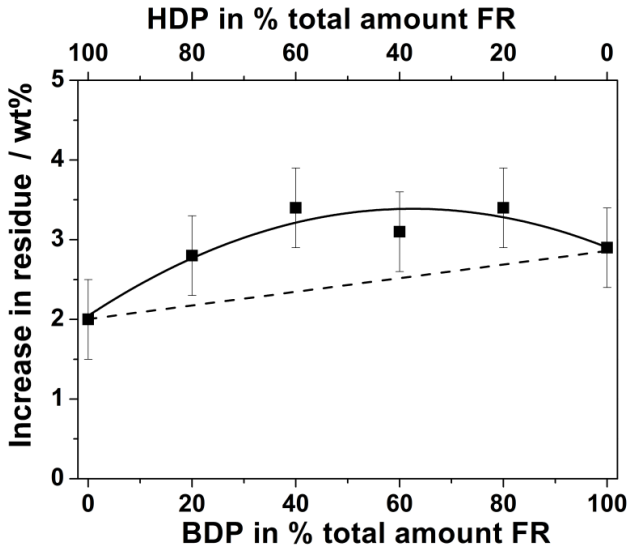

Figure 4.4.5 Interaction BDP-HDP: Binary system BDP+HDP

BDP and HDP work in a synergistic manner when blended in PC/ABS_{PTFE}, in the condensed phase. The combination of BDP and HDP delivered an increase in residue that is larger than the increase in residue expected for a superposition of the effects of each component. To quantify this synergy, the synergistic effect (SE_A) concerning the absolute increase in residue obtained in the TGA has been evaluated for the different blends in *Table 4.4.2*. A clear synergy occurred in this increase in residue for all mixtures of BDP+HDP. The intermediate mixtures with a ratio of BDP/HDP 40:60 showed the highest synergistic effect as large as SEA = 1.44. Or in other words the increase in residue was nearly one and a half than what expected for superposition.

Assuming that the increase in residue does not show an extensive nonlinear behavior against BDP or HDP concentration, the synergistic increase in residue was suggested coming from a reaction or strong interaction between the two flame retardants promoting the charring of PC. An additional cross-linking occurred between the flame retardants and PC, most probably via a transesterification reaction between rearranged PC and BDP and/or HDP.

Table 4.4.2 Quantification of the synergy on the increase in residue (Δ%R) by the synergistic effect SE_A. A clear synergy (SE_A > 1) is visible for intermediary mixtures of flame retardants.

PC/ABS+BDP/HDP	100:0	80:20	60:40	40:60	20:80	0:100
SE_A	1	1.25	1.22	1.44	1.28	1

4.4.2 A route to an aryl phosphate-aryl phosphate synergy?

The possibility of a reaction between BDP and HDP was investigating to explain the aryl phosphate-aryl phosphate synergy in the increase of residue and the reduction of PC mass loss. Binary mixtures of BDP+HDP were analysed thermally under nitrogen in the TGA, see *Figure 4.4.6*.

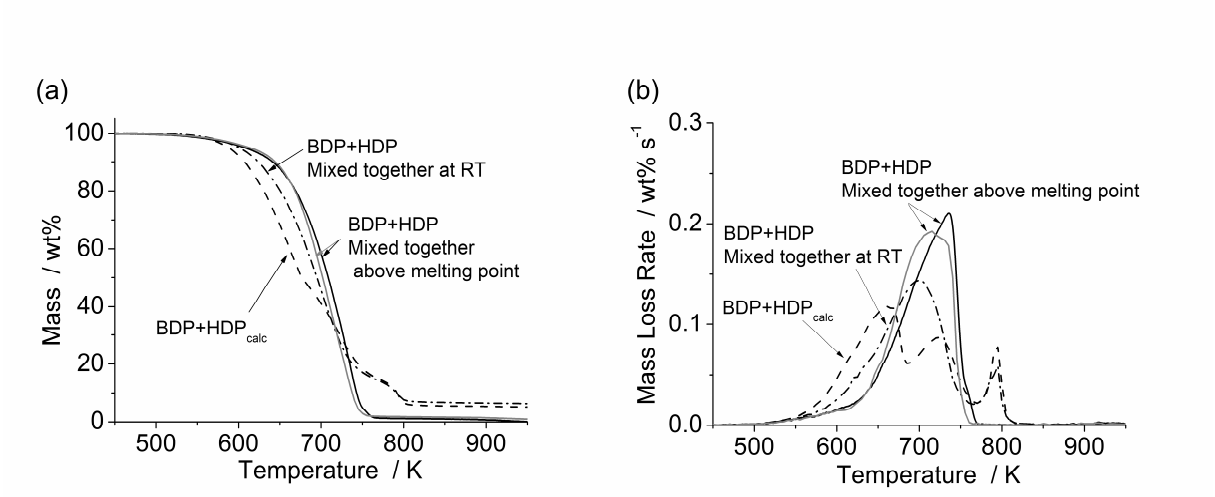

Figure 4.4.6 TGA of BDP+HDP 60:40 binary system. (a) Mass and (b) mass loss rate of BDP+HDP 60:40 mixed at room temperature and mixed at 387 K and calculated BDP+HDP 60:40

BDP and HDP were first mixed together at room temperature before their introduction in the TGA. They demonstrated a higher thermal stability than expected from the calculated BDP+HDP mass evolution. The decomposition occurred in one step instead of the three expected. The interactions between BDP and HDP were even stronger when the binary

system was mixed above the melting point of both BDP and HDP (387 K). The temperature at 10 % of mass loss, $T_{10\%}$, was increased by 36 K, and the maximum decomposition temperature T_{Max} was increased by 55 K compared to the calculation (*Table 4.4.3*).

HDP interacted with BDP to form intermediary compounds instead of an early volatilisation as expected. These intermediary compounds are thermally more stable than HDP. They decompose in the temperature range 550-700 K.

Table 4.4.3 TGA results from BDP+HDP 60:40 binary system and comparison with calculated BDP+HDP 60:40.

	Calculated BDP+HDP	BDP+HDP mixed at room temperature (296 K)	BDP+HDP mixed above melting point (387 K)
$T_{2\%}$ / K	561	570	567
$T_{10\%}$ / K	607	623	643
T_{Max} / K	660	700	715
	725	-	734
Residue / wt%	5.7	5.6	1.7

The fit of the decomposition temperature of PC was shown to be the major criterion for increased char formation from PC by aryl phosphate flame retardants [58]. In the case of the binary mixture BDP+HDP, the shift in the decomposition range of the intermediary products fits the start of the decomposition temperature of PC in the PC/ABS_{PTFE} blend (*Figure 4.4.7*), inducing more reaction with PC. Cross-linking reactions occurred between the phosphorus-containing species and PC decomposition products, in correlation with the increase in TGA residue under nitrogen.

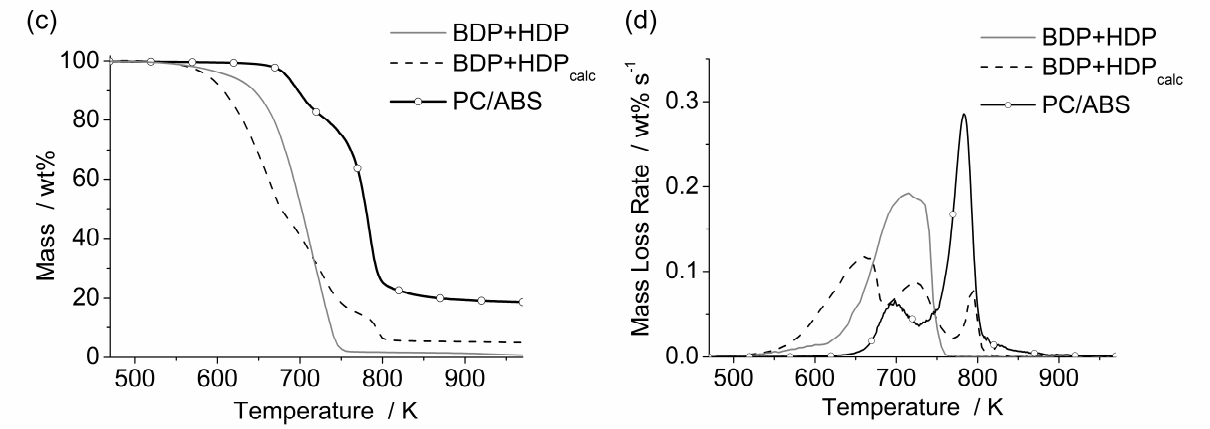

Figure 4.4.7 (a) mass and (b) mass loss rate of PC/ABS$_{PTFE}$, binary system BDP+HDP 60:40 mixed at 387 K, and calculated BDP+HDP 60:40.

Transmission FTIR was used to identify any chemical change during decomposition of the binary mixture BDP+HDP 60:40 in the condensed phase. The spectra at different temperatures are reported in *Figure 4.4.8*. At room temperature (initial stage) the characteristic vibrations of aromatic phosphate esters were visible: the phosphate group (ν P-O-C_{Ar} at 958, 1186 and 1165 cm^{-1} and ν P=O at 1300 cm^{-1}) as well as aromatics groups (ν C=C-H at 3071 cm-1, ν C_{Ar}=C_{Ar} at 1590 and 1489 cm^{-1} and deformation δ C-H for mono-substituted phenyl rings at 753 and 688 cm^{-1} and 1,4-disubstituted phenyl rings at 841 cm^{-1}). The bands of the isopropylidene group –$C(CH_3)_2$ (–CH_3 stretching vibration at 2970 and 2874 cm^{-1} and deformation at 1408, 1387 and 1365 cm^{-1}) are characteristic of BDP.

At 673 K, corresponding to 25 % mass loss in TGA, a strong reduction in the aromatic intensities as well as the reduction of the phosphate ester vibration indicated the release of volatile aryl phosphates or aryl polyphosphates into the gas phase. The intensity of the bands of phosphorous groups is higher than that of the aromatics. An increasing release of phenyl end groups in the gas phase is suggested as well as the formation of higher molecular weight oligomeric phosphates. This is an intermediate step to the formation of phosphates of higher molecular weight.

At the maximum of the decomposition of the BDP+HDP 60:40 mixture (737 K) a shift in the frequency in the phosphate P-O-C vibration appeared, from 958 to 964 cm^{-1}. Changes in the chemical environment of the phosphorus atom and especially hydrolysis were indicated. The changes are further supported by the presence of a new broad band at 896 cm^{-1}

corresponding to P-O-P vibrations. Polyphosphates or poly phosphoric acid species are formed and cross-linking of the phosphorus with some poly aromatic structures occurred.

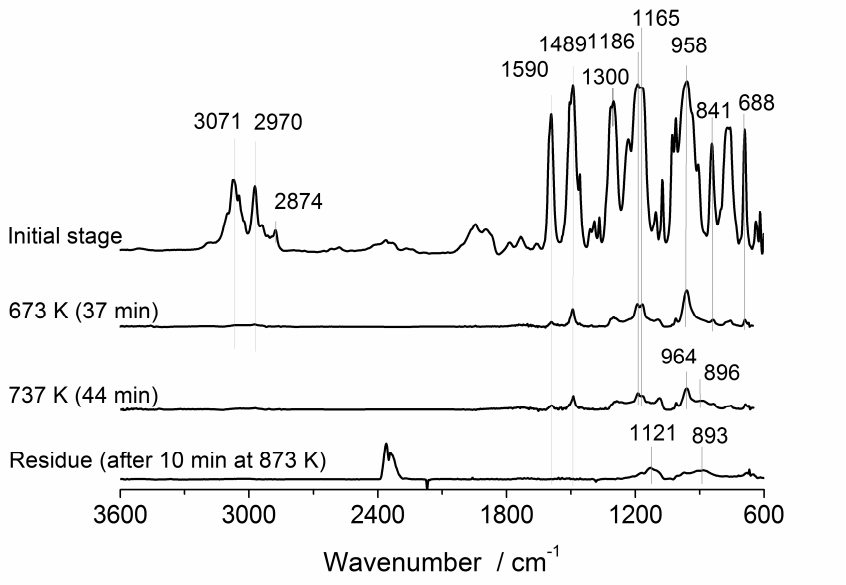

Figure 4.4.8 FTIR Spectra of the condensed phase (Linkam hot stage) of the BDP+HDP 60:40 mixture at different temperatures (heating rate 10 K min-1): initial stage at room temperature, 673 K (25% ML), 737 K (max. of decomposition,80% ML) and after 20 min storage at 873 K (residue).

The residue obtained after storage at 873 K for 20 min showed mainly two broad bands centred at 1121 cm^{-1} and 893 cm^{-1}, corresponding to the cross-linked polyphosphates.

From the investigations of the binary system BDP+HDP, it is suggested that HDP reacts with BDP to form intermediate products less volatile than HDP. From FTIR experiments it is known that these products have structures similar to HDP and BDP, since no P-OH bond or P-O-P bond is visible under 730 K. It is thus proposed that higher-molecular-weight oligomers were formed via transesterification between HDP and BDP. As possible reaction scheme is proposed in *Figure 4.4.9a*. Phosphate esters were then retained in the condensed phase up to the start of the decomposition of PC. These intermediate products were then decomposed/volatilised above 750 K or reacted with PC decomposition or rearrangement products, for example via Fries rearrangement *(Figure 4.4.9b*). The intermediate products promote increased char formation from PC through cross-linking. The change in the decomposition temperature of these intermediate compounds, which corresponds to the early decomposition of PC, is one of the main processes explaining the increase in residue of the blends and thus the aryl phosphate-aryl phosphate synergy.

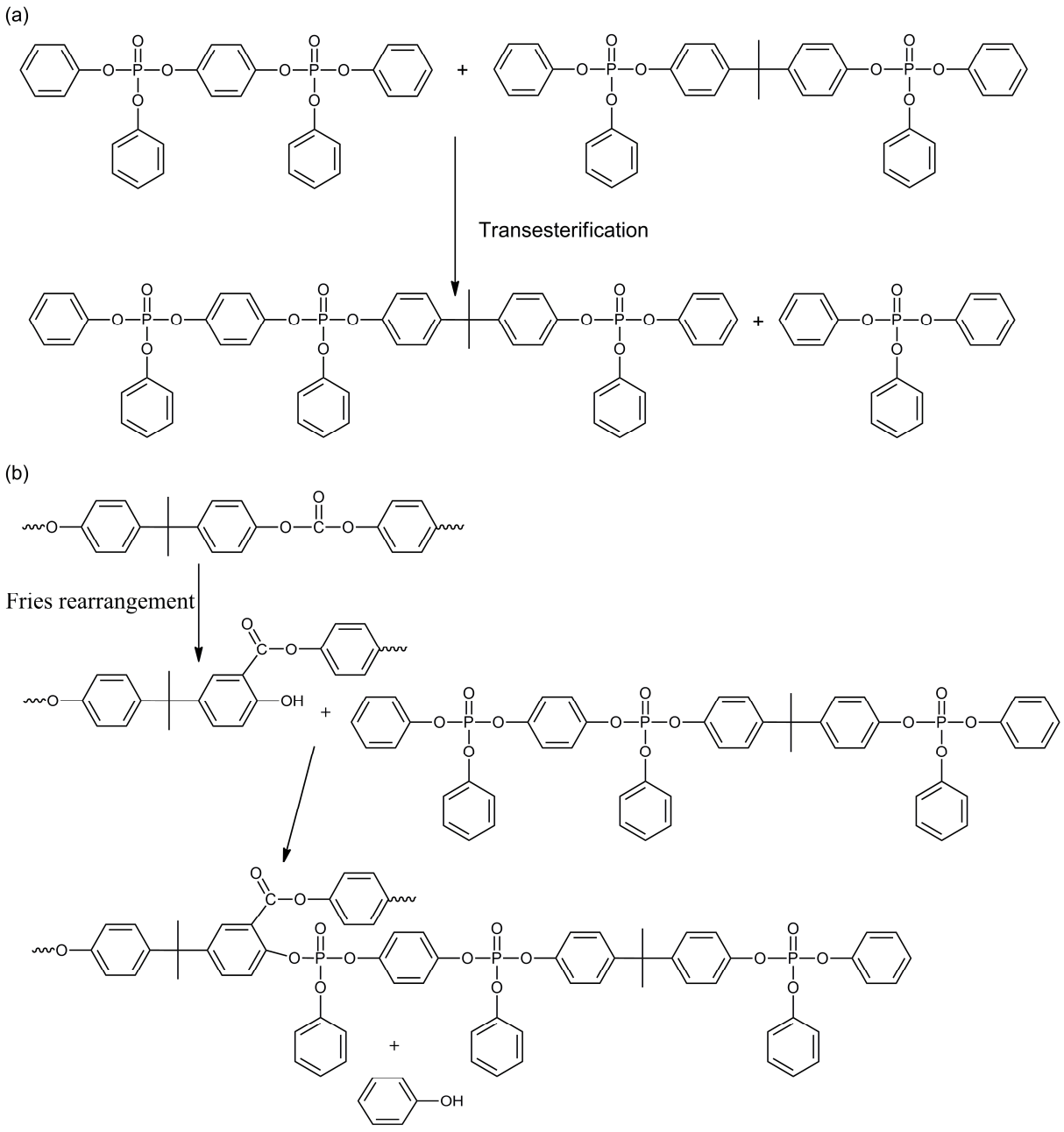

Figure 4.4.9 (a) Proposed reaction pathway of BDP with HDP to form intermediate products via transesterification (b) Cross linking between PC rearrangement products with BDP-HDP intermediate products.

4.4.3 Fire behaviour

The results of flammability (reaction to a small flame) are reported in *Table 4.4.4* for PC/ABS_{PTFE} and PC/ABS_{PTFE}+BDP/HDP blends. The Limiting Oxygen Index (LOI) increased for all the flame-retarded blends compared to PC/ABS, by a 6.1 to 8.2 % O_2

increase, thanks to the char forming action and the gas flame poisoning action of the BDP/HDP mixture, that are consistent with the cone calorimeter results.

Table 4.4.4 Flammability results (reaction to a small flame) of PC/ABS_{PTFE} and PC/ABS_{PTFE}+BDP:HDP blends

PC/ABS_{PTFE}+ BDP:HDP	/	100:0	80:20	60:40	40:60	20:80	0:100
LOI in %	23.3	29.4	30.1	31.5	31.4	31.5	31.1
UL94 3.2 mm	HB	V-0	V-0	V-0	V-0	V-0	V-0
UL94 1.6 mm	HB	V-0	V-0	V-0	V-0	V-0	V-0

A slight synergy was suggested for the intermediate mixtures of BDP/HDP, with an increase from 29 % for PC/ABS_{PTFE}+BDP/HDP 100:0 to 31.5 % for PC/ABS_{PTFE}+BDP/HDP 60:40. Unfortunately, this increase is hardly larger than two times the magnitude of the uncertainty of 1 %. In UL 94 test, all PC/ABS_{PTFE}+BDP/HDP achieved the best classification of the test, V-0 at both the 3.2 and 1.6 mm, as opposed to the horizontal burning (HB) rating for PC/ABS, because of shorter burning time and stronger residue formation from the flame retarded blends, combined with the shrinkage of the blends due to the presence of PTFE.

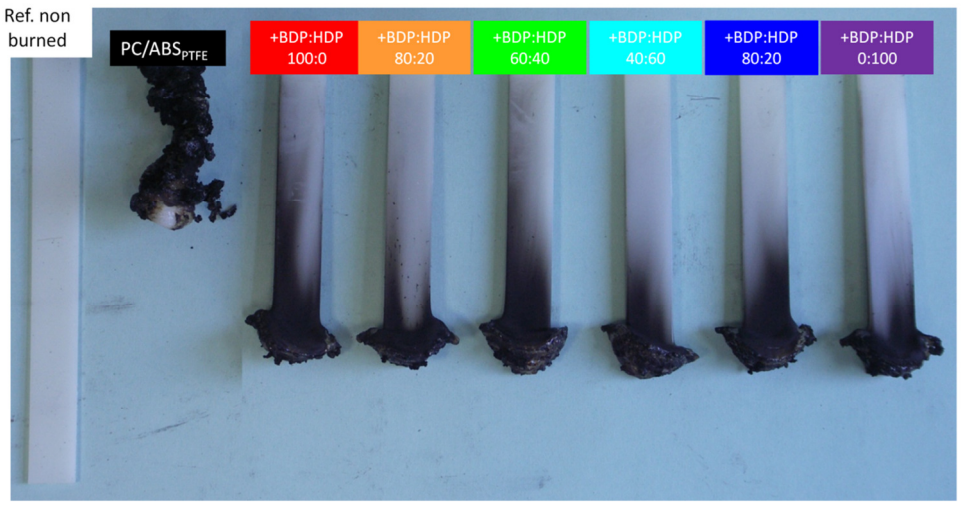

Figure 4.4.10 UL94-V residue for the PC/ABS_{PTFE}+BDP:HDP blends (3.2 mm).

The PC/ABS$_{PTFE}$+BDP:HDP showed in the cone calorimeter a typical burning for char forming polymers with a strong increase in the HRR curve shortly after the ignition, and after residue is formed, the HRR diminished due to an effective barrier formation at the surface of the burning material [109] *(Figure 4.4.11 and Appendix Table A.4.2*). The burning is not uniform because of strong deformation of the samples during combustion with the formation of char to the top, then the falling of the char because of the melted underlying layer, and sometimes the melted layer retract, as observed in the UL94, thanks to the presence of PTFE fibrils. The measurements at 70 kW m^{-2} were more reproducible than 35 kW m^{-2} because of less deformation before ignition.

The time to ignition t_{ig} of the PC/ABS$_{PTFE}$ + BDP:HDP blends were similar or slightly higher than the unprotected material, independent of the external heat fluxes. From the TGA results, the pyrolysis of the blends with higher amount of HDP started to decompose at a lower temperature than PC/ABS$_{PTFE}$. The pyrolysis products at this temperature have thus a low flammability and did not influence the ignition time.

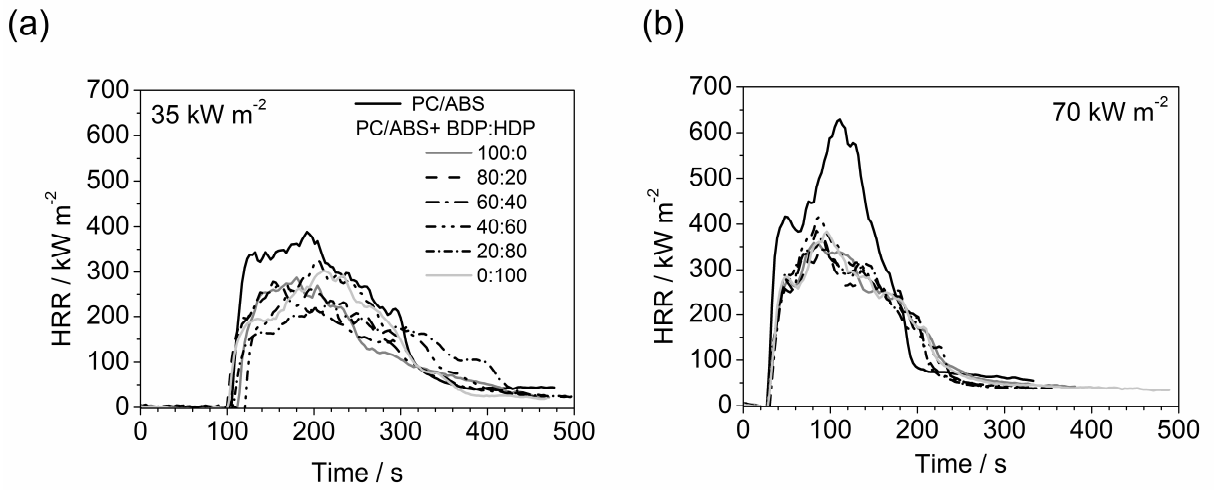

Figure 4.4.11. Heat Release Rate (HRR) curves of the PC/ABS$_{PTFE}$+BDP:HDP blends in the cone calorimeter (a) at an irradiance of 35 kW m^{-2} and (b) at 70 kW m^{-2}.

The peak heat release rate (PHRR) represents the maximum rate of heat released by the flaming combustion of the material. The addition of the flame retardants in PC/ABS$_{PTFE}$ clearly reduced the PHRR compared to PC/ABS$_{PTFE}$, quite independent of the FR composition. The PHRR is reduced by 20-36 % at 35 kW m^{-2}. The reduction is even stronger

at 70 kW m^{-2}, with PHRR values 34 % to 43 % lower than for PC/ABS_{PTFE} (*Figure 4.4.12*). The whole data are given in the *Appendix in Table A.4.2.*

The different composition of the mixture influenced the reduction in PHRR only slightly, at all the external heat fluxes. No significant trend emerged from the PHRR value even when the lowest peaks were obtained from the intermediate BDP/HDP mixtures (40:60 and 60:40). The PHRR was strongly influenced by the height of the char tower that is to say by the distance between the char tower and the cone heater. This distance is dependent on the deformation of each sample. The slight possible differences between the blends are masked by the high uncertainty from sample to sample of the same material.

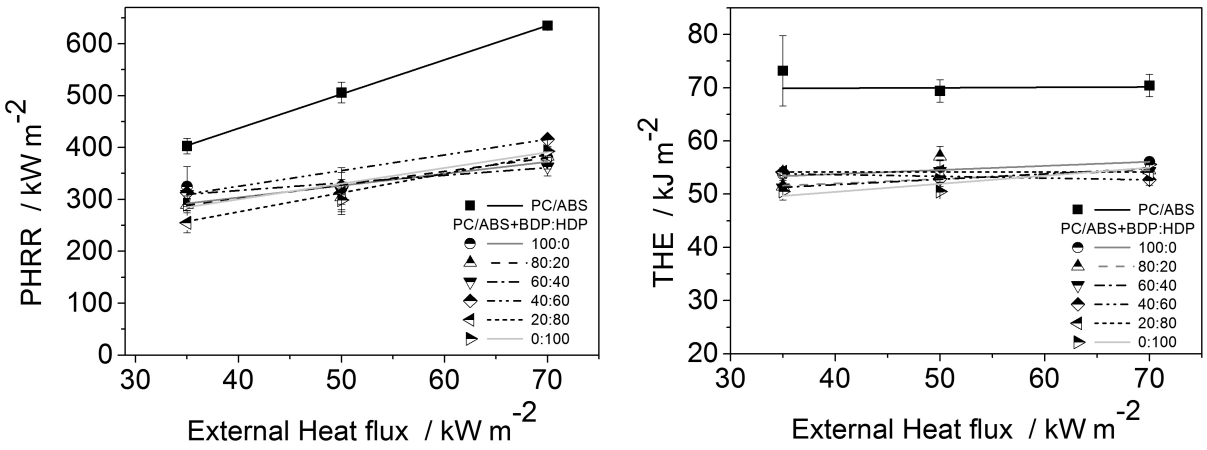

Figure 4.4.12 Peak heat release rate (PHRR) and THE (total heat evolved) at different external heat fluxes (35, 50 and 70 kW m^{-2}) of PC/ABS_{PTFE} and the PC/ABS_{PTFE}+BDP:HDP mixtures in the cone calorimeter

The Total Heat Evolved (THE) evaluates the second main fire risk: fire load. The THE is the total amount of heat released when a material burns. THE was reduced by about 21 – 27 % for all flame-retarded blends with the addition of BDP:HDP mixture to PC/ABS_{PTFE} (*Figure 4.4.13*). This reduction was in the order of the reduction achieved with BDP or HDP in the blend. However, a slight trend emerged in the case of the intermediate BDP/HDP mixtures, with greater reduction of THE at 70 kW m^{-2} for PC/ABS_{PTFE}+BDP/HDP 40:60 than for PC/ABS_{PTFE}+BDP or PC/ABS_{PTFE}+HDP. The reduction for intermediate BDP/HDP mixtures is clearer at a heat flux of 70 kW m^{-2} than at 35 kW m^{-2}, even though, strictly speaking, the small differences are within the margin of error.

The THE per Mass Loss (THE/ML) is related to the effective heat of combustion of the volatiles in the gas phase. The reduction in THE/ML is an indicator of the gas-phase action of the flame retardant in the flame. For all the flame-retarded blends, the THE/ML was reduced by 17-21 % compared to PC/ABS_{PTFE} at 35 kW m^{-2} (developing fire) until 70 kW m^{-2} (fully developed fire) and the residues were increased *(Figure 4.4.13*). The flame retardant mixtures BDP:HDP have a flame mode of action through flame poisoning. The combustion in the flame was inhibited. The phosphates resulting from the decomposition of the intermediate products of the reaction between HDP and BDP released in the flame form several types of phosphorus radicals in the flame, where PO-radicals are believed to play the major role [20]. These radicals react with the highly reactive $H^{\bullet}$ or $OH^{\bullet}$ radicals during combustion [50].

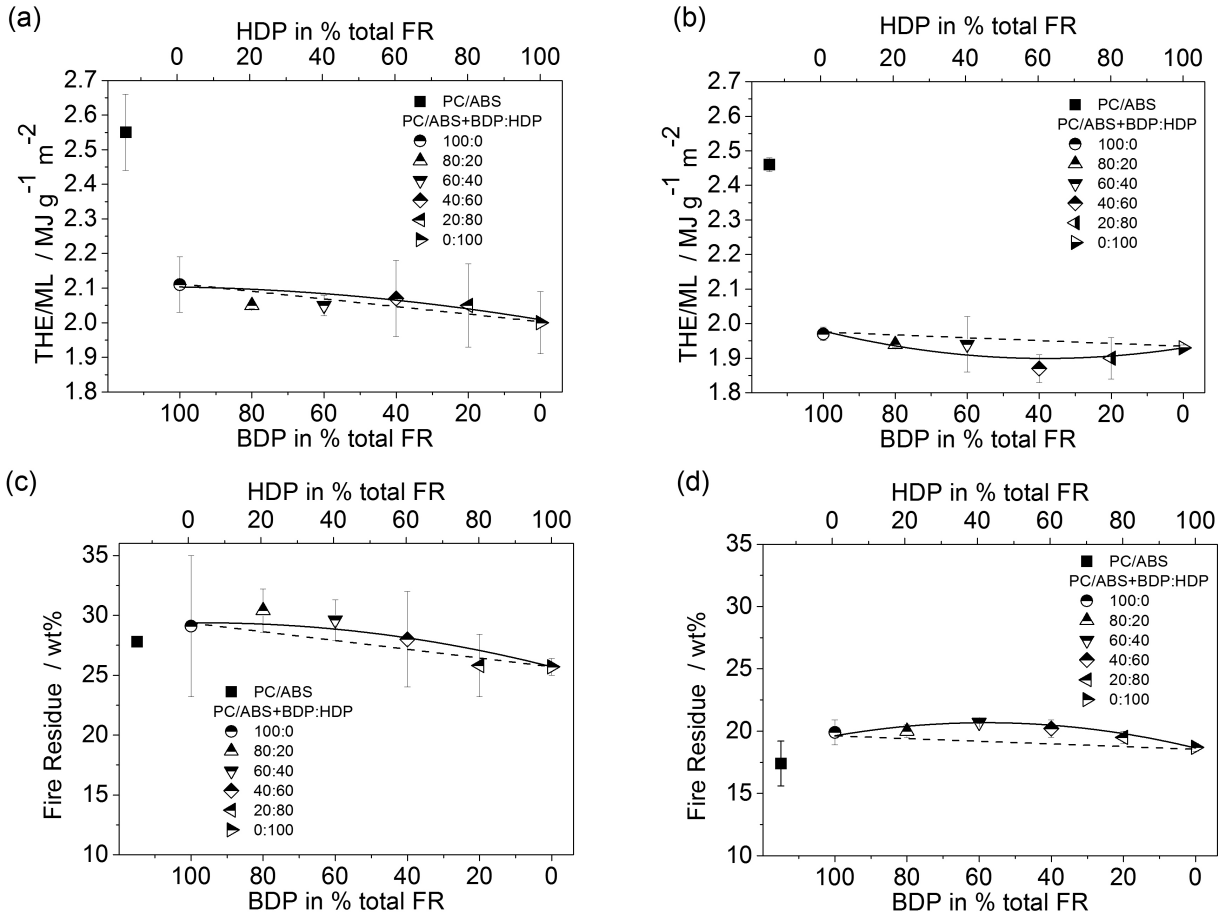

Figure 4.4.13 THE/ML (effective heat of combustion) (a, b) and residues (c, d) of the different PC/ABS_{PTFE}+BDP:HDP blends in the cone calorimeter at an irradiance of 35 kW m^{-2} (a, c) and 70 kW m^{-2} (b, d). The continuous line is a polynomial fitting and the dash line is linear fitting of BDP and HDP values.

At 35 kW m^{-2}, with an increase of HDP versus BDP in the mixture, the THE/ML decreased by 17% for BDP:HDP 100:0 to 22% for BDP:HDP 0:100, indicating a stronger gas phase action from HDP. The residues at flame out, even if higher in presence of the flame retardant mixtures, reduced with increasing HDP content. This is related to the enhanced release of the volatile HDP compared to BDP, highlighted in the TG under nitrogen. HDP has a higher phosphorus content, so in the case for the mixtures with higher concentrations in HDP, more phosphorous species are released at a lower decomposition temperatures than for the one with high BDP concentrations. The synergy observed for the residue formation in the TGA is only suggested at 35 kW m^{-2}, but is not significant enough due to the high uncertainty of the measurement.

At 70 kW m^{-2}, irradiance corresponding to a fully developed fire, the synergy between HDP and BDP is more pronounced, thanks to smaller error range. The best flame inhibition, indicated by a reduced THE/ML was obtained for the intermediate mixtures, especially BDP/HDP 40:60 (*Figure 4.4.13 b*). This synergy occurred simultaneously in the condensed phase, with increased residues for the blends PC/ABS_{PTFE}+BDP/HDP 40:60 and 60:40 (*Figure 4.4.13 d*) compared with PC/ABS_{PTFE} +BDP or PC/ABS_{PTFE}+HDP.

Calculation on the SEA for the absolute increase in residue (*Table 4.4.5*) confirmed synergy between HDP and BDP in the condensed phase, for an incident heat flux of 35 kW m^{-2}. The SEA (residue) were close to or even above 2 for the mixtures 60:40 and 40:60. Or in other words the increase in residue was twice than what expected for superposition.

No clear synergism was observed for the reduction in THE/ML for the BDP/HDP combinations at 35 kW m-2 irradiation, when SE_A was considered. SE_R was also close to 1 and only > 1 for BDP/HDP ratios of 80:20 and 60:40 indicating a slight synergy. At 70 kW m^{-2}, an analogous synergy was found for the residue (maximum of SE_A = 1.63). The SE_A (THE/ML) and SE_R (THE/ML) were consistent to each other, and revealed synergy on the reduction of THE/ML. The highest value of SE_R = 1.21 for the 40:60 mixture indicated significant synergy also in flame inhibition.

Table 4.4.5 Synergistic effect index on the absolute difference (SE_A) and on the relative difference (SE_R), respectively, calculated for the fire residue and the effective heat of combustion at 35 KW m^{-2} and 70 kW m^{-2} for the different PC/ABS_{PTFE}+BDP:HDP blends. Values higher than 1 indicate synergism.

PC/ABS_{PTFE}+ BDP/HDP	Irradiance 35 kW m^{-2}			Irradiance 70 kW m^{-2}		
	SE_A (residue)	SE_A (THE/ML)	SE_R (THE/ML)	SE_A (residue)	SE_A (THE/ML)	SE_R (THE/ML)
100:0	1	1	1	1	1	1
80:20	1.85	1.08	1.12	1.15	1.04	1.08
60:40	2.13	1.03	1.08	1.63	1.03	1.08
40:60	1.98	0.95	0.99	1.57	1.15	1.21
20:80	1.07	0.95	0.98	1.36	1.07	1.11
0:100	1	1	1	1	1	1

An increase of the TSR/ML and TCOR/ML (*Figure 4.4.14*) for all the flame retarded systems compared to the non-flame retarded PC/ABS_{PTFE} confirms the gas phase activity of the HDP-BDP mixtures. The TSR/ML is increased between 35% and 43% at 35kW m^{-2}, and 35 and 55% at 70 kW m^{-2}. From the previous mentioned results, the gas phase activity (THE/ML) is increased for the intermediate blends, especially at higher heat fluxes, and the TSR/ML followed this trend with higher TSR/ML for the intermediate blends. The effective CO release TCOP/ML is increased between 62-70% at 35 kW m^{-2} and 86-103% at 70 kW m^{-2} for the flame retarded blends. The values are slightly higher following the increase in amount of HDP in the blends.

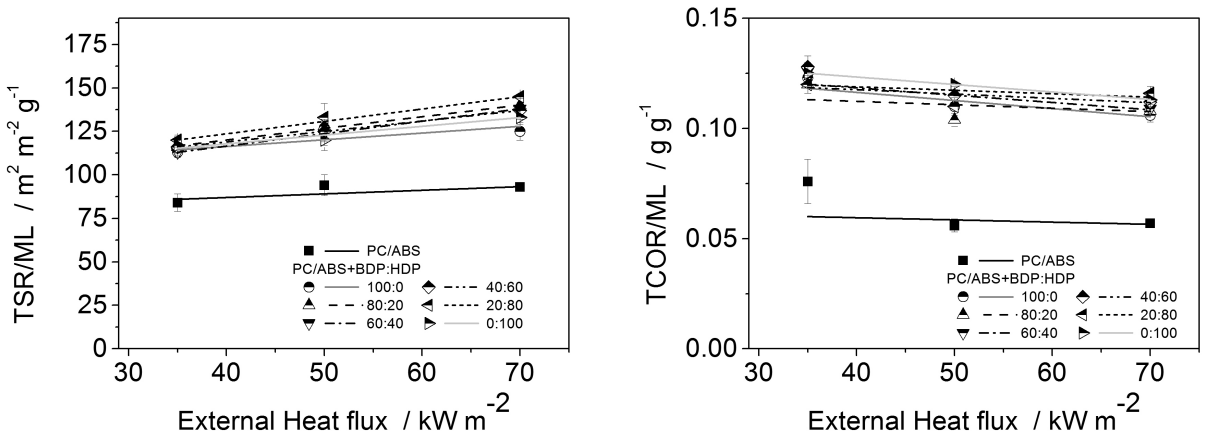

Figure 4.4.14 TSR/ML (effective smoke release) and TCOR/ML (effective CO release) by different external heat fluxes in the cone calorimeter (35, 50 and 70 kW m^{-2}) for the different PC/ABS$_{PTFE}$+BDP:HDP blends

The gas and condensed phase activities of the BDP-HDP mixtures confirmed in the cone calorimeter tests correlated well with the results of the pyrolysis investigations, where a gas phase action of the mixture was proven by the presence of phosphorus-containing derivatives by spectroscopy and in the thermogravimetry with the increase in residues for the intermediate mixtures.

All the flame retarded systems showed by 35kW m^{-2} in comparison to PC/ABS$_{PTFE}$ a more stable residues, with higher amount of residue at the end of the test (after flame out) in the order PC/ABS$_{PTFE}$+BDP:HDP 60:40 (28.9wt%) ≈ PC/ABS$_{PTFE}$+BDP:HDP 40:60 (28.0wt%) > PC/ABS$_{PTFE}$+BDP:HDP 100:0 (25.9 wt%) ≈ PC/ABS$_{PTFE}$+BDP:HDP 20:80 (25.8wt%) > PC/ABS$_{PTFE}$+BDP:HDP 100:0 (24.2 wt%) ≈ PC/ABS$_{PTFE}$+BDP:HDP 80:20 (24.0 wt%). This is confirmed by elemental analysis (*Table 4.4.6*) where the amount of phosphorus retained in the condensed phase correlated well with the amount of residue. The more phosphorus stays in the residue, the more cross-linking reactions can occur, and the higher the resulting residue can be.

Table 4.4.6 Phosphorus content in cone residues (by 35 kW m^{-2} at end of test) from elemental analysis for PC/ABS_{PTFE} and the PC/ABS_{PTFE}+BDP:HDP blends (values are average of two measurements)

PC/ABS_{PTFE}+ BDP/HDP	/	100:0	80:20	60:40	40:60	20:80	0:100
P in residue / wt%	0	51	48	51	52	43	33
P lost / wt%	0	49	52	49	48	57	67

ATR-FTIR spectra of the fire residues obtained by cone calorimeter experiments after flame-out are presented (*Figure 4.4.15*). For better comparison, the intensities of the ATR spectra were normalised to the intensity of the peak at 1575 cm^{-1}. For PC/ABS_{PTFE} at 35 and 70 kW/m² the characteristic peaks of PC char were visible at 1575 cm^{-1} (C=C polyaromatics) and at 875, 812 and 745 cm^{-1} from di-, tri-, tetra-, and penta-substituted aromatic rings [113]. The broad peak between 1250 and 1150 cm^{-1} corresponds to the inclusion of oxygen functionalities in the char (C-O) from rearrangements of PC and oxidation.

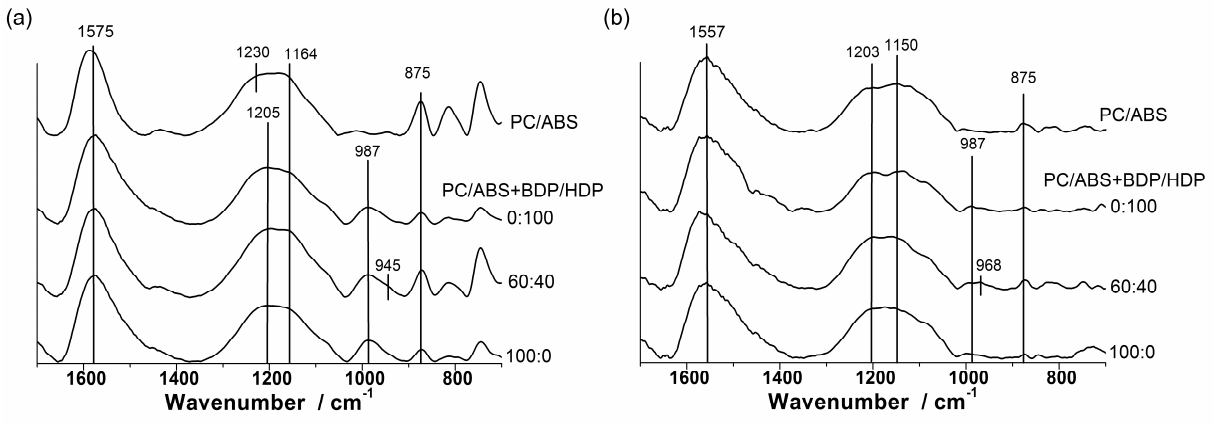

Figure 4.4.15. ATR-FTIR spectra of cone calorimeter test residues from PC/ABS_{PTFE} and PC/ABS_{PTFE}+BDP/HDP blends obtained at (a) 35 kW m^{-2} and (b) 70 kW m^{-2}.

For the blends PC/ABS_{PTFE}+BDP/HDP the characteristic bands of the char from PC/ABS_{PTFE} were present. Furthermore, a new broad peak centred at 987 cm^{-1} was observed for all PC/ABS_{PTFE}+BDP/HDP blends, at both 35 and 70 kW m^{-2}. It corresponded to the inclusion of phosphorus species in the phosphor carbonaceous char (between the

carbonaceous fraction consisting of polyaromatic species organised in stacks characteristic of a pre-graphitisation stage [52]). In the case of PC/ABS_{PTFE}+ BDP/HDP 60:40 a shoulder was observed between 970 and 945 cm^{-1}, which highlighted the formation of other phosphorus species in the residues, in agreement with the increased residues in cone calorimeter experiments. We suggest that amorphous polyphosphate/pyrophosphate structures are formed.

The intensity of the band of the phosphorus-carbon complex at 990-950 cm^{-1} is clearly reduced for fire residues obtained at 70 kW m^{-2} as compared to those obtained at 35 kW m^{-2}, and that for all the PC/ABS_{PTFE}+BDP/HDP blends. At 70 kW m^{-2} the release of phosphorus in the gas phase is enhanced and less phosphorus remained in the condensed phase.

Chapter 5 NEW PHOSPHORUS-NITROGEN-CONTAINING FLAME RETARDANT FOR POLYCARBONATE/ACRYLONITRILE-BUTADIENE-STYRENE: HEXAPHENOXY TRICYCLO PHOSPHAZENE

5.1 Hexaphenoxytricyclophosphazene as flame retardant in PC, ABS and PC/ABS_{PTFE}

PC/ABS_{PTFE} was flame retarded with a commercially available phosphorus-nitrogen-containing flame retardant, hexaphenoxyphosphazene. Polyphosphazene polymers are known to have a high thermal resistance [81], but are more difficult to process than additives. Other phosphorus and nitrogen additives showed in different systems [87] a positive effect on flame retardancy, or even a synergistic effect, like for intumescence. Even if hexaphenoxytricyclo phosphazene (DPZ) is commercially available as flame retardant, little is known on its mode of action. Studies of this flame retardant in PC/ABS_{PTFE} blend is completely missing until now. A complete overview of the effectiveness of this flame retardant, of its decomposition and the interaction with PC/ABS, and the active flame retardancy mechanisms is as far as known not existing.

5.1.1 Pyrolysis

To better understand the effect of DPZ in the PC/ABS_{PTFE} blend, DPZ was added in PC and in ABS separately at a constant amount of 8 wt%.

The thermal decomposition of ABS, DPZ and ABS/DPZ_{PTFE} is given in *Figure 5.1.1*. The thermal decomposition of ABS and DPZ are a one step process. The addition of DPZ into ABS shifted the start of the decomposition $T_{2\%}$ of $ABS/8DPZ_{PTFE}$ to lower temperatures, due to the earlier release of DPZ (*Table 5.1.1*). The temperature of the maximum mass loss rate T_{Max} of $ABS/8DPZ_{PTFE}$ is shifted of 12K to higher temperatures. DPZ showed no char forming action on the non-charring ABS, with no increase in residue. Thus the main flame retardant action is also expected in the gas phase.

The addition of DPZ in PC induced an earlier start of the decomposition of PC/8DPZ, with $T_{2\%}$ 100K earlier than PC. This new decomposition step was related to the lower thermal stability of DPZ, which started to decompose in this temperature range, and left almost no residue. The two decompositions of DPZ and PC are normally in two different temperature ranges, but when mixed together, the two steps overlapped. The mass loss for this additional step corresponded to the initial mass of DPZ present in the composition, plus some

decomposition of PC. The main decomposition of PC is slightly affected by the presence of the flame retardant, with a T_{Max} reduced from 3K. The amount of residue in the case of PC/8DPZ and PC/8DPZ$_{PTFE}$ is increased compared to the expected residue of both components, and indicated a light condensed phase action of DPZ as secondary mechanism in PC. The main flame retardant action of DPZ in PC is expected to be in the gas phase.

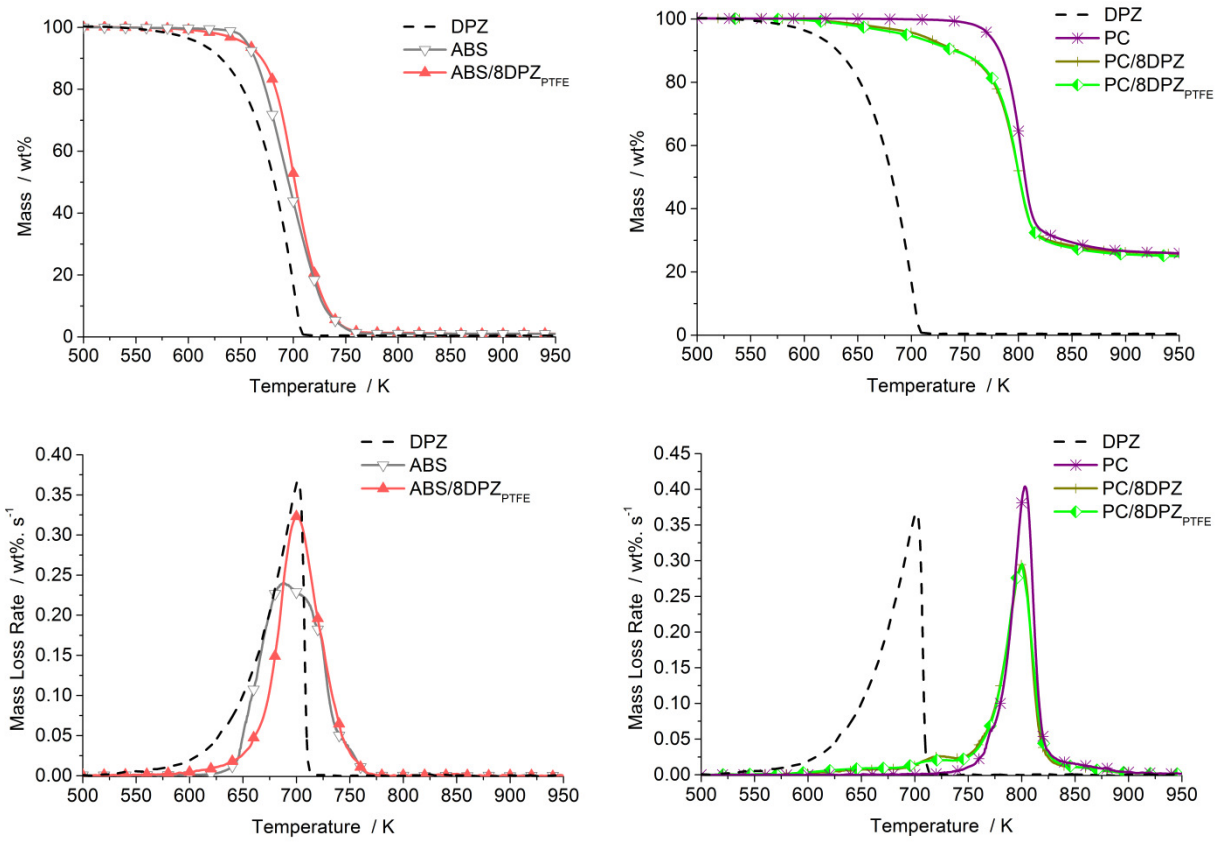

Figure 5.1.1 Thermal behaviour of ABS/DPZ blends and their single components (left) and PC/DPZ blends and their single component (right) under inert atmosphere (10K min^{-1}, N_2)

The addition of PTFE to PC/DPZ$_{PTFE}$ had only an influence on $T_{2\%}$ and T_{Max} 1, around 10 K and 5 K lower, respectively, than PC/8DPZ (*Table 5.1.1*). The same effect occurred for ABS/DPZ$_{PTFE}$ blends, where $T_{2\%}$ and T_{Max1} were also shifted to lower temperatures with the addition of PTFE (*Appendix Table A.4.4*). The second mass loss step and the residues were similar with and without PTFE. The influence of PTFE on the onset of the decomposition of PC/ABS was already observed previously by Pawlowski et al [46].

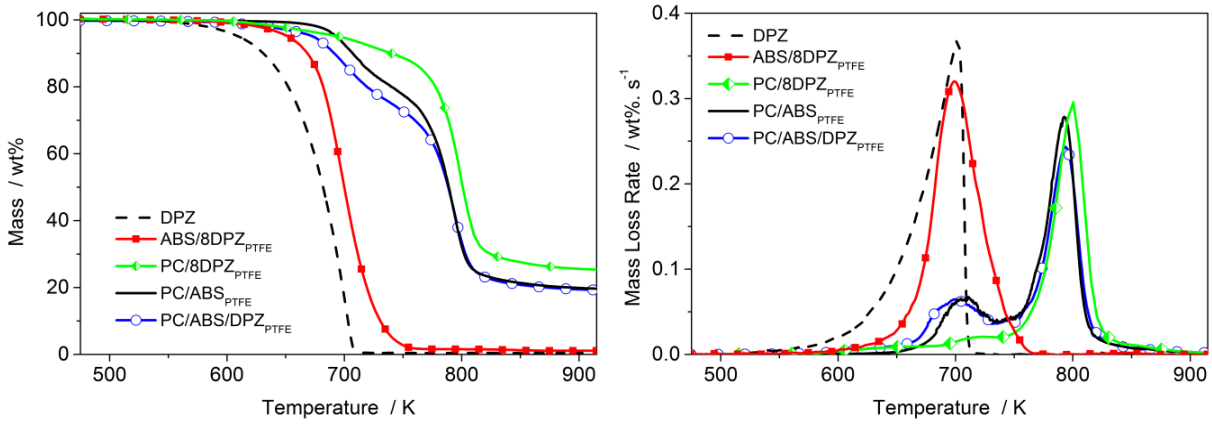

Figure 5.1.2 Thermal behaviour of PC/ABS/DPZ $_{PTFE}$, ABS/DPZ $_{PTFE}$ and PC/DPZ $_{PTFE}$ under anaerobic conditions (nitrogen, 30 ml/min)

When DPZ is added to the PC/ABS$_{PTFE}$ blend, the thermal decomposition of PC/ABS/8DPZ$_{PTFE}$ started at a temperature 47K lower (*Figure 5.1.2* and *Table 5.5.1*) than PC/ABS$_{PTFE}$, and is intermediate between the $T_{2\%}$ of ABS/DPZ$_{PTFE}$ and of PC/DPZ$_{PTFE}$.

Table 5.1.1 Thermogravimetric results of DPZ as flame retardant in PC/ABS$_{PTFE}$, PC and ABS blends (under N_2, 10 K min^{-1}). Value in bracket means shoulder step.

	PC/ABS PTFE	+8DPZ	PC	+8DPZ	+8DPZ PTFE	DPZ	ABS	+8DPZ$_{PTFE}$
$T_{2\%}$ in K	678	631	758	653	643	587	649	624
Mass Loss I								
ML1 in wt%	19.2	27.1	-	9.7	10.5	99.5	98.2	97.7
$T_{Max\ 1}$ in K	707	701	-	724	719	703	688 (708)	700
Mass Loss II								
ML2 in wt%	57.2	51.0	69.0	60.3	60.3	-	-	-
$T_{Max\ 2}$ in K	793	793	803	800	800	-	-	-
Residue								
Residue in wt%	23.7	21.9	31.0	30.0	29.2	0.5	2.4	2.3
Expect. residue	-	21.7	-	28.6	28.5	-	-	2.2

Furthermore the temperature of the maximum mass loss rate of the first step is shifted to lower temperatures by the addition of DPZ into PC/ABS_{PTFE}, and was similar to the one of ABS/DPZ_{PTFE} blend. The second mass loss step is really similar to the second step of PC/ABS_{PTFE}, with a similar T_{Max2}. DPZ did not increased significantly the amount of residue formed by PC/ABS_{PTFE}, and confirmed the fact that it did not increased the residue for ABS or for PC alone.

The evolved gas spectra of the PC/DPZ_{PTFE} and ABS/DPZ_{PTFE} are given in *Figure 5.1.3*. Already during the first decomposition step (shoulder) of PC/DPZ_{PTFE}, at 42 min, characteristic decomposition products of PC, such as phenol and bisphenol A derivatives (1259, 1177 cm^{-1} and 1600, 1509, 2937, 3085 cm^{-1}), CO_2 (2360 cm^{-1}) and methane (3016 cm^{-1}) are released, indicating the early start of the decomposition of PC due the presence of DPZ. Moreover new broad bands are present around 1353 cm^{-1}, 1489 and 1462 cm^{-1} which are attributed to nitrogen containing species, such as partly aromatic imines as long of a shoulder at 2258 cm^{-1} (aromatic nitriles or cyanates), that is not present in the decomposition products of DPZ.

Reactions between the decomposition products of DPZ and the one of PC occurred. The new amines or ureas moieties formed during the decomposition of DPZ and reactions with decomposing PC are able to react with the carbonates linkages. The phenols derivatives formed during the hydrolysis of PC are in turn able to hydrolyse the phosphazene cycles that further dehydrated to form CO_2 and C≡N linkages (nitriles or cyanates). A small shoulder at 3660 cm^{-1} indicated the further hydrolysis of DPZ with the formation of phosphate P-OH acids groups. The second step of the decomposition at 49.7 min related principally to the further decomposition of PC, with the characteristic decomposition products of PC described previously. The amount of carbonates released was changed (1221, 1773 cm^{-1}), that indicated a possible reaction in the condensed phase between the phosphoric acids derivatives formed in the first step and the decomposing polymer matrix that supported the light increase in residue in the TGA.

During the main decomposition step of $ABS/8DPZ_{PTFE}$ at 40 min (*Figure 5.1.3*), decomposition products of polystyrene (mainly styrene, 910, 699; 3078; 3039 cm^{-1}) and of acrylonitrile (954 cm^{-1}) and other nitrilic derivatives (2307 cm^{-1}) are observed that indicated the main decomposition of ABS, especially the SAN part, before the decomposition of DPZ.

The decomposition and volatilisation of DPZ occurred during the small shoulder after the main step, at 44.6 min. In this step decomposition and volatilization products of DPZ were visible, with the presence of the P=N bands at 1263 cm^{-1} for tricyclophosphazene; P-OC bands at 1194; 1176 and 1163 cm^{-1} str as and at 948 cm^{-1} str sym of P-N and P-OC bands. DPZ decomposed in a less extend with the presence of a band at 3649 cm^{-1}, resulting from the release of phenols and from phosphoric acid derivatives. This band does not exist in the spectrum of DPZ in TG-FTIR, and is an indication of a minor chemical reaction between DPZ and the decomposition products of ABS, probably due to the presence of the polar nitrile groups. The formation of P-NH-P groups from the decomposition of DPZ is possible, however it cannot be definitely concluded because the bands were overlapped by C=C alkene or aromatics bands (3074 cm^{-1}, broad band at 1453 cm^{-1}, and 870 and 697 cm^{-1}). Additionally during this step, typical products of decomposition and rearrangements of SAN and polybutadiene rubber with styrenic compounds were released, aliphatic alkenes (within butadiene) and some cycloalkenes evolved ($CH=CH_2$ at 1453 cm^{-1}; C=C bands at 1593 and 1490 cm^{-1}; C-H bands at 3078 and 3033 cm^{-1}, aliphatic CH_2 bands at 2973; 2937; 720 cm^{-1}) that are typical products of the decomposition of the polybutadiene part.

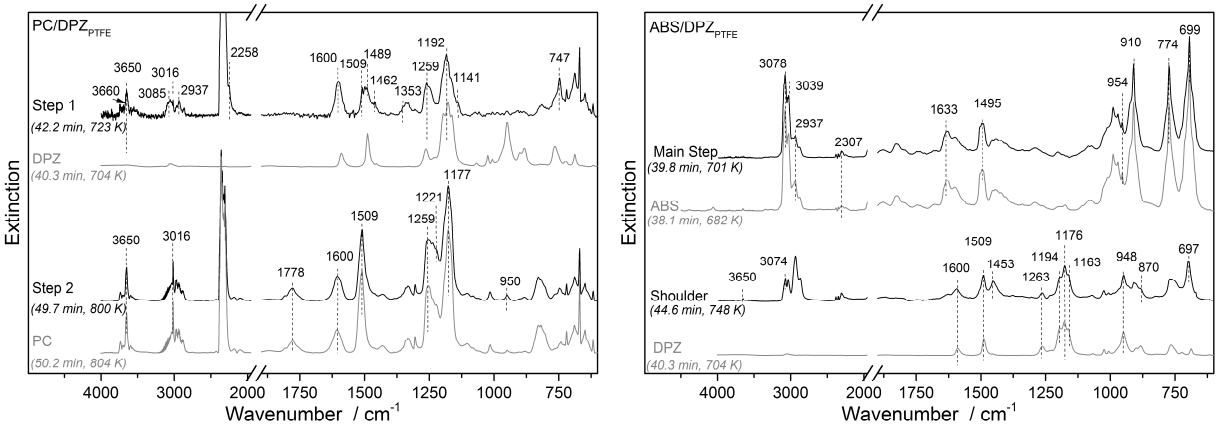

Figure 5.1.3 FTIR Spectra in the gas phase of PC/DPZ$_{PTFE}$ (left) and of ABS/DPZ $_{PTFE}$ (right) (TG-FTIR, 10 K min^{-1}, N_2)

The FTIR spectra of PC/ABS/DPZ$_{PTFE}$ at the different decomposition steps are given in *Figure 5.1.4*. During the first decomposition step at 40 min, characteristic decomposition products of ABS were observed, as long as some decomposition products of DPZ and PC (P=N str at 1264 cm^{-1}, P-O-C at 1188, 1161 cm^{-1} and 950 cm^{-1}). The phosphorus bands are

overlapped by the C-O str band at 1259 and 1177 cm^{-1} of phenol derivatives. The presence of phenols is supported by the PhO-H band at 3650 cm^{-1}. Some nitriles derivatives are observed at 2252 and 2194 cm^{-1}, and related to the reaction between nitrogen-containing species and the OH groups produced during the decomposition of the polymer matrix. Like in PC/8DPZ$_{PTFE}$, DPZ induced the earlier decomposition of the polycarbonate. At 45 min, in the intermediate shoulder between the two steps, the decomposition of the PC is continuing, with the stronger release of small molecules like methane (3016 cm^{-1}) and CO_2 (2360 cm^{-1}) and of the phenol derivatives. The release of nitrogen compounds from DPZ is occurring, and the broad bands were a sign of change in the chemical environment of the P-N (823 and 878 cm^{-1}). The C=C_{Ar} band at 1490 cm^{-1} indicated that a part of the aromatics contained more electronegative atoms, and thus cross-linking reactions occurred with nitrogen or phosphorus in the condensed phase. In the main step at 49.2 min, the increase in the amount of formed carbonates groups (-O(C=O)O- 1778 cm^{-1} and –OCO-O- 1235 cm^{-1}) that was observed in PC/DPZ$_{PTFE}$ occurred only in a limited way in PC/ABS/DPZ$_{PTFE}$. The decomposition products were similar to the one of PC in PC/ABS$_{PTFE}$ (phenol derivatives 3650 cm^{-1}; CH_4 3016 cm^{-1}; CO_2 2360 cm^{-1}; CO 2091 cm^{-1}). This supported the decrease action in the condensed phase of DPZ in PC/ABS$_{PTFE}$ than in PC. Furthermore phosphorus and P-N species were released in the gas phase (P-O-C 950 cm^{-1}, P-N 764 and 883 cm^{-1}). A stronger release of DPZ in the gas phase and thus an increased action of DPZ in the gas phase is expected in PC/ABS$_{PTFE}$ than in PC.

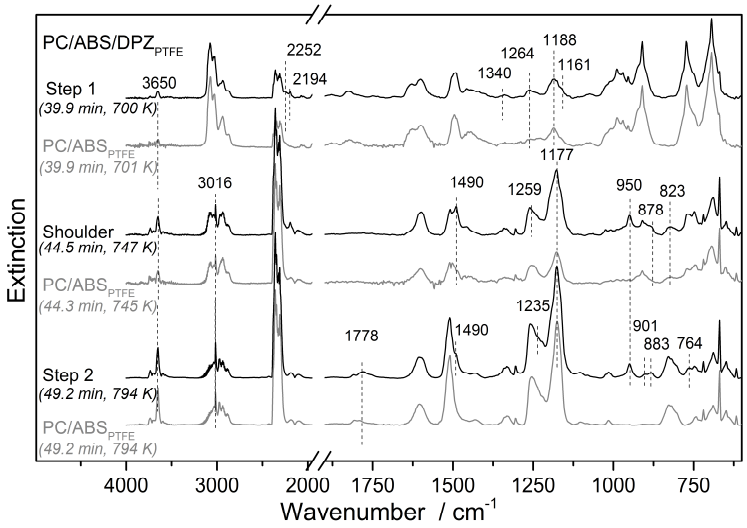

Figure 5.1.4 FTIR spectra of the evolved gases in the gas phase of PC/ABS/DPZ$_{PTFE}$ and of PC/ABS$_{PTFE}$ (10K min^{-1}, N$_2$)

To explain the difference between PC/ABS$_{PTFE}$ and PC observed in the presence of DPZ, the thermal decomposition of the phosphazene has been analysed in condensed and gas phase. To get a more comprehensive insight of the mechanisms and the influence of the structures of the phenoxyphosphazene, a mixture of phosphazene oligomers (DPZ-m mixture consisted in 70% of cyclic trimer, 20% of cyclic tetramer, and 10% of linear oligomers) has been chosen. Since DPZ is included in DPZ-m, conclusions drawn here are valid for DPZ.

DPZ-m showed a really similar thermal decomposition in the TG than DPZ in one main mass loss step under anerobic conditions. T2% of DPZ-m was 2 K higher than DPZ, and T_{Max} was 5 K lower. Almost no residue was formed (0.3 wt%) by DPZ-m, as for DPZ. The FTIR spectra of the evolved gases (from TG-FTIR) and the condensed phase (linkam hot stage) of DPZ-m are represented in *Figure 5.1.5*. At the start in the condensed phase (*Figure 5.1.5 a*), the characteristic bands of the cyclic trimer are present (P=N at 1265 cm, P-N at 903; 881; 724 cm^{-1}, P-O-C_{Ar} at 1176; 1161; 947 cm^{-1}). The cyclic tetramers and oligomers were visible (P=N cyclic tetramer and oligomers at 1352 cm^{-1} (broad), P-N at 818, 824 cm^{-1}) as long as the phenoxy substituents (CH str at 3068; 3041 cm^{-1}, C=C str at 1591; 1488 cm^{-1}, C-H def monosubstuted phenyl ring at 766; 688 cm^{-1}). The spectrum of DPZ (99.8% trimer) (not shown) was similar as the one of DPZ-m, only the tetramers and oligomers bands were missing.

During the decomposition in the condensed phase (25.5 min), the P=N band at 1262 cm^{-1} of the cyclic trimer decreased strongly, that indicated a partial volatilization of DPZ or a loss of the phosphazene ring. A change in the environment of the P-O-C occurred. The band at 1194 cm^{-1} broadened and the bands at 947 cm^{-1} broadened too and shifted to lower wavenumber. The aromatics band intensity decreased in the same time (1590; 1489 cm^{-1}) that indicated the loss of the organic part and rearrangement of the P-O into the formation of P-O-P groups. The tetramers had a lower volatility than the trimers, and the amount of tetramers decreased at a later point than the one of the trimers. All the bands corresponding to P-N decreased strongly.

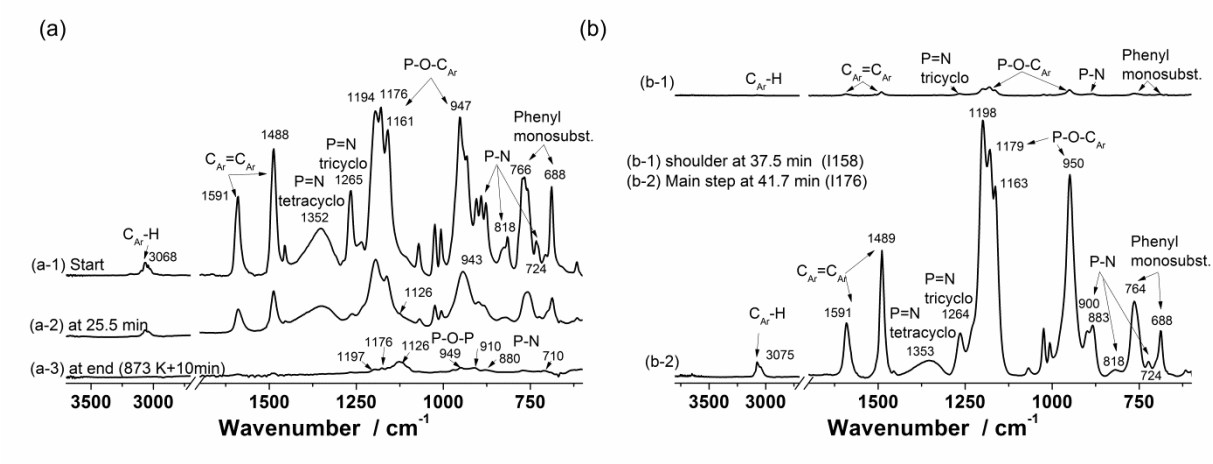

Figure 5.1.5 Condensed phase FTIR spectra (linkam hot stage) (a) and evolved gas FTIR spectra (TG-FTIR) (b) of DPZ-m decomposition at different temperatures.

The biggest part of the nitrogen element is then lost and released in the gas phase. At the end of the decomposition, at 600°C, characteristic bands for inorganic species is observed. Most of the elements retained were phosphorous species, with P-O-P bands from polyphosphoric derivatives (1197; 1126; 910 cm^{-1}). The P-N bands were shifted, indicating reaction at the P-N groups, and the intensities were strongly reduced (880; 770; 710 cm^{-1}). Some P-O-C and P-OH moieties stayed in the condensed phase (at 1176 and 949 cm^{-1}), and indicated that the transformation into poly- and metaphosphates was not totally complete. The formation of the P-O-P and, in a less extent, P-N bond supported a cross-linking of DPZ molecules into phosphorus oxynitride PON_x, and polyphosphoric acid, as long as the volatilization of DPZ into cyclic trimer and cyclic tetramer for the main part. A small

presence of the aromatics rings, but shifted, is also observed, and suggested the formation of char by condensation of the aromatic rings.

The results of the condensed phase are supported by the gas evolved in the gas phase in the TG-FTIR under nitrogen (*Figure 5.1.5 b*). In the first small shoulder at 37.54 min, cyclic trimer were observed (P=N at 1264 cm^{-1}, P-N at 899; 883; 724 cm^{-1}; P-O-C_{Ar} at 1179; 1163; 950 cm^{-1}, and monosubstituted phenyl rings C_{Ar}=C_{Ar} str at 1591; 1489 cm^{-1} and C_{Ar}-H def at 764; 688 cm^{-1}) [80]. At 41.7 min, the bands of the trimers increased and new bands of the tetramers were visible (P=N at 1353 cm^{-1} (broad) [129] and P-N at 879 cm^{-1}), indicating the later volatilization of the tetramers. The bands of the aromatics were broadened, that indicated that possible rearrangements of the organic part of the decomposition products occurred. Moreover, some decomposition products condensed in the transfer-line (at 230°C), and indicated that bigger molecules from the decomposition and rearrangements of DPZ into higher molecular weights products occurred.

5.1.2 Mechanisms

The decomposition of DPZ followed different decomposition pathways. The volatilisation of the trimer was important and competed with decomposition followed by cross-linking in the condensed phase that leads to an increase in residue [130, 131]. The favoured pathways were dependent on the environment that means on the polymer matrix. When DPZ is added in PC, the charring is increased, that indicated that the mechanisms in the condensed phase occurred as well as the volatilisation. DPZ is sensible to hydrolysis [46, 132], and so the phosphazene ring is destructed, leading to the formation of phosphoric acid derivatives, that act in the condensed phase for cross-linking and char promotion. The nitrogen species released acted in the gas phase for flame dilution and cooling of the flame. [133, 134]. Mainly P-N and C-N derivatives are released. No primary or secondary amines were produced, and thus indicate their direct reactions when formed with the phenols of PC. The formation of aromatic tertiary amine is a consequence, whose are difficult to detect in FTIR. Moreover the phenol derivatives R-OH produced during the decomposition of PC are able to react with DPZ to form via transesterification R-O-P bound and the release of phenol. The secondary or primary amines formed by hydrolysis of DPZ are nucleophilic and react with the carbonyl from PC decomposition, like amide bound. These products could further

dehydrate to produce C=N and C≡N bounds, that are release in the gas phase. The char is increased through the reaction of the P-O-P formed that cross-linked with PC to form phosphate esters. A partly organic/inorganic and aromatic char structures is formed during the decomposition.[135]. A possible intumescent effect is thus achieved by the presence of the phosphoric acids in the condensed phase and the release of pyrolysis gases and nitrogen-containing species in the gas phase as blowing agent [54, 136].

When DPZ was added in PC/ABS_{PTFE}, no condensed action is observed, and the increase in residue in the TG is only marginal. Most of the flame retardant is observed in the gas phase that indicated that for this blend the volatilisation of DPZ is the main process. In the gas phase, the ring will further decompose if a flame is present, and flame poisoning through the phosphorus and flame dilution through the nitrogen elements are expected. A possible interaction between the decomposing ABS and DPZ is proposed for the low interaction between DPZ and the PC in PC/ABS_{PTFE}.

5.1.3 Flammability and ignitability

The addition of DPZ as flame retardant in PC increased both the oxygen index and the UL94 rating at 1.6 and 3.2 mm, indicating the effect of the flame retardant on the flammability properties (*Table 5.1.2*). However in the absence of PTFE, burning drips formed and inflamed the cotton, leading to the classification V-2 for both thicknesses. The addition of PTFE as anti-dripping agent in $PC/8DPZ_{PTFE}$ effectively improved the UL94 classification to the best ranking V-0, with the absence of burning drips and short burning times (under 1 second). The presence of a flow limit in the viscosity of the melt from PTFE is the reason for it [103]. DPZ acted as good flame retardant in combination with PTFE in PC. The good properties of DPZ are also reflected in the ignitability of the PC/DPZ_{PTFE} blends under forced flaming combustion (cone calorimeter), with quite similar time to ignition at 35 kW m^{-2} to delayed t_{ig} at 50 and 70 kW m^{-2}.

DPZ showed also a flame retardant action in the highly flammable ABS (with 0.45% of PTFE) (*Table 5.1.2*). The oxygen index increased by around 2-3% by the addition of DPZ compared to literature value of ABS, and the rating in the UL94 test did not changed compared to literature value of ABS. The loading of 8% of DPZ in the blend is too low to achieve values above 25-28% OI, what is expected for most of flame retarded applications. The addition of DPZ improved the ignitability of the $ABS/8DPZ_{PTFE}$ blends under forced

flaming combustion, with higher or similar time to ignition compared to ABS. The ignitability under forced flaming conditions of the ABS/DPZ_{PTFE} blends is slightly improved in the presence of DPZ, especially at 35 and 50 kW m^{-2}.

*Table 5.1.2 Flammability results (LOI, UL94) and ignitability results (time of ignition t_{ig}) for the DPZ as flame retardant in PC, ABS and PC/ABS_{PTFE} blends. *Data from [1] and **Data from [137]*

Material	LOI (%)	UL94 classification (3.2 mm)	UL94 classification (1.6 mm)	t_{ig} in s		
				at 35 kW m^{-2}	at 50 kW m^{-2}	at 70 kW m^{-2}
PC	27-28*	HB*	V-2*	157 ± 13	65 ± 1	33 ± 1
PC/8DPZ	34.4	V-2	V-2	139 ± 3	68 ± 1	39 ± 1
PC/8DPZ_{PTFE}	42.2	V-0	V-0	149 ± 3	79 ± 5	38 ± 2
ABS	18-19**	n.R**	n.R**	62 ± 2	30 ± 1	18 ± 1
ABS/8DPZ_{PTFE}	21.6	n.R	n.R	65 ± 4	35 ± 1	18 ± 1
PC/ABS_{PTFE}	24.1	HB	HB	82 ± 2	48 ± 3	27 ± 2
PC/ABS/DPZ_{PTFE}	29.4	V-1	V-1	110 ± 7	49 ± 1	28 ± 2

When DPZ is added to PC/ABS_{PTFE}, the oxygen index is improved of 5 % v/v O_2, and PC/ABS/8DPZ_{PTFE} achieved the second best classification in the UL94 test (V-1). The samples extinguished between 10 and 30 seconds after removal of the external flame, without dripping. The samples ignited later in the cone calorimeter in the presence of DPZ at 35 kW m^{-2}, or with the same time at higher heat fluxes. This confirmed the results of the TG-FTIR, where DPZ decomposition products are released mainly during the first decomposition step of PC/ABS/8DPZ_{PTFE} that provided flame inhibition and flame dilution.

5.1.4 Fire behaviour

The fire behaviour under forced flaming combustion of PC, ABS and PC/ABS_{PTFE} blends flame retarded with DPZ has been investigated in the cone calorimeter at different external heat fluxes. The addition of DPZ in ABS added with 0.45% of PTFE clearly reduced the heat release rate curves and reduced the peak heat release rate (PHRR), between -30 to -40%

(*Figure 5.1.8* and *Table 5.1.3*). A detail overview of the cone calorimeter data are given in *Table A.4.3, A.4.4* and *A.4.5* in the appendix. ABS/8DPZ$_{PTFE}$ did not charred, and a typical curve for thermally thick non charring material is observed. The reduction in the fire hazards is thus possible through the gas phase action of DPZ. The effective heat of combustion THE/ML is reduced between 18 to 22% for all three fire scenarios tested in the presence of 8% of DPZ in ABS. The total heat evolved is reduced of about 20%. This is possible through flame poisoning by the phosphorus-containing and nitrogen-containing species released in the gas phase, as observed in the TG-FTIR.

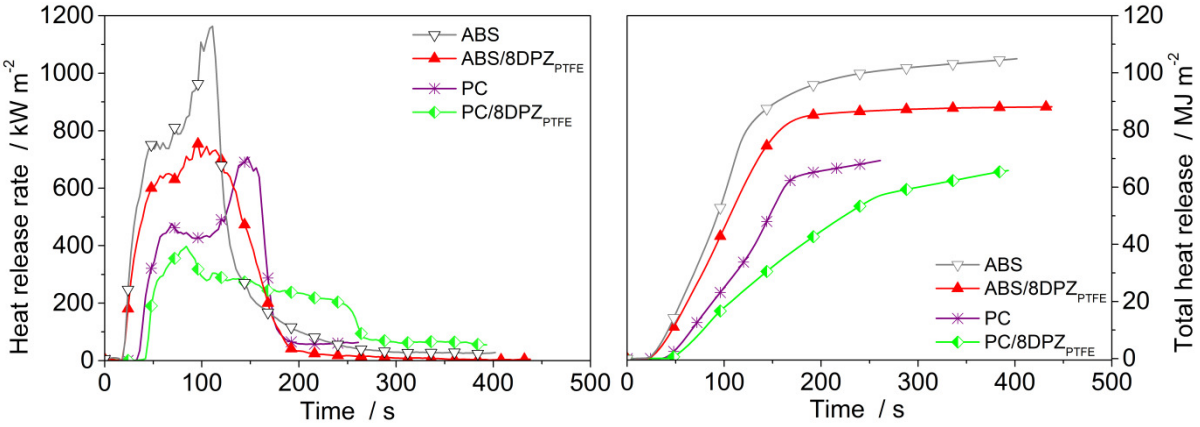

Figure 5.1.8 Heat release rate (HRR) and total heat release rate (THR) of the blends of DPZ in ABS and in PC in the cone calorimeter at 70 kW m^{-2}

The addition of DPZ in PC/DPZ$_{PTFE}$ reduced the main fire hazards. In this charring material, an intumescent like effect is observed in the presence of DPZ, with high char column or "tower" sometimes touching the cone heater or even higher than the highest point of the heater, with a total height of the char of around 50 to 60 mm (*Figure 5.1.10*). A flame-retardant system is coming to intumescence, if three important factors are fulfilled [53, 54]. First a substance needs to be present in the system, which can form acidic functions when the temperatures rise. Further, a carbon-rich material is requested that will be the basis for the formation of char. A last component that serves as blowing agent, producing volatile gases, which will blow up the residue has eventually to be present. In some cases, a substance can play more than one of the cited functions.

In the PC system flame retarded by the phosphazene, the phosphorus group is the acidic former. The opening of the phosphazene ring during the thermal decomposition caused the

formation of phosphoric acids groups. These participate to the cross-linking of the polymer through dehydration, and are the basis of the carbonaceous char. The gaseous decomposition products from the matrix and the flame retardant, especially the nitrogen-containing species, serve as blowing agent. The residue will expand and a multicellular protection layer against heat and mass transport will be form between the heat source and the pyrolysis zone. The PHRR is then reduced in PC between 20% at 35 kW m^{-2} to almost 50% at 70 kW m^{-2}.

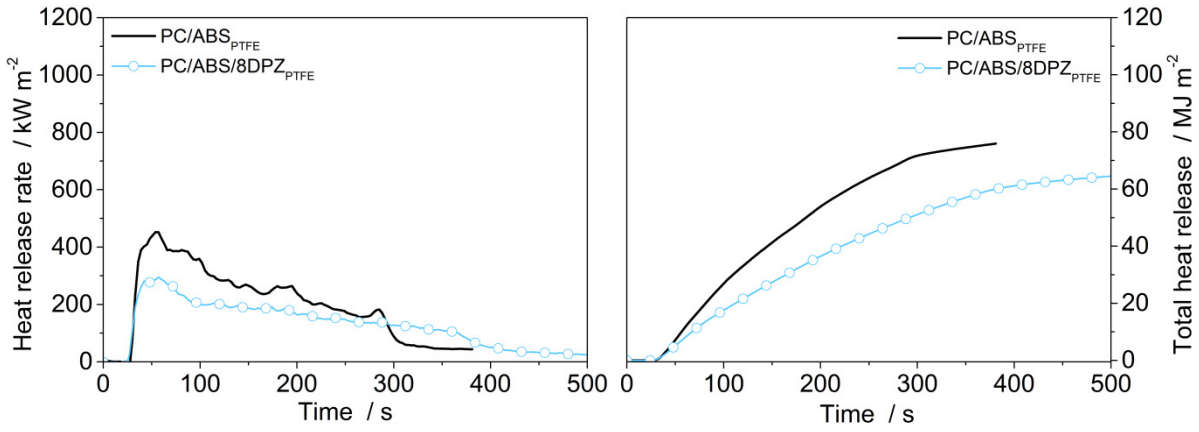

Figure 5.1.9 Heat release rate (HRR) and total heat release rate (THR) of the blend of DPZ in PC/ABS$_{PTFE}$ in the cone calorimeter at 70 kW m^{-2}

In PC, DPZ worked via a condensed phase action with the increase in residue of about 1 to 23% in the cone calorimeter. The char formation is relatively low for intumescent flame retardant, and the protection layer is not effective enough, with the presence of big cells inside of the char tower. This increase in residue in the TGA was of 1 wt%. This difference is related to different expansion of the char in the TGA (especially in the case of intumescence) depending on the initial weight of the sample and the geometry and size of the crucible in the TGA. Expansion of char can be reduced in TGA if the sample size and crucible dimensions hindered the formation of an effective protecting layer. DPZ showed additionally a gas phase action, with a light reduction of the THE/ML, indicating flame inhibition.

Figure 5.1.10 Action of DPZ flame retardant by enhancement of the char formation by an intumescence process: PC/8DPZ (top left) and PC/8DPZ$_{PTFE}$ (top right), PC/ABS$_{PTFE}$ without flame retardant (bottom left); PC/ABS/8DPZ$_{PTFE}$ (bottom right); in the cone calorimeter (50 or 70 kW m^{-2}) after flame out

When DPZ is added to the PC/ABS$_{PTFE}$ blend (*Figure 5.1.9*), a similar interaction is observed as for PC with intumescent-like expansion of the char. A heat release rate curve for char forming polymer is obtained. A high char tower formed in the forced flaming conditions of the cone calorimeter (*Figure 5.1.10*). DPZ acts mainly in PC/ABS$_{PTFE}$ like in PC, because PC is the main component in the PC/ABS$_{PTFE}$ blend, even if some little differences existed.

Table 5.1.3 Results of the cone calorimeter at 35, 50 and 70 kW m^{-2} of DPZ as flame retardant in PC, ABS and PC/ABS_{PTFE} (and relative change to PC, ABS or PC/ABS_{PTFE} values)

Material	PC/8DPZ$_{PTFE}$ (Change to PC)	ABS/8DPZ$_{PTFE}$ (Change to ABS)	PC/ABS/8DPZ$_{PTFE}$ (Change to PC/ABS_{PTFE})
External heat flux: 35 kW m^{-2}			
THE in MJ m^{-2}	60.9 ± 0.9 (-2%)	84.7 ± 4.5 (-23%)	61.4 ± 0.7 (-11%)
PHRR in kW m^{-2}	374 ± 68 (-21%)	490 ± 14 (-28%)	313 ± 35 (+8%)
Residue in wt.%	27.0 ± 0.1 (+10%)	3.0 ± 0.2 (-31%)	22.7 ± 2.7 (-7%)
THE/ML in MJ m^{-2} g^{-1}	2.30 ± 0.03 (-4%)	2.7 ± 0.1 (-25%)	2.25 ± 0.01 (-14%)
TSR/ML in m^2 m^{-2} g^{-1}	76 ± 2 (-11%)	142 ± 4 (+26%)	96 ± 5 (+9%)
TCOP/ML in g g^{-1}	0.026 ± 0.001 (+69%)	0.034 ± 0.001 (+58%)	0.037 ± 0.002 (+112%)
External heat flux: 50 kW m^{-2}			
THE in MJ m^{-2}	61.7 ± 2.1 (-3%)	85.9 ± 1.7 (-17%)	62.3 ± 3.2 (-14%)
PHRR in kW m^{-2}	407 ± 24 (-23%)	539 ± 48 (-41%)	354 ± 34 (+12%)
Residue in wt.%	22.4 ± 0.1 (+1%)	2.1 ± 0.1 (-36%)	20.3 ± 0.4 (+7%)
THE/ML in MJ m^{-2} g^{-1}	2.22 ± 0.06 (-6%)	2.76 ± 0.05 (-18%)	2.23 ± 0.12 (-14%)
TSR/ML in m^2 m^{-2} g^{-1}	83 ± 4 (-6%)	144 ± 1 (+23%)	107 ± 1 (+16%)
TCOP/ML in g g^{-1}	0.033 ± 0.001 (+106%)	0.035 ± 0.001 (+61%)	0.038 ± 0.002 (+118%)
External heat flux: 70 kW m^{-2}			
THE in MJ m^{-2}	60.4 ± 2.5 (-5%)	83.3 ± 2.5 (-19%)	62.8 ± 0.1 (-12%)
PHRR in kW m^{-2}	380 ± 18 (-47%)	744 ± 10 (-35%)	325 ± 30 (-23%)

Residue in wt.%	25.3 ± 2.6 (+23%)	± 0.3 (0%)	18.9 ± 1.5 (+10%)
THE/ML in MJ m^{-2} g^{-1}	2.25 ± 0.01 (-2%)	2.66 ± 0.07 (-22%)	2.22 ± 0.03 (-11%)
TSR/ML in m^2 m^{-2} g^{-1}	97 ± 5 (+2%)	140 ± 12 (+17%)	117 ± 3 (+21%)
TCOP/ML in g g^{-1}	0.029 ± 0.001 (+81%)	0.036 ± 0.001 (+52%)	0.030 ± 0.003 (+90%)

The effect of DPZ on the two main hazard parameters, the peak heat release rate and the total heat evolved is represented for PC and PC/ABS_{PTFE} in *Figure 5.1.11*. DPZ reduced effectively the peak heat release rate (PHRR) in PC, with an increased action by increased external heat flux. This action is stronger in PC than in PC/ABS_{PTFE}, where the PHRR is only reduced at 70 kW m^{-2}. The better action in PC probably came from the absence of PTFE compared to PC/ABS_{PTFE}. PTFE induced deformations of the melted polymer. The presence of the flame retardant reduced the second main hazard: the fire load (THE). This reduction is much stronger in the case of PC/ABS_{PTFE}, compared to PC.

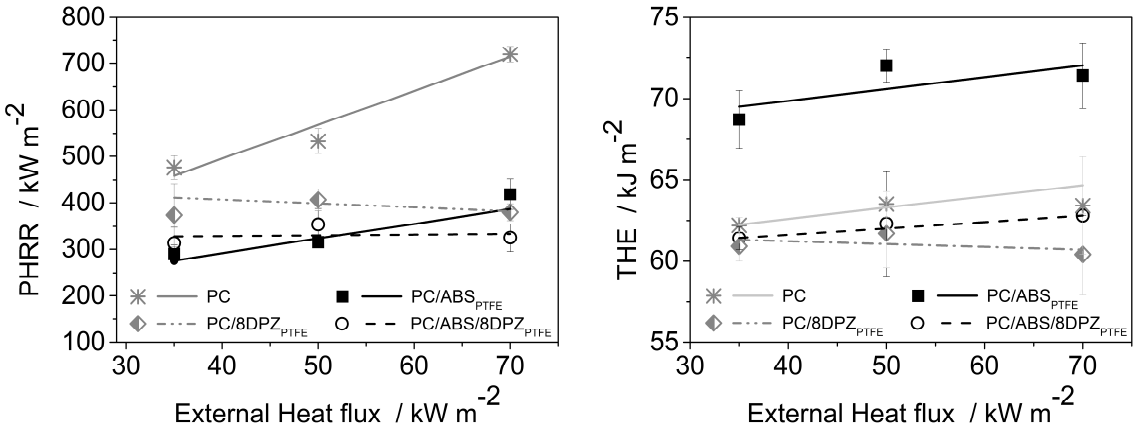

Figure 5.1.11: Action of DPZ flame retardant on the peak heat release rate (PHRR) (left) and the Total Heat Evolved (THE) (right) in PC and PC/ABS_{PTFE} blends in different fire scenarios

The residue of $PC/ABS/8DPZ_{PTFE}$ is decreased at 35 kW m^{-2} and increased from 7 to 10% compared to PC/ABS_{PTFE} at higher heat inputs (*Table 5.1.3*, *Figure 5.1.12*). It indicated that the condensed phase action of DPZ still occurred in the blend. However this effect is

lower than what is obtained for PC/DPZ$_{PTFE}$ (20% of increase). It is supposed that the presence of ABS induced interactions with DPZ, that leads to non-char forming species in the condensed phase. The amount of released gases originating from the flame retardant is thus increased. This is confirmed by the increased gas phase action of DPZ in the PC/ABS$_{PTFE}$ blend, with a reduction of -11 to -14% of the THE/ML.

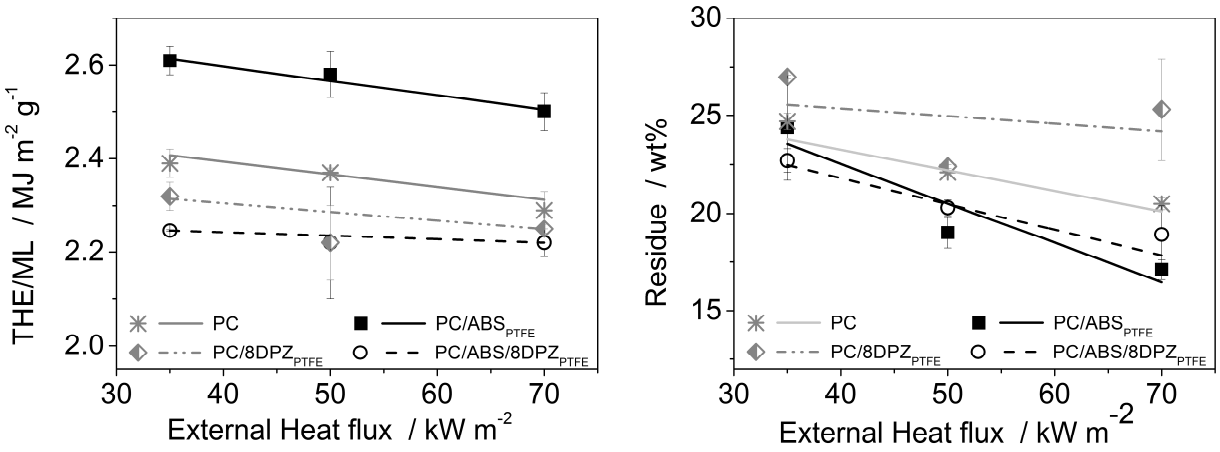

Figure 5.1.12 Action of DPZ flame retardant on the effective heat of combustion (THE/ML) (left) and the residue formation (right) in PC and PC/ABS$_{PTFE}$ blends in different fire scenarios

The evolution of the effective smoke release (TSR/ML) and the effective CO release (TCOP/ML) is given in *Figure 5.1.13*, when DPZ is added in PC, the effective smoke release TSR/ML is reduced. But the addition of DPZ in PC/ABS$_{PTFE}$ increased the smoke release, which is related to the increase in gas phase activity. The increase of the CO release due to the less complete combustion in the gas phase is stronger in PC/ABS$_{PTFE}$ compared to PC for the same reasons. The combustion efficiency was calculated for the blend with DPZ-m, which contained a stronger part of tetramers and of linear oligomers (not shown), and a combustion efficiency between 0.85 at 35kW m^{-2} until 0.79 at 70kW m^{-2} was obtained for phenoxyphosphazene, instead of the 0.96 (closed to 1, complete combustion in the gas phase) of PC/ABS$_{PTFE}$ without flame retardant. DPZ acted by flame poisoning in the gas phase. Since the temperature of decomposition is quite the same for the trimer, similar combustion efficiency is expected.

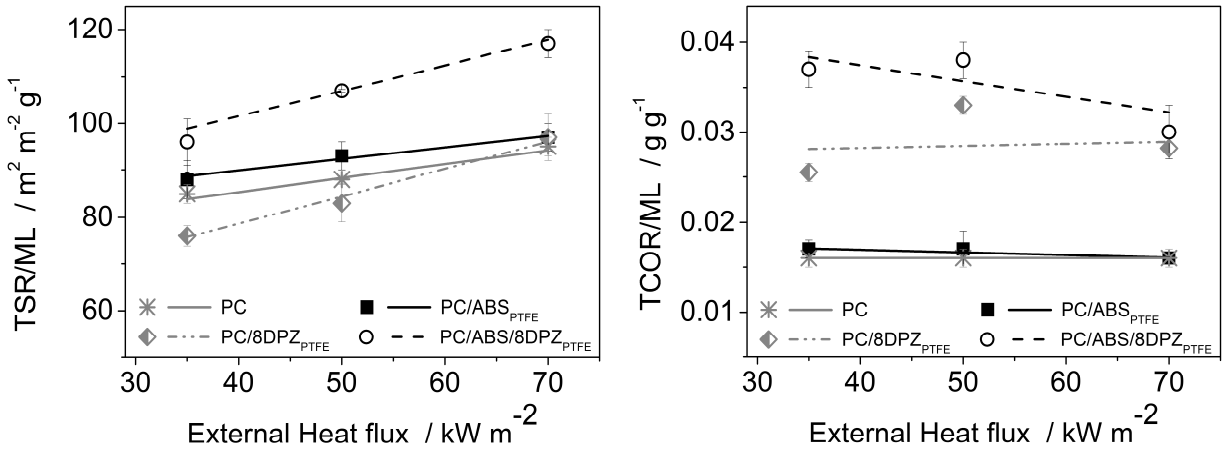

Figure 5.1.13: Action of DPZ flame retardant on the effective smoke release (TSR/ML) (left) and the effective CO release (TCOR/ML) (right) in PC and PC/ABS$_{PTFE}$ blends at different fire scenarios

DPZ-m flame retardant was further tested in the PC/ABS$_{PTFE}$ blend. Both flame retardants, DPZ and DPZ-m are compared in PC/ABS$_{PTFE}$ *Figure A.5.1* of the appendix. DPZ-m has a similar effect compared with DPZ on the fire behaviour of the blend, what is not surprising because of the high percentage of DPZ trimer in the DPZ-m mixture (70%).

The efficiency of DPZ as flame retardant in PC based blends (PC and PC/ABS$_{PTFE}$) and in ABS is represented in *Figure 5.1.14*, with the two main fire risks, the fire load (THE) and the fire propagation propensity (PHRR/t_{ig}) where t_{ig} is the time to ignition [110, 138].

When DPZ is added to PC, both fire risks are decreased, even if the fire propensity is the parameter which is the most reduced, thanks to the reduction of the PHRR. In the case of PC/ABS$_{PTFE}$ with the addition of DPZ, both fire risks are decreased. The fire load (THE) is diminished even more in PC/ABS$_{PTFE}$ than in PC, due to the strong action of DPZ in the gas phase, and its interaction with ABS. In ABS, DPZ is able to limit both fire risks, especially the fire load.

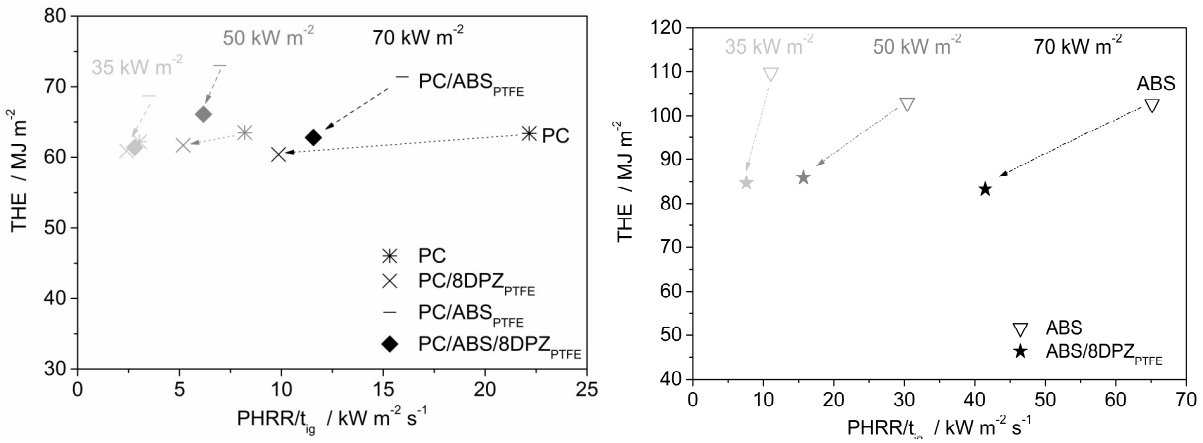

Figure 5.11.14 Assessment of the fire risks according to Petrella at different external heat fluxes by the addition of DPZ in PC or in PC/ABS$_{PTFE}$ blends (left) or in ABS (right) (mean values at 35, 50 and 70 kW m^{-2})

DPZ is an effective flame retardant in both PC and ABS, and is thus adapted for the flame retardancy in the PC/ABS$_{PTFE}$ blend. DPZ acted principally in the gas phase in ABS via flame inhibition, DPZ acts via a condensed phase and a gas phase mechanism in PC, and principally in the gas phase in PC/ABS$_{PTFE}$, with a minor action in the condensed phase with increase of the char formation.

5.2 Combination of phosphazene and an aryl phosphate flame retardants in polycarbonate/acrylonitrile-butadiene-styrene

Since BDP acted both via a condensed and gas phase action, as investigated in Chap 4, and DPZ acted mainly via a gas phase action as evaluated in Chap 5.1, the influence of the mixture of both flame retardants in PC/ABS_{PTFE} was of interest. Different ratios of the mixtures were investigated, with a constant amount of phosphorus element in all the blend of 1.1 %, to avoid any bias due to the different phosphorus amount.

5.2.1 Pyrolysis

The addition of the BDP:DPZ mixtures in PC/ABS_{PTFE} influenced the thermal decomposition of the blend. In *Figure 5.2.1* the TG and DTG-signals of the PC/ABS_{PTFE}+BDP:DPZ blends is given with the different BDP:DPZ ratios. The correlated data are summarized in *Table 5.2.1*.

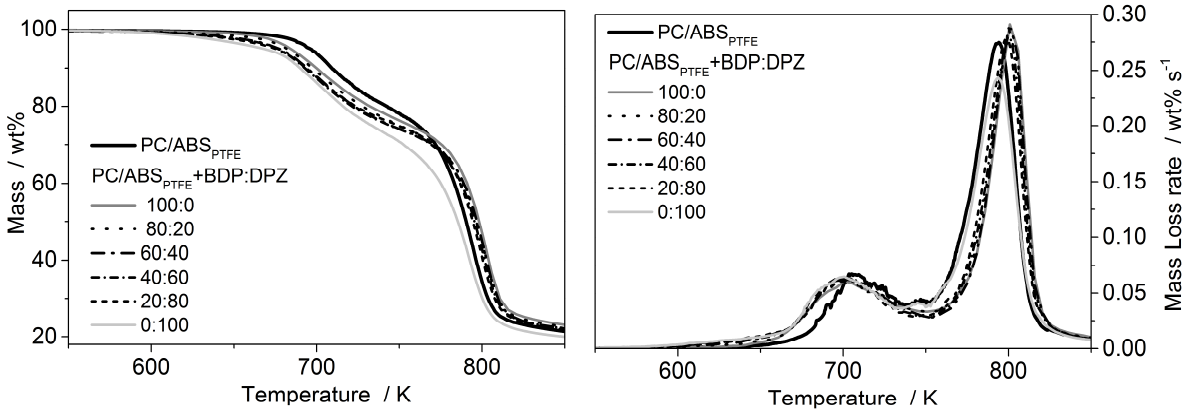

Figure 5.2.1 TG and DTG curves of PC/ABS_{PTFE}+BDP:DPZ blends with different BDP:DPZ ratios and PC/ABS_{PTFE} (under N2, 10K min^{-1})

All the materials decomposed in two steps like PC/ABS_{PTFE}. The temperature of the decomposition of the first step is shifted to lower temperatures (between 8 to 3 K lower) for all the flame retardants mixtures. The start of the decomposition $T_{2\%}$ is decreased with increasing amount of DPZ, due to the lower stability of DPZ, as it was observed with the

BDP:HDP mixtures, where HDP had a lower thermal stability than BDP (*Chap 4.2*). The decomposition of PC during the second step is shifted to higher temperatures with all the different BDP:DPZ ratios, except for BDP:DPZ 0:100, where the temperatures T_{Max} is the same than PC/ABS_{PTFE}. All the BDP:DPZ mixtures influenced the thermal decomposition of PC/ABS_{PTFE}.

A further difference between the changing BDP:DPZ mixture ratios is the amount of char formed. All the flame retardant mixtures formed more char than the expected residues calculated based on the residues of the single components. The residues of the mixtures with higher amount of BDP are higher, for example 2.8 wt % higher in the 80:20 mixture. Only the BDP:DPZ 40:60 mixture showed the same amount of residue than the BDP alone mixtures (4.1 wt % more), but this difference is due to broader error range for this material.

Table 5.2.1 Thermogravimetric results of PC/ABS_{PTFE}+BDP:DPZ blends and PC/ABS_{PTFE} (under N_2, 10K min^{-1})

PC/ABS_{PTFE} + BDP:DPZ	/	100:0	80:20	60:40	40:60	20:80	0:100
T2% in K	678	665	654	646	638	637	633
			Mass Loss I				
ML1 in wt%	19.2	24.6	25.8	26.6	27.0	25.6	27.1
T_{Max} 1 in K	707	704	699	700	699	704	701
			Mass Loss II				
ML2 in wt%	57.2	50.5	50.3	49.9	49.9	51.2	51.0
T_{Max} 2 in K	793	803	802	801	802	799	793
			Residue				
Residue in wt%	23.7	24.9	23.8	23.4	25.5	22.5	21.9
Expected residue in wt%	-	20.9	21.0	21.2	21.4	21.5	21.7
Increase in residue in wt%		+4.0	+2.8	+2.2	+4.1	+1.0	+0.2

The interactions between BDP and DPZ have been evaluated, based on the mixture BDP+DPZ 40:60 in the thermogravimetry under nitrogen *Figure 5.2.2*. The mixture BDP+DPZ 40:60 has a lower stability than the calculated TG curve from the superposition of BDP+DPZ of the curve of the single component. $T_{2\%}$ and T_{Max} are both at lower temperatures than what was expected. The formed residue is lower than expected, and indicated that both components react with each other to form more volatile gases that are not inducing char formation.

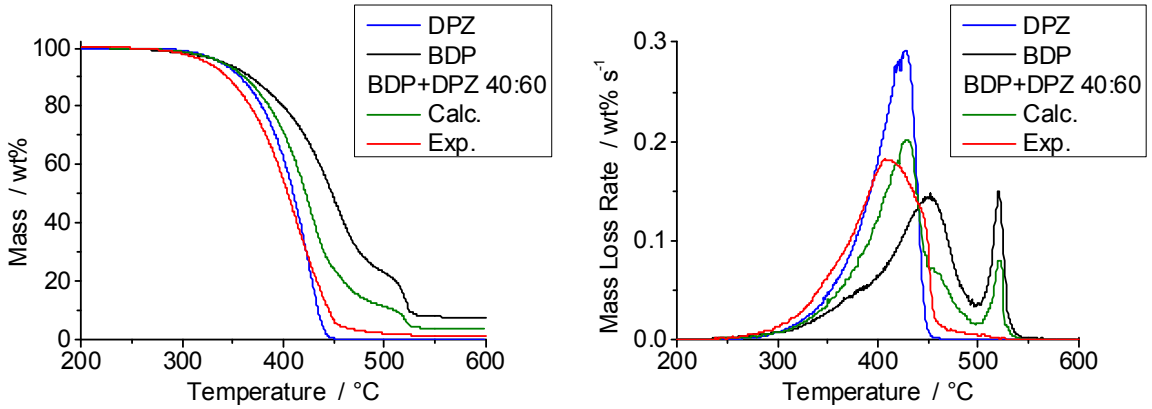

Figure 5.2.2 Thermogravimetric results of BDP, DPZ and BDP+DPZ 40:60 mixture (under N_2, 10K min^{-1})

The results from the TGA of BDP+DPZ suggested an antagonism between DPZ and BDP. DPZ is an easy phosphorylating agent, and is able to react with BDP at earlier temperatures. The formed intermediates are more volatile and formed less species that remained in the condensed phase.

BDP is less available for char formation. Such an effect was already observed when BDP was combined with inorganic additives such as zinc borate [66, 69] where anorganic phosphoborates were formed and reduced the availability of the phosphorus for the char formation with the polycarbonate decomposition products.

5.2.2 Fire behaviour

In the flammability tests (*Table 5.2.2*), the PC/ABS_{PTFE}+BDP:DPZ blends with the different BDP:DPZ ratios showed a decreased rating in the UL94 test from V-0 to V-1 with increasing amount of DPZ in the BDP:DPZ mixture. The gas phase action of the DPZ flame retardant was not sufficient to reach the V-0 rating. The LOI values were really similar between all the flame retarded blends, and were in the same domain than the single BDP or DPZ flame retardant value, that were around +6 vol % O_2 higher than PC/ABS_{PTFE}.

The ignitability is changed with the addition of the flame retardant mixtures in the polymer matrix. The material ignited under forced flaming combustion at a later time with the mixtures with the intermediates ratios of BDP:DPZ (60:40 and 40:60), compared to the one with the single flame retardant. This may be due to the different intermediates that are produced from the interactions of BDP and DPZ, as already supposed from the TG of the mixture BDP+DPZ.

Table 5.2.2 Flammability results (LOI, UL94) and ignitability results (time of ignition t_{ig} in the cone calorimeter) for PC/ABS_{PTFE}+BDP:DPZ blends and PC/ABS_{PTFE} blends (n.R: non rating)

PC/ABS_{PTFE}+	LOI (%)	UL94 (3.2 mm)	UL94 (1.6 mm)	t_{ig} in s		
				at 35 kW m^{-2}	at 50 kW m^{-2}	at 70 kW m^{-2}
-	24.1	HB	HB	82 ± 2	48 ± 3	27 ± 2
+BDP:DPZ 100:0	30.0	V-0	V-0	84 ± 4	45 ± 1	32 ± 1
+BDP:DPZ 80:20	29.3	V-0	V-1	108 ± 6	49 ± 5	29 ± 1
+BDP:DPZ 60:40	30.2	V-1	V-1	150 ± 59	52 ± 4	29 ± 1
+BDP:DPZ 40:60	29.9	V-1	V-1	105 ± 2	58 ± 9	27 ± 1
+BDP:DPZ 20:80	30.2	V-1	V-1	93 ± 7	48 ± 1	28 ± 1
+BDP:DPZ 0:100	29.4	V-1	V-1	110 ± 7	49 ± 1	28 ± 2

Under forced flaming combustion in the cone calorimeter, all the PC/ABS$_{PTFE}$+BDP:DPZ blends charred and deformed. With increasing amount of DPZ, the char structures were higher and the char structures contained more big cells. The formation of the char structures was really dependent on the scenario and the samples and the different deformations of the material. In the samples containing a higher amount of DPZ (BDP:DPZ ratio 40:60 and 20:80), the char structure was sometimes high and instable, that a part or the entire char tower fell down on the side of the sample. In this case the protecting barrier effect of the char is lost or reduced, and more pyrolysis gases could escape in the gas phase. Characteristic values from the cone calorimeter measurements are summarized in the *Table A.4.6* in the *Appendix*.

In *Figure 5.2.3* is represented the dependency of the THE and the PHRR in function of the external irradiance. While the PHRR is only slightly decreased with increasing external heat flux for the blends containing the BDP: DPZ mixtures, the reduction in THE raised with higher external heat fluxes from 11-12 % to 12-21% for the flame retarded blends. The best results in reduction in PHRR were obtained for DPZ single flame retardant, whereas the best results for the reduction of the THE were obtained for BDP. The intermediate mixtures showed similar results.

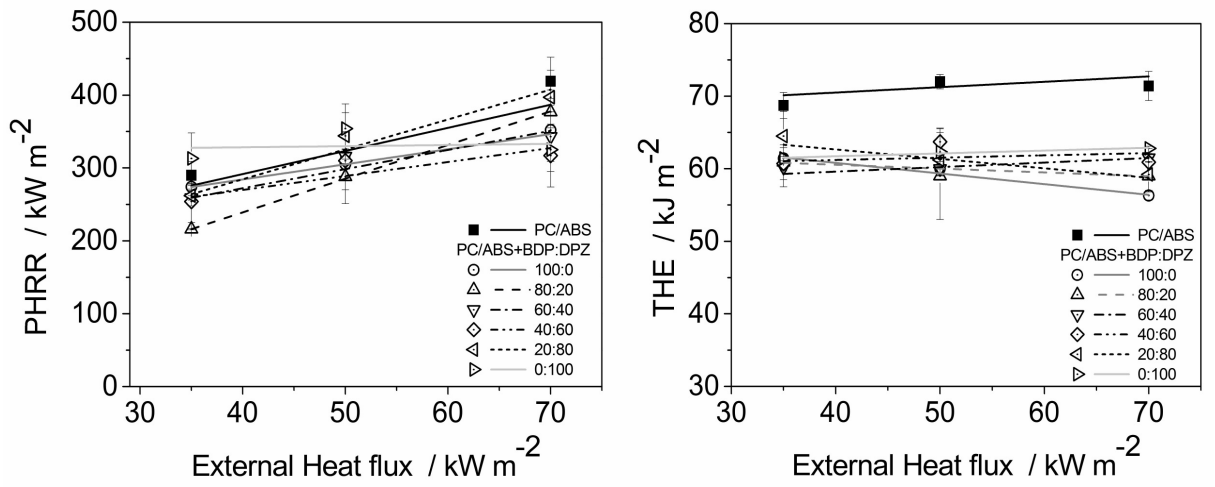

Figure 5.2.3 PHRR and THE in different fire scenarios for the PC/ABS$_{PTFE}$+BDP:DPZ blends

The dependency of the THE of the PC/ABS$_{PTFE}$+BDP:DPZ blends in function of the external heat fluxes can be explained, if the values for the residues and the THE/ML are

considered in detail (*Figure 5.2.4*). For low irradiances, the THE/ML of the BDP:DPZ flame retarded systems were reduced quite similarly by ca. 14-17% compared to PC/ABS_{PTFE}. The amount of residue formed were in the same range for all the flame retarded systems, independently of the BDP:DPZ ratios. At higher heat fluxes, the THE/ML is dependent of the BDP:DPZ compositions. The THE/ML reduced linearly with increasing ratio of BDP that means a stronger gas phase action. The same linear relationship existed for the residue, because of the non-charring tendency of DPZ. Instead of synergy, a simple superposition of the effect of BDP and DPZ in the BDP:DPZ combinations occurred.

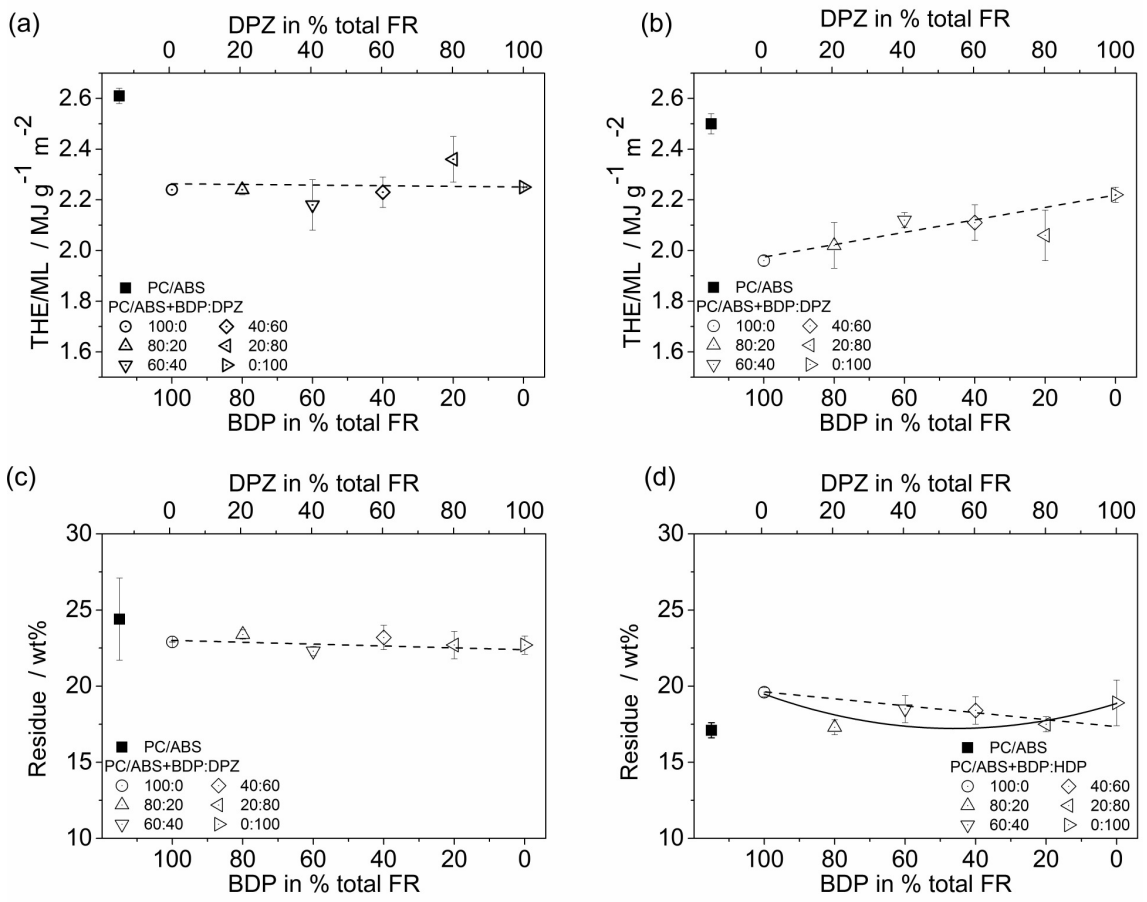

Figure 5.2.4 THE/ML (effective heat of combustion) (a, b) and residues (c, d) of the different PC/ABS_{PTFE}+BDP:DPZ blends in the cone calorimeter at an irradiance of 35 kW m^{-2} (a, c) and 70 kW m^{-2} (b, d).

More incomplete combustion products are formed through flame poisoning of the BDP:DPZ mixtures in form of smoke and carbon monoxide (CO), compared to the

combustion of non-flame retarded material. This induced an increase of the effective smoke release and the effective CO release (TSR/ML and TCOP/ML) for all the investigated mixtures. With increasing fire scenarios, the flame inhibition was increased, and thus the TSR/ML was as well increased. All the investigated mixtures showed gas phase mechanisms. (*Figure 5.2.5*). BDP had the highest gas phase activity of the BDP:DPZ mixtures, and this is supported by the highest TSR/ML and TCOP/ML.

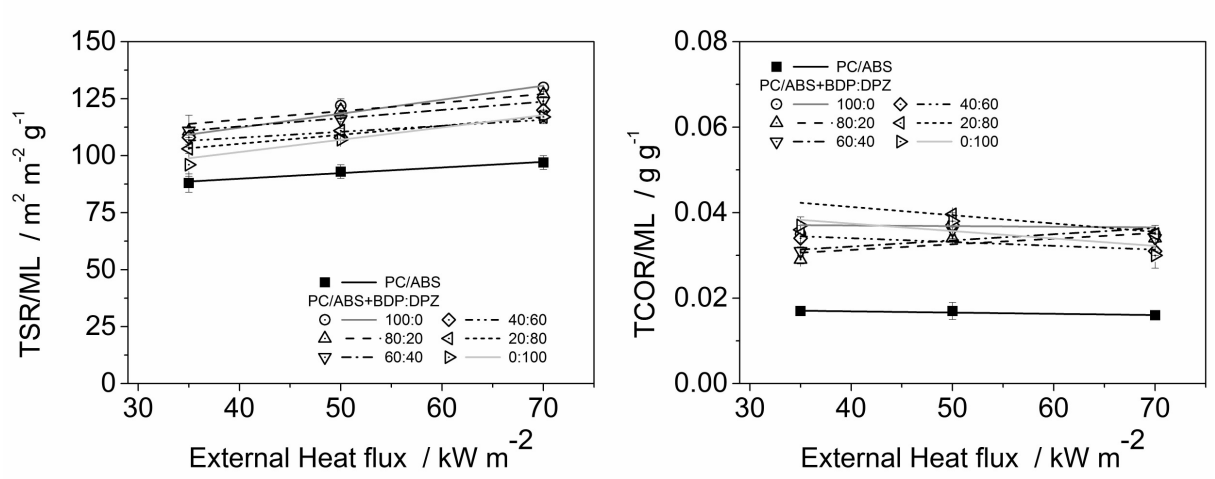

Figure 5.2.5 Action of BDP:DPZ flame retardant mixtures on the effective smoke release (TSR/ML) (left) and the effective CO release (TCOP/ML) (right) in PC/ABS$_{PTFE}$ in different fire scenarios

The results of the elemental analysis on the cone residues at 35 kW m^{-2} (*Table 5.2.3*) confirmed a linear decrease in the amount of phosphorus retained in the condensed phase, due to the lower amount of BDP present in the blend. BDP formed more cross-linked structures with the decomposing polymer matrix than did DPZ. On the contrary, DPZ formed an intumescent char that is looser, with big cells, and is not as efficient as BDP, for the same amount of phosphorus added inside the blends. Almost all the nitrogen element of DPZ was released in the gas phase, as only 3 to 4% remained in the condensed phase. The released nitrogen elements were used for the blowing up of the decomposing polymer melt into a foam-like char. An insulating layer is thus formed, protecting the underlying decomposing material. A dilution effect can also be observed in the flame when the gas reached the flame zone.

Table 5.2.3.Results of elemental analysis on the residues from cone calorimeter tests at 35kW m^{-2} (average of two measurements)

PC/ABS_{PTFE}+BDP:DPZ	100:0	80:20	60:40	40:60	20:80	0:100
$P_{in\ residue}$ in wt%	43%	42%	48%	40%	35%	36%
$N_{in\ residue}$ in wt%	N/A	2%	4%	4%	3%	4%

A possible interaction (synergistic or additive action) between BDP and DPZ has been quantified by the synergistic effect SE_A in *Table 5.2.4*. There is no synergy in the condensed phase between BDP and DPZ as seen on the SEA of the residue, both in the TGA and in the cone calorimeter. These results supported the conclusions made in the LOI, UL94 and cone calorimeter part. The residues in the cone calorimeter at 35 kW m^{-2} show a SE_A close to 1, without clear tendency.

Table 5.2.4 Absolute synergistic effect (SE_A) calculated on the residue under pyrolysis in the TGA and the residues and THE/ML from the cone calorimeter at 35 and 70 kW m^{-2}

Materials	TG under inert atmosphere	Cone calorimeter test			
	Increase in residue	Irradiance 35 kW m^{-2}		Irradiance 70 kW m^{-2}	
PC/ABS +BDP:DPZ	SE_A (increase in residue)	SE_A (Residue)	SE_A (THE/ ML)	SE_A (Residue)	SE_A (THE/ ML)
100:0	1.00	1.00	1.00	1.00	1.00
80:20	0.81	0.91	1.00	N/A	0.95
60:40	0.77	N/A	1.17	0.61	0.82
40:60	1.92	0.89	1.04	0.60	0.95
20:80	0.79	1.13	0.69	1.55	1.25
100:0	1.00	1.00	1.00	1.00	1.00

An antagonism can be seen, with values clearly smaller than 1, around 0.80 in TGA in inert atmosphere and 0.60 in the cone calorimeter at 70 kW m^{-2} (forced flaming combustion). This support the earlier decomposition of the BDP+DPZ mixture observed in the TGA in part

5.3.2, without increase in residue. In the case of a gas phase action in the cone calorimeter experiments, no clear interaction between the two flame retardants occurred, and the effects resulted more from an addition of the effect of each flame retardant (SEA closed to 1, or slightly under 1).

Chapter 6 COMPARISON OF THE FLAME RETARDANTS IN PC/ABS$_{PTFE}$

6.1 Effect of single flame retardants in PC/ABS$_{PTFE}$

Four aryl phosphates and two phosphazene flame retardants have been tested in PC/ABS$_{PTFE}$ blends, at the same level of phosphorus element in the blends, 1.1 wt%. The structure of the aryl phosphates had an influence on the fire retardancy mechanisms and so on the fire behavior. When the structural unit of the core unit (bridge) of the bridged aryl phosphate played a minor role, as far as all were based on aromatics (BDP, HDP and BBDP), the substitution of the side units has a bigger influence on the flame retardancy mechanisms. This influence can be illustrated in the Petrella plot (*Figure 6.1.1*). When the phosphate ester flame retardants BDP, BBDP, HDP are added to PC/ABS$_{PTFE}$, the two main fire risks according to Petrella [138] are reduced: the flame spread, represented by the PHRR divided per time of ignition (PHRR/t_{ig}) and the fire load represented by the total heat evolved (THE), which is the THR taken at flame out.

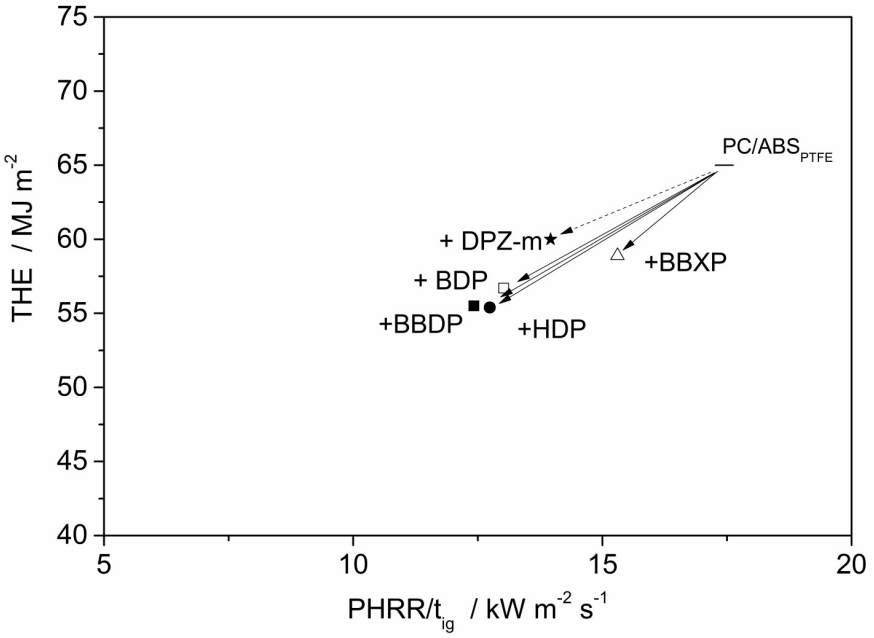

Figure 6.1.1 Assessment of the fire risks according to Petrella at an external heat flux of 70 kW m^{-2} by the addition of single flame retardant in PC/ABS$_{PTFE}$ blends (mean values)

In the case of all flame retardants, both of these main parameters are reduced. The aryl phosphates acted both via a condensed phase and a gas phase action. In the condensed phase, interaction between the decomposing PC with the presence of C-OH groups and the hydrolysed flame retardants formed cross-links and more species remained in the condensed phase. Less pyrolysis gases was then released in the gas phase, which reduced the total heat evolved. Moreover the increased char formed acted as a physical barrier between the flame and the pyrolysis zone against heat, which in turn reduced the temperature in the pyrolysis zone. Phosphorous species were in the same time released in the gas phase. They acted by flame inhibition, and reduced the effective heat of combustion of the pyrolysis gases in the gas phase. Less heat is then produced in the flame that will continue the decomposition of the underlying material. BDP, HDP and BBDP acted effectively through these combined mechanisms for the reduction of the fire risks. BDP, HDP and BBDP achieved a V-0 classification at 3.2mm in PC/ABS$_{PTFE}$, the materials were then fulfilling the UL94 standard for electronics applications in the European zone [6, 101]. However, BBXP aryl phosphate was less efficient in PC/ABS$_{PTFE}$ due to change action because of the substitution. The action in the gas phase and in the condensed phase was slightly reduced compared to BBDP. The reduced actions of the flame retardant played a major role on the fire risks. Both of the fire load and the PHRR/t_{ig} were not reduced so effectively as with BBDP, because less phosphorus reached the gas phase. In the condensed phase, the char formation from BBXP was not increased as much as expected. BBXP decomposed with the formation of aromatic-phosphorous cross-linked species by its own, and the interactions with PC decomposing species was reduced. The char amount was slightly increased, and a barrier effect was observed for BBXP that reduced both fire risks. But the condensed and gas phase mechanisms were not enough to compete with BBDP.

The phosphazene flame retardant showed a different mode of action. DPZ (and DPZ-m) was acting as an intumescent system, where the acidic source role was played by the flame retardant, the carbon-rich source for the formation of char was played by the polycarbonate matrix and the blowing agents came from the flame retardant and the matrix decomposition products. The residues expanded and a multicellular protection layer against heat and mass transport was formed. Even if the blowing of the residue was fast, the char layer formed was not optimal, and the increase in residue of PC/ABS/DPZ$_{PTFE}$ occurred only for higher external heat fluxes under forced flaming conditions. The low overlapping in decomposition temperatures between the phosphazene and the char former PC induced lower interactions in the condensed phase. Moreover the formed char contained big cells, and was sometimes

falling on the side. The barrier protection was thus decreased. Phosphorous and nitrogen-containing species, as blowing agent, were released in the gas phase. The phosphazene acted in the gas phase by flame inhibition and by flame dilution through the release of nitrogen-and phosphorus-containing species. Both main fire risks, the THE and the PHRR/t_{ig} were reduced. If the phosphazene is compared with the aryl phosphates, BDP showed a stronger reduction in both main fire risks, especially on the fire load. The cross-linking interactions of BDP with PC were higher than DPZ, and more char was formed. The increased condensed phase action of BDP compared to the phosphazene induced stronger reduction of the fire risks. DPZ reduced mainly the fire risks thanks to its gas phase action.

The effect of the addition of the single flame retardant was investigated on the rheological properties of the blends. The additives changed the viscosity and the shear stress, mainly depending on the category of the flame retardant (*Figure 6.1.2*). All aryl phosphates reduced the viscosity of the PC/ABS$_{PTFE}$+Aryl phosphate blends, which is in part due to the increase in free volume. The plasticizing effect is really similar for all bridged aryl phosphates. However the effect is reduced in the case of the phosphazene. Plasticizing effect is advantageous for compounding and injection molding. Moreover all single flame retardants possess a flow limit, which is characterized by a plateau in the shear stress at low angular frequency. This is characteristic of the effect of the anti-dripping agent, and confirmed the observation from the UL94 test.

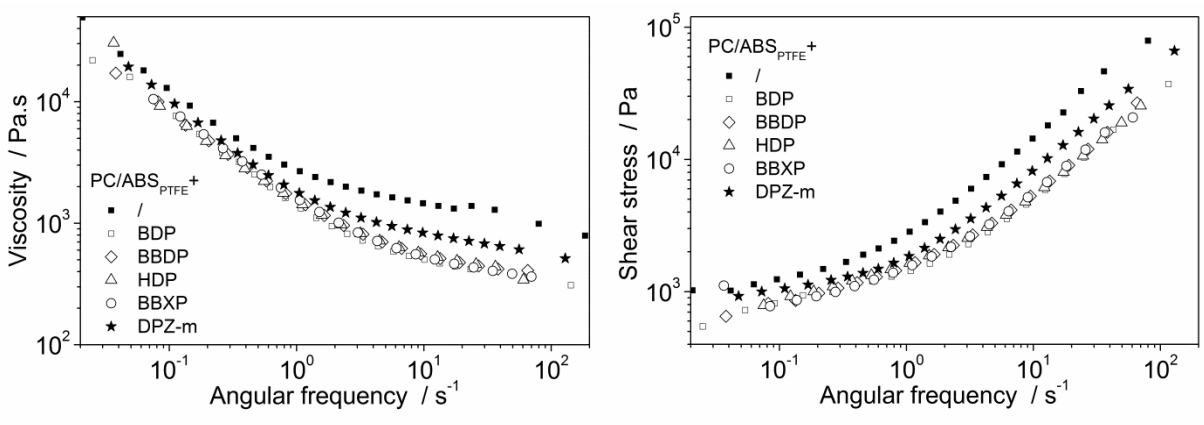

Figure 6.1.2 Effect of the addition of the single flame retardant on the rheological properties of the PC/ABS$_{PTFE}$ blends, on the viscosity at 250°C (left) and on the shear stress (right).

The increased plasticity due to the flame retardant is modifying the glass transition temperatures (T_g) of the blends. PC/ABS$_{PTFE}$ is a two phase blend, and possesses two separated glass transitions. The first Tg originated from the ABS rich phase (Tg of ABS is 382 K), and the second T_g originated from the PC rich-phase (T_g of PC 421 K). Both of these temperatures are reduced by the addition of the flame retardants (*Table 6.1.1*).

Table 6.1.1 Effect of the addition of the single flame retardants on the glass transition temperatures of the blends (T_g).

PC/ABS$_{PTFE}$+	/	BDP	BBDP	HDP	BBXP	DPZ-m
First T_g ± 1°K	382	363	365	363	376	373
Second T_g ± 1°K	416	378	384	379	388	396

The reduced plasticizing effect from the phosphazene is confirmed by the reduced change for both of the first and the second T_g to lower temperature. The dynamics of the flame retardant is thus probably changed due to the presence of the six phenyl ring on the phosphazene ring. Thus the reduced dynamics resulted in a reduction of the apparent viscosity, and is confirmed in the rheological curves of *Figure 6.1.2*.

6.2 Effect of the flame retardant combinations in PC/ABS$_{PTFE}$

Two different combinations containing BDP were tested in PC/ABS$_{PTFE}$, namely BDP:HDP and BDP:DPZ at different ratios. When the synergistic effect index (SE_A) (part 2.3.3) between the two flame retardant is calculated, different effects can be observed between these mixtures, for example on the residue increase in the TGA, *Figure 6.2.1*. A clear synergy is observed in the case of BDP:HDP, with value of SE_A above 1. On the opposite, BDP:DPZ, showed an antagonism in the residue formation, with value of SE_A under 1 for the intermediate mixtures. BDP:HDP worked synergistically in the condensed phase, thanks to the formation of more stable intermediate phosphates, that increased the cross-linking with

polycarbonate decomposition products. This is due to the similar flame retardant mechanisms between BDP and HDP.

On the contrary, the replacement of BDP by DPZ induced a reduced char formation tendency, instead of the hoped synergy between the main gas phase mechanism and intumescent action of DPZ, and the condensed phase action of BDP. The main reason is the reaction of BDP and DPZ which limit the formation of char by cross-linking with PC, but also decreased the intumescence effect from DPZ.

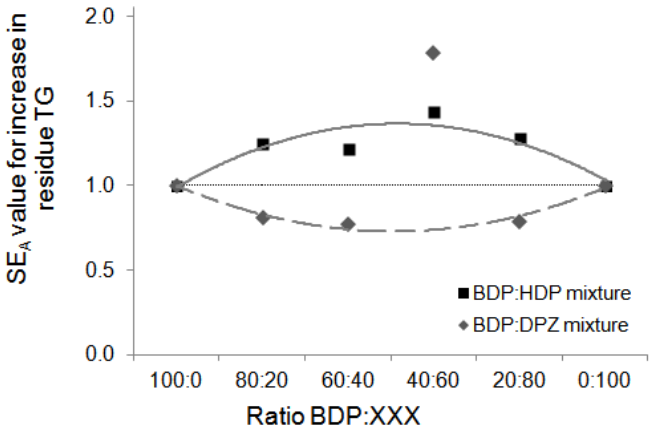

Figure 6.2.1 SEA value on the residue increase in the TGA under nitrogen for PC/ABS$_{PTFE}$+BDP:HDP or BDP:DPZ mixtures

In the forced flaming conditions (cone calorimeter, *Figure 6.2.2*), the synergy on the residue increase observed in the TGA for BDP:HDP is visible at irradiances of 35 and 70 kW m^{-2}, and is predominant for 35 kW m^{-2}. The tendency to antagonism in the residue formation for the BDP:DPZ is low at 35 kW m^{-2} but is more pronounced at 70 kW m^{-2}. For the gas phase action, the THE/ML showed only little synergy in the case of BDP:HDP at 70kW/m^2, the other blends only show superposition.

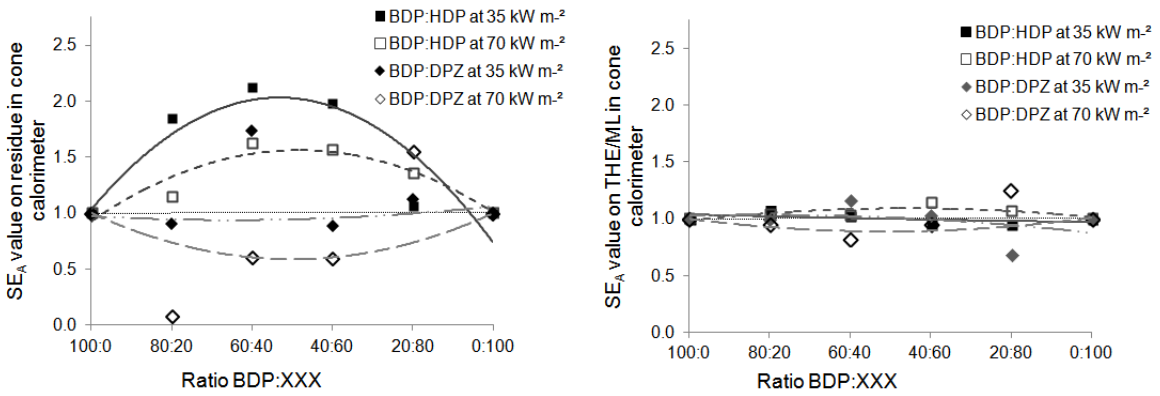

Figure 6.2.2 SEA value on the residue in the cone calorimeter (left) and on the effective heat of combustion THE/ML (right) at 35 and 70 kW m^{-2} for PC/ABS$_{PTFE}$+BDP:HDP or BDP:DPZ mixtures

The influences of the flame retardant mixtures on the two main fire risks are represented in the Petrella plot in *Figure 6.2.3* at 70 kW m^{-2}..

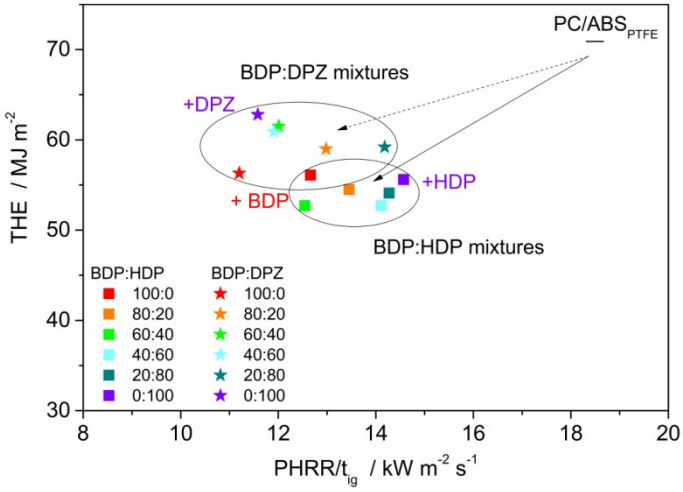

Figure 6.2.3 Assessment of the fire risks according to Petrella at an external heat flux of 70 kW m^{-2} by the addition of the BDP:HDP mixtures or BDP:DPZ mixtures in PC/ABS$_{PTFE}$ blends (mean values)

Both kinds of mixtures reduced the two main fire risks. The formation of the intermediate cross-links for the BDP:HDP blends successfully achieved a better reduction in both parameters. The fire load (THE) is more reduced in the case of the two aryl phosphates mixtures than did the phosphate –phosphazene mixtures, probably due to the increase in

residue formed, that retained PC decomposition products into the condensed phase, and the char layer worked as a physical barrier to heat. In the case of BDP:DPZ mixtures, they worked in a rather antagonistic way, the presence of one reducing the mode of action of the other. No improved flame retardant properties can be achieved

The interactions between the two flame retardants in a mixture played a major role on the thermal decomposition mechanisms and the fire behaviour. The addition of two flame retardants could lead to superposition of the effects, as it is observed in the gas phase, to antagonisms as it can be observed in the residue of PC/ABS$_{PTFE}$+BDP:DPZ with intermediate ratios, or to synergy. Synergy is observed in the condensed phase by the increase in residue for the BDP:HDP mixtures. The synergy between two flame retardants has the advantages, to achieve better flame retardancy performances with the same amount of flame retardant additives in the blends. An increase in flame retardancy is achieved by the combinations of two flame retardants, and the gained properties were not observed by single flame retardant. Synergy is an effective way of protecting flammable material, and the BDP:HDP system gave the best properties in terms of pyrolysis and fire behaviour.

Chapter 7 CONCLUSIONS

Bisphenol A polycarbonate/acrylonitrile-butadiene-styrene (PC/ABS) is an engineering thermoplastic polymer that proved advantageous mechanical and processing properties for electrical engineering and electronics applications like thin wall housings. These applications have however high requirements on flame retardancy. PC/ABS without additives does not fulfil the criteria, and flame retardants are needed to achieve the right level of fire safety. In the past, halogen-containing flame retardants have been commonly used to protect PC/ABS products. However ecological and health concerns have progressively led to their replacement by bromine and chlorine-free systems. Phosphorus-containing flame retardants are one of the adequate alternatives, especially organophosphate esters. The understanding of the mode of action of the flame retardant in the polymer is needed to better improve the flame retardancy concept. The mode of action of the flame retardant is not only depending on its chemical structure but also on its interaction with the surrounding polymer matrix and possible other additives. The interactions of the flame retardant with PC/ABS were studied for some commonly used aryl phosphates, however systematic investigations of structure-properties relationships on newly commercialised aryl phosphates in PC/ABS are missing, and a complete understanding of them is lacking. Phosphorus-containing flame retardants are an emerging class of additives only sporadically investigated in PC/ABS literature, and less is known about their real modes of action. Furthermore combinations of two organic flame retardants based on phosphorus have been rarely fully characterised for this polymer.

In the present work, the mechanisms and mode of action of single oligomeric phosphorus-containing or phosphorus- nitrogen- containing flame retardants were investigated in PC/ABS_{PTFE} depending on the flame retardant structure and the fire behaviour characterized. Combinations of two phosphorus-containing flame retardants were investigated at different ratios in PC/ABS_{PTFE}. The mode of actions and possible interactions or synergy were identified, quantified and discussed.

Bridged aryl bisphosphates with different bridging units (core) and with different side chain unit were varied and tested in PC/$ABS_{PTFE.}$ All of the investigated aryl phosphates act in the gas phase via flame inhibition and in the condensed phase via cross-linking reactions of the phosphate groups with the early decomposing products of PC during pyrolysis. PC

decomposition was shifted to higher temperatures, an increase in residue amount and a change towards a more inorganic-carbonaceous residue occurred.

The change of the aromatic core structure between BDP, HDP and BBDP induced only slight changes in the mode of action of the flame retardant aryl phosphates. BDP and BBDP had similar condensed phase action, and only HDP has a slightly reduced action in the condensed phase due to its lower decomposition temperature. The temperature of decomposition of the flame retardant, corresponding to the occurrence of early decomposition products of PC, is one of the key parameters for the interaction in condensed phase. The interaction between aryl phosphate and PC stabilized the carbonate linkages. One hypothesis is that aryl phosphate reacts more easily via hydrolysis/alcoholysis than PC. The formed acid groups may transesterify the carbonate groups. Moreover, they cross-link with early decomposition products of PC such as Fries rearrangement products.

All aryl phosphates release species containing phosphorus in the gas phase and show their main flame retardancy action by flame inhibition. The predominant mechanism of flame inhibition of all flame retardants influences the performance in the flammability testing. The UL94 rating is enhanced to the best classification V-0 for all of the flame retardants at 3.2 and 1.6 mm thickness, instead of the HB rating of PC/ABS_{PTFE}, the worst classification in this test. The LOI is increased of +5 % O_2 in comparison to the unprotected PC/ABS_{PTFE}. No significant differences were observed for PC/ABS_{PTFE}+BDP, +HDP and +BBDP with respect to fire performance in the cone calorimeter. The peak heat release rate and the fire load (THE) were reduced, quite independently of the aryl core structures.

The change of the side chain unit of the bridged aryl phosphate, by the addition of a 2,6-dimethyl substitution on phenoxy groups between BBDP and BBXP has a much stronger influence on the efficiency of the flame retardant. The condensed phase action was not as efficient in PC/ABS_{PTFE} as for BBDP, and flame inhibition was reduced. Elemental analyses on the residue proved that more phosphorus remained in the condensed phase that is not available for flame inhibition in the gas phase. Competing reactions of decomposition of BBXP occurred, that were not observed for BBDP, because of the higher hydrolytic stability of the flame retardant and the change of the environment of the phosphorus atoms. In this case rearrangements and intra and inter reactions occurred during the decomposition of BBXP. Though these reactions formed more char from BBXP, they deteriorate the flame retardant activity of BBXP in the condensed phase with the decomposition products of PC and in the gas phase, by reducing the amount of phosphorus released.

Further a combination of two aryl phosphates at different flame retardant ratios was added in PC/ABS_{PTFE}: HDP has the lowest residue formation of the aryl phosphate tested previously, and BDP the highest increase in residue formation. When they are combined together in the polymer, an increase in residue was observed in TGA under nitrogen and for residues under well-ventilated conditions in cone calorimeter tests. The char yields were higher compared to the calculation from the superposed actions of both components. A slight synergy was also observed in LOI (between +6.1 and +8.1 % O_2). All of the BDP:HDP combinations induced the best classification V-0 in the UL94 flammability tests, even at 1.6 mm thickness. Investigations of the condensed phase of the binary system BDP+HDP in the 60:40 ratio revealed that both components interact with each other. Intermediate products of higher thermal stability than the volatile HDP are formed. Thus interactions in the condensed phase between aryl phosphates and decomposition products of PC are enhanced and lead to increased charring.

The aryl phosphate mixtures also enable a strong gas-phase action through flame inhibition. The action relates to the phosphorus content introduced in the PC/ABS_{PTFE}+BDP/HDP blends, with increased gas-phase action in the case of the volatile HDP. The overlapping in the decomposition temperature ranges between aryl phosphate and PC is still a prerequisite for the reaction between aryl phosphates and PC. When BDP and HDP are combined, the temperature of the intermediate products overlaps with the decomposition of PC. This aryl phosphate – aryl phosphate synergy is at work in PC/ABS_{PTFE}, with higher or equal amounts of residues obtained than BDP, due to the increased charring of PC in the condensed phase.

A phosphorus-nitrogen-containing flame retardant a tricyclophenoxyphosphazene DPZ was further investigated in PC/ABS_{PTFE}. Stepwise addition in PC or in ABS highlighted the possible interactions between DPZ and the PC/ABS_{PTFE} components. DPZ acts principally in PC, ABS and PC/ABS_{PTFE} in the gas phase, with some minor condensed phase action. In ABS the gas phase action is the only flame retardant mode of action. The flame retardant is completely released in the gas phase, as almost no charring from ABS occurred. The release nitrogen- and phosphorus-containing species act via flame inhibition and flame dilution. The predominant gas phase action is reflected by the results in flammability tests. The LOI value was increased of around +2-3% O_2 compared to literature data, but the UL94 did not changed compared to ABS. The good flame inhibition induced a reduction of the PHRR and the fire load. In PC and PC/ABS_{PTFE}, DPZ acts mainly via flame inhibition and flame dilution, but

also via cross-linking with the decomposing PC thanks to the reactive phosphorous group. Phosphate groups remained in the condensed phase, whereas nitrogen containing species and a part of the phosphorous-containing species were released in the gas phase. DPZ induces an intumescent like effect in PC/ABS_{PTFE}, with a fast increase in the volume of the char formed. However the condensed phase action was not effective, and the residue formed were only slightly increased compared to PC/ABS_{PTFE}. Two main phenomena are responsible for the low increase in char formation. Possible reactions between the amines from the decomposition of DPZ and PC matrix lead to release in the gas phase of decomposition products instead of the formation of char via cross-links. Further the low overlapping in decomposition temperatures between the phosphazene and the char former PC induced lower interactions in the condensed phase. DPZ meliorates the flammability properties of PC/DPZ_{PTFE} and $PC/ABS/DPZ_{PTFE}$, with a change from a V-2 to a V-0 classification in the UL94 test and an increase of the LOI of +14-15% in PC, and a change from HB to V-1 and an increase of +5.3 % of the OI in PC/ABS_{PTFE}. The residue formation under well-ventilated conditions in the cone calorimeter was higher in PC than in PC/ABS_{PTFE}, which indicates that DPZ was better reacting with PC in the absence of ABS, probably because of better overlap of the decomposition temperatures between DPZ and PC in this case.

Finally, DPZ was combined with the char forming BDP at different ratios in $PC/ABS_{PTFE.}$ All the BDP:DPZ combinations acted in the gas phase by flame inhibition and via condensed phase by cross-links with the decomposing polymer matrix. The condensed phase action, and thus the increase in the char formation, was proportional with the amount of BDP in the blend. A superposition effect of both flame retardants was achieved under forced flaming conditions by the combinations of BDP and DPZ in the gas phase, but no synergistic effect between the two flame retardants occurred. In the condensed phase, a superposition tending to an antagonistic effect was observed on the char forming tendency for the mixtures with a ratio close to 1:1. The superposition of the effect of both flame retardant in the mixture is supported in the flammability tests (reaction to a small flame). With increase amount of DPZ in the mixture, the UL94 classifications changed from V-0 to V-1, an increase in the OI between +5.2 and + 6.1 % O_2 was obtained. No phosphorus-nitrogen synergy was observed for these combinations. An analysis of BDP+DPZ 40: 60 binary system indicated that when they are combined, the decomposition of the mixture starts at an earlier time and most of the decomposition products are release before PC decomposition started. On the opposite of

BDP+HDP, the replacement with DPZ reduced the temperature of decomposition, and thus the interaction with decomposing PC.

The occurrence and the efficiency of gas phase or condensed phase activity is dependent on different factors: the decomposition temperature of the polymer matrix, and especially of PC, the hydrolytic stability of the phosphorous groups and the chemical environment of the phosphorous groups. The aryl phosphates BDP, BBDP and to a less extent HDP investigated in this work possess the best properties as single flame retardant in PC/ABS_{PTFE}. The phosphazene is forming fewer cross-links in the condensed phase, and thus a reduced efficiency on the reduction of the main fire risks is obtained. Moreover the use of an aryl phosphate combination based on BDP and HDP enhanced even more the charring of PC in the condensed phase. It was shown that the structure-property relationship of a flame retardant is a key parameter for further optimisation of the flame retardant material. An improvement can be achieved by changing the flame retardant compositions too. This knowledge opens new insight into the flame retardancy concepts of PC/ABS_{PTFE}. Preparing tailored multi component systems is a solution to optimize the performances of products for specific applications.

REFERENCES

1. Bayer Material Science A, Bayblend the Polycarbonate Blend.

2. Grigo U, Kircher K, Mueller PR, Polycarbonate, In: *Kunststoff Handbuch - 3 Technische Thermoplaste: Polycabonate, Polyacetale, Polyester, Celluloseester*, Bottenbruch L, ed., Hanser Verlag, Munich, **1992**.

3. Levchik SV, Weil ED, Flame Retardants in Commercial Use or in Advanced Development in Polycarbonates and Polycarbonate Blends, *Journal of Fire Sciences*, **2006**, 24, 137-151.

4. Levchik SV, Weil ED, Overview of Recent Developments in the Flame Retardancy of Polycarbonates, *Polymer International*, **2005**, 54, 981-998.

5. Weil ED, Levchik SV, Flame Retardants in Commerical Use or Advanced Development in Polycarbonates and Polycarbonate Blends, In: *Flame Retardants for Plastics and Textiles*, Weil ED, Levchik SV, eds., Hanser, **2008**, 121-140.

6. Eckel T, The Most Important Flame Retardant Plastics, In: *Plastics Flammability Handbook*, Troitzsch J, ed., Hanser Verlag, Munich, **2004**, 158-172.

7. Van Krevelen DV, Some Basic Aspects of Flame Resistance of Polymeric Materials, *Polymer*, **1975**, 16, 615-620.

8. Freitag D, Fengler G, L M, Routes to New Aromatic Polycarbonates with Special Material Properties, *Angewandte Chemie International edition*, **1991**, 1598-1610.

9. Green J, Phosphorus-Bromine Flame Retardant Synergy in Polycarbonate/Abs Blends, *Polymer Degradation and Stability*, **1996**, 54, 189-193.

10. Joseph P, Edbdon JR, Recent Developments in Flame-Retarding Thermoplastics, In: *Fire Retardant Materials*, Horrocks A, Price D, eds., Woodhead Publishing, Cambridge, **2001**, 240-243.

11. Lu SY, Hamerton I, Recent Developments in the Chemistry of Halogen-Free Flame Retardant Polymers, *Progress in Polymer Science*, **2002**, 27, 1661-1712.

12. Levchik SV, Weil ED, A Review of Recent Progress in Phosphorus-Based Flame Retardants, *Journal of Fire Sciences*, **2006**, 24, 345-364.

13. Green J, Phosphorus-Containing Flame Retardants, In: *Fire Retardancy of Polymeric Materials*, Grand AF, Wilkie CA, eds., CRC Press, Cambridge, **2000**, 147-170.

14. Joseph P, Ebdon JR, Phosphorus-Based Flame Retardants, In: *Fire Retardancy of Polymeric Materials*, Wilkie CA, Morgan AB, eds. 2nd ed., CRC Press, Boca Raton, **2010**, 107-127.

15. Levchik SV, Bright DA, Moy P, Dashevsky S, New Developments in Fire Retardant Non-Halogen Aromatic Phosphates, *Journal of Vinyl & Additive Technology*, **2000**, 6, 123-128.

16. Levchik SV, Bright DA, Dashevsky S, Moy P, Application and Mode of Fire-Retardant Action of Aromatic Phosphates, In: *Specialty Polymer Additives*, Al-Malaika S, Golovoy A, Wilkie CA, eds., Blackwell Science, Oxford, **2001**, 259.

17. Wilkie CA, McKinney MA, Thermal Properties and Burning Behavior of the Most Important Plastics, In: *Plastics Flammability Handbook, 3rd Ed*, Troitzsch J, ed., Hanser Verlag, Munich, **2004**, 124-127.

18. Price D, Anthony G, Carty P, Introduction: Polymer Combustion, Condensed Phase Pyrolysis and Smoke Formation, In: *Fire Retardant Materials*, Horrocks AR, Price D, eds., Woodhead Publishing, Cambridge, **2001**, 14-19.

19. Di Blasi C, The Combustion Process, In: *Plastics Flammabilty Handbook*, Troitzsch J, ed. 3rd ed., Hanser Verlag, Munich, **2004**.

20. Lewin M, Weil ED, Mechanisms and Modes of Action in Flame Retardancy of Polymers, In: *Fire Retardant Materials*, Horrocks A, Price D, eds., Woodhead Publishing, Cambridge, **2001**, 30-68.

21. Lyon RE, Janssens ML, Polymer Flammability, **2005**. No. DOT/FAA/AR-05/14.

22. Lyon RE, Walters RN, Stoliarov SI, Thermal Analysis of Polymer Flammability, *Abstracts of Papers of the American Chemical Society*, **2004**, 228, U439-U439.

23. Hastie JW, Molecular Basis of Flame Inhibition, *Journal of Research of the National Bureau of Standards Section a-Physics and Chemistry*, **1973**, A 77, 733-754.

24. Granzow A, Flame Retardation by Phosphorus Compounds, *Accounts of Chemical Research*, **1978**, 11, 177-183.

25. Lyon R, Solid-State Thermochemistry of Flaming Combustion, In: *Fire Retardancy of Polymeric Materials*, Grand AF, Wilkie CA, eds., Marcel Dekker Inc, New York, **2000**, 391-447.

26. Lyon R, Plastics and Rubber, In: *Handbook of Building Materials for Fire Protection*, Harper CA, ed., Mc Graw-Hill, New York, **2004**, 3.1-3.51.

27. Rutkowski JV, Levin BC, Acrylonitrile Butadiene Styrene Copolymers (ABS) - Pyrolysis and Combustion Products and Their Toxicity - a Review of the Literature, *Fire and Materials*, **1986**, 10, 93-105.

28. Yang MH, The Thermal Degradation of Acrylonitrile-Butadiene-Styrene Terpolymer under Various Gas Conditions, *Polymer Testing*, **2000**, 19, 105-110.

29. Dicortemiglia MPL, Camino G, Costa L, Guaita M, Thermal Degradation of ABS, *Thermochimica Acta*, **1985**, 93, 187-190.

30. Wilkie CA, McKinney MA, Thermal Properties and Burning Behavior of the Most Important Plastics, In: *Plastics Flammability Handbook, 3rd Ed*, Troitzsch J, ed., Hanser Verlag, Munich, **2004**, 72-73.

31. Factor A, Char Formation in Aromatic Engineering Polymers, In: *Fire and Polymers Hazards Identification and Prevention Acs Symposium Series*, Nelson GL, ed., ACS, Washington, **1990**, 274-287.

32. Levchik SV, Wilkie CA, Char Formation, In: *Fire Retardancy of Polymeric Materials*, Grand AF, Wilkie CA, eds. 3rd edition ed., Marcel Dekker, New York, **2000**, 171-215.

33. Duquesne S, Bourbigot S, Char Formation and Characterization, In: *Fire Retardancy of Polymeric Materials*, Wilkie CA, Morgan AB, eds., CRC Press, Boca Raton, **2010**, 239-259.

34. Stoliarov SI, Crowley S, Walters RN, Lyon RE, Prediction of the Burning Rates of Charring Polymers, *Combustion and Flame*, **2010**, 157, 2024-2034.

35. Bottenbruch L, Technische Thermoplaste: Polycarbonate, Polyacetale, Polyester, Celluloseester. Kunststoff-Handbuch, Carl Hanser, Munich, **1992**.

36. Eckel T, Janke N, Peucker U, Seidel A, Wittmann D, Flame-Resistant Polycarbonate Compositions, *Patent EP 1 309 655 (A1)*, Assigned to Bayer AG, **2002**.

37. Bozi J, Czegeny Z, Meszaros E, Blazso M, Thermal Decomposition of Flame Retarded Polycarbonates, *Journal of Analytical and Applied Pyrolysis*, **2007**, 79, 337-345.

38. Landry S, Changing Chemical Regulations and Demands, In: *Fire Retardancy of Polymeric Materials*, Wilkie CA, Morgan AB, eds. 2nd ed., CRC Press, Boca Raton, **2010**, 671-702.

39. Lyon RE, Emrick T, Non-Halogen Fire Resistant Plastics for Aircraft Interiors, *Polymers for Advanced Technologies*, **2008**, 19, 609-619.

40. Babrauskas V, Simonson M, Fire Behaviour of Plastic Parts in Electrical Appliances—Standards Versus Required Fire Safety Objectives, *Fire and Materials*, **2007**, 31, 83-96.

41. Weil ED, Levchik SV, Ravey M, Zhu WM, A Survey of Recent Progress in Phosphorus-Based Flame Retardants and Some Mode of Action Studies, *Phosphorus Sulfur and Silicon and the Related Elements*, **1999**, 146, 17-20.

42. Jang BN, Jung I, Choi J, Study of a Novel Halogen-Free Flame Retardant System through TGA and Structure Analysis of Polymers, *Journal of Applied Polymer Science*, **2009**, 112, 2669-2675.

43. Green J, Mechanisms for Flame Retardancy and Smoke Suppression -a Review, *Journal of Fire Sciences*, **1996**, 14, 426-442.

44. Bright DA, Dashevsky S, Moy P, Williams B, Resorcinol Bis(Diphenylphosphate), a Non-Halogen Flame-Retardant Additive, *Journal of Vinyl & Additive Technology*, **1997**, 3, 170-174.

45. Murashko EA, Levchik GF, Levchik SV, Bright DA, Dashevsky S, Fire Retardant Action of Resorcinol Bis(Diphenyl Phosphate) in a PC/ABS Blend. I. Combustion Performance and Thermal Decomposition Behavior, *Journal of Fire Sciences*, **1998**, 16, 278-296.

46. Pawlowski KH, Schartel B, Flame Retardancy Mechanisms of Triphenyl Phosphate, Resorcinol Bis(Diphenyl Phosphate) and Bisphenol Bis(Diphenyl Phosphate) in Polycarbonate/Acrylonitrile-Butadiene-Styrene Blends, *Polymer International*, **2007**, 56, 1404-1414.

47. Davis A, Golden JH, Stability of Polycarbonate, *Journal of Macromolecular Science-Reviews in Macromolecular Chemistry*, **1969**, C 3, 49-68.

48. Schartel B, Pawlowski KH, Perret B, Pmse 152-Flame Retardancy Mechanisms in Halogen-Free PC/ABS Blends, *Abstracts of Papers of the American Chemical Society*, **2008**. 1053.

49. Camino G, Costa L, Luda di Cortemiglia MP, Overview of Fire Retardant Mechanisms, *Polymer Degradation and Stability*, **1991**, 33, 131-154.

50. Schartel B, Phosphorus-Based Flame Retardancy Mechanisms-Old Hat or a Starting Point for Future Development?, *Materials*, **2010**, 3, 4710-4745.

51. Fenimore CP, Jones GW, Phosphorus in the Burnt Gas from Fuel-Rich Hydrogen-Oxygen Flames, *Combustion and Flame*, **1964**, 8, 133-137.

52. Bourbigot S, Le Bras M, Flame Retardants, In: *Plastics Flammability Handbook*, Troitzsch J, ed. 3rd. ed., Hanser, Munich, **2004**, 133-157.

53. Camino G, Lomakin S, Intumescent Materials, In: *Fire Retardant Materials*, Horrocks A, Price D, eds., Woodhead Publishers Limited, Cambridge, **2001**, 328-333.

54. Bourbigot S, Duquesne S, Intumescence-Based Fire Retardants, In: *Fire Retardancy of Polymeric Materials*, Wilkie CA, Grand AF, eds. 2nd ed., CRC Press, Boca raton, **2010**, 129-158.

55. Bourbigot S, Lebras M, Delobel R, Breant P, Tremillon JM, Carbonization Mechanisms Resulting from Intumescence .2. Association with an Ethylene Terpolymer and the Ammonium Polyphosphate Pentaerythritol Fire-Retardant System, *Carbon*, **1995**, 33, 283-294.

56. Jang BN, Wilkie CA, A TGA/FTIR and Mass Spectral Study on the Thermal Degradation of Bisphenol a Polycarbonate, *Polymer Degradation and Stability*, **2004**, 86, 419-430.

57. Murashko EA, Levchik GF, Levchik SV, Bright DA, Dashevsky S, Fire-Retardant Action of Resorcinol Bis(Diphenyl Phosphate) in PC-ABS Blend. II. Reactions in the Condensed Phase, *Journal of Applied Polymer Science*, **1999**, 71, 1863-1872.

58. Perret B, Pawlowski KH, Schartel B, Fire Retardancy Mechanisms of Arylphosphates in Polycarbonate (PC) and PC/Acrylonitrile-Butadiene-Styrene - the Key Role of Decomposition Temperature, *Journal of Thermal Analysis and Calorimetry*, **2009**, 97, 949-958.

59. Wawrzyn E, Schartel B, Ciesielski M, Kretzschmar B, Braun U, Döring M, Are Novel Aryl Phosphates Competitors for Bisphenol a Bis(Diphenyl Phosphate) in Halogen-Free Flame-Retarded Polycarbonate/Acrylonitrile-Butadiene-Styrene Blends?, *European Polymer Journal*, **2012**, 48, 1561-1574.

60. Lee K, Yoon K, Kim J, Bae J, Yang J, Hong S, Effect of Novolac Phenol and Oligomeric Aryl Phosphate Mixtures on Flame Retardance Enhancement of ABS, *Polymer Degradation and Stability*, **2003**, 81, 173-179.

61. Lopez-Cuesta J-M, Laoutid F, Multicomponent Fr Systems: Polymer Nanocomposites Combined with Additional Materials, In: *Fire Retardancy of Polymeric Materials*, Wilkie CA, Morgan AB, eds. 2nd ed., CRC Press, Boca Raton, **2010**, 309-313.

62. Feyz E, Jahani Y, Esfandeh M, Effect of a Nanoclay/Triphenyl Phosphate Hybrid System on the Fire Retardancy of Polycarbonate/Acrylonitrile–Butadiene–Styrene Blend, *Journal of Applied Polymer Science*, **2011**, 120, 3435-3442.

63. Feyz E, Jahani Y, Esfandeh M, Comparison of the Effect of an Organoclay, Triphenylphosphate, and a Mixture of Both on the Degradation and Combustion Behaviour of CABS Blends, *Macromolecular Symposia*, **2010**, 298, 130-137.

64. Levchik SV, Weil ED, Developments in Phosphorus Flame Retardants, In: *Advances in Fire Retardant Materials*, Horrocks A, Price D, eds., Woodhead Publishing, Cambridge, **2008**, 42-43.

65. Pawlowski KH, Schartel B, Flame Retardancy Mechanisms of Aryl Phosphates in Combination with Boehmite in Bisphenol a Polycarbonate/Acrylonitrile-Butadiene-Styrene Blends, *Polymer Degradation and Stability*, **2008**, 93, 657-667.

66. Pawlowski KH, Schartel B, Fichera MA, Jager C, Flame Retardancy Mechanisms of Bisphenol A Bis(Diphenyl Phosphate) in Combination with Zinc Borate in Bisphenol A Polycarbonate/Acrylonitrile-Butadiene-Styrene Blends, *Thermochimica Acta*, **2010**, 498, 92-99.

67. Tang Z, Li Y, Zhang YJ, Jiang P, Oligomeric Siloxane Containing Triphenylphosphonium Phosphate as a Novel Flame Retardant for Polycarbonate, *Polymer Degradation and Stability*, **2012**, 97, 638-644.

68. Iji M, Serizawa S, Silicone Derivatives as New Flame Retardants for Aromatic Thermoplastics Used in Electronic Devices, *Polymers for Advanced Technologies*, **1998**, 9, 593-600.

69. Wawrzyn E, Schartel B, Seefeldt H, Karrasch A, Jäger C, What Reacts with What in Bisphenol a Polycarbonate/Silicon Rubber/Bisphenol A Bis(Diphenyl Phosphate) During Pyrolysis and Fire Behavior?, *Industrial & Engineering Chemistry Research*, **2011**, 51, 1244-1255.

70. Weil ED, Synergists, Adjuvants, and Antagonists in Flame-Retardant Systems, In: *Fire Retardancy of Polymeric Materials*, Grand AF, Wilkie CA, eds., Woodhead Publishing, Cambridge, **2000**, 123-129.

71. Eckel T, Bödinger M, Wittmann D, Alberts H, Horn K, Flame-Resistant Polycarbonate Moulding Materials Which Are Dimensionally Stable at High Temperatures and Have High Flow Line Strength, *Patent EP 0983 315*, Assigned to Bayer Material Science, AG, **1998**.

72. Eckel T, Wittmann D, Oeller M, Alberts H, Flame-Retardant, Stress Crack Resistant Polycarbonate Abs Moulding Composition, *Patent EP 0640655*, Assigned to Bayer AG, **1994**.

73. Weil ED, Zhu W, Patel N, Mukhopadhyay SM, A Systems Approach to Flame Retardancy and Comments on Modes of Action, *Polymer Degradation and Stability*, **1996**, 54, 125-136.

74. Willard JJ, Wondra RE, Quantitative Evaluation of Flame-Retardant Cotton Finishes by Limiting-Oxygen Index (LOI) Technique, *Textile Research Journal*, **1970**, 40, 203-210.

75. Gaan S, Sun G, Hutches K, Engelhard MH, Effect of Nitrogen Additives on Flame Retardant Action of Tributyl Phosphate: Phosphorus-Nitrogen Synergism, *Polymer Degradation and Stability*, **2008**, 93, 99-108.

76. Maruyama K, Motoshige R, Flame Retardant Thermoplastic Resin Composition, *Patent EP 0728811 B1*, Assigned to Mitsubishi, **2003**.

77. Sato I, Flame Retardant Polycarbonate Resin Composition, *Patent EP 1548065*, Assigned to Sumito Dow, **2005**.

78. Shaw RA, Smith BC, Fitzsimmons BW, Phosphazenes (Phosphonitrilic Compounds), *Chemical Reviews*, **1962**, 62, 247-281.

79. Lyon RE, Speitel L, Walters RN, Crowley S, Fire-Resistant Elastomers, *Fire and Materials*, **2003**, 27, 195-208.

80. Allcock HR, Recent Advances in Phosphazene (Phosphonitrilic) Chemistry, *Chemical Reviews*, **1972**, 72, 315-356.

81. Allen CW, The Use of Phosphazenes as Fire Resistant Materials, *Journal of Fire Sciences*, **1993**, 11, 320-328.

82. Liu R, Wang X, Synthesis, Characterization, Thermal Properties and Flame Retardancy of a Novel Nonflammable Phosphazene-Based Epoxy Resin, *Polymer Degradation and Stability*, **2009**, 94, 617-624.

83. Facchin G, Guarino L, Modesti M, Minto F, Gleria M, Thermosetting Resins and Azo Dyes Based on Phosphazenes, *Journal of Inorganic and Organometallic Polymers*, **1999**, 9, 133-150.

84. Gleria M, De Jaeger R, Aspects of Phosphazene Research, *Journal of Inorganic and Organometallic Polymers*, **2001**, 11, 1-45.

85. El Gouri M, El Bachiri A, Hegazi SE, Rafik M, El Harfi A, Thermal Degradation of a Reactive Flame Retardant Based on Cyclotriphosphazene and Its Blend with DGEBA Epoxy Resin, *Polymer Degradation and Stability*, **2009**, 94, 2101-2106.

86. Muraki T, Ueta M, Ihara E, Inoue K, Enhancement of Thermal Stability of Polystyrene and Poly(Methyl Methacrylate) by Cyclotriphosphazene Derivatives, *Polymer Degradation and Stability*, **2004**, 84, 87-93.

87. Levchik GF, Grigoriev YV, Balabanovich AI, Levchik SV, Klatt M, Phosphorus-Nitrogen Containing Fire Retardants for Poly(Butylene Terephthalate), *Polymer International*, **2000**, 49, 1095-1100.

88. Lim JC, Flame Retardant Thermoplastic Resin Composition, *Patent US 6630524*, Assigned to Cheil, **2003**.

89. Lim JC, Seo GH, Yang SJ, Suh GH, Flame Retardant Thermoplastic Resin Composition Comprising a Polycarbonate Resin, a Rubber Modified Graft Copolymer and a Flame Retardent, *Patent KR2003055443-A*, Assigned to Cheil Ind Inc, **2003**.

90. Kurose T, Takahashi T, Sugimoto M, Taniguchi T, Koyama K, Uniaxial Elongational Viscosity of PC/a Small Amount of PTFE Blend, *Nihon Reoroji Gakkaishi*, **2005**, 33, 173-182.

91. Nishihara H, Tanji S, High-Order Structure and Flame Retardation Effect of Poly(Tetrafluoroethylene) in Thermoplastic Resin Compositions, *Polymer Journal*, **1998**, 30, 322-326.

92. Lewin M, Synergism and Catalysis in Flame Retardancy of Polymers, *Polymers for Advanced Technologies*, **2001**, 12, 215-222.

93. Lewin M, Synergistic and Catalytic Effects in Flame Retardancy of Polymeric Materials-an Overview, *Journal of Fire Sciences*, **1999**, 17, 3-19.

94. Weil ED, Additivity, Synergism and Antagonism in Flame Retardancy, In: *Flame Retardancy of Polymeric Materials*, Kuryla WC, Papa AJ, eds., Marcel Dekker, New York, **1975**, 185-243.

95. Wu GM, Schartel B, Yu D, Kleemeier M, Hartwig A, Synergistic Fire Retardancy in Layered-Silicate Nanocomposite Combined with Low-Melting Phenysiloxane Glass, *Journal of Fire Sciences*, **2012**, 30, 69-87.

96. Hatakeyama K, Quinn FX, Thermal Analysis Fundamentals and Applications to Polymer Science, 2nd ed, John Wiley & Sons Ltd., New York, **1999**.

97. Price DM, Hourston DJ, Dumont F, Thermogravimetry of Polymers, In: *Encyclopedia of Analytical Chemistry*, Meyers RA, ed., John Wiley Sons Ltd, Chichester, **2000**.

98. Wunderlich B, Thermal Analysis of Polymeric Materials, Springer, Berlin, **2005**.

99. Materazzi S, Thermogravimetry- Infrared Spectroscopy (TG-FTIR) Coupled Analysis, *Applied Spectroscopy Reviews*, **1997**, 32:4, 385-404.

100. Kunze R, Schartel B, Bartholmai M, Neubert D, Schriever R, TG-MS and TG-FTIR Applied for an Unambiguous Thermal Analysis of Intumescent Coatings, *Journal of Thermal Analysis and Calorimetry*, **2002**, 70, 897-909.

101. UL94 - Standard for Flammability of Plastic Materials for Parts in Devices and Appliances, Underwriters Laboratories Inc., **2009**.

102. IEC 60695-11-10: 1999 - Fire Hazard Testing - Part 11-10: Test Flames - 50 W Horizontal and Vertical Flame Test Methods, **1999**.

103. Kempel F, Schartel B, Marti JM, Butler KM, Rossi R, Idelsohn SR, et al., Modelling the Vertical Ul 94 Test: Competition and Collaboration between Melt Dripping, Gasification and Combustion, *Fire and Materials*, **2015**, 39, 570-584.

104. EN ISO 4589-2:1999/A1:2006 - Determination of Burning Behaviour by Oxygen Index - Part 2: Ambient-Temperature Test, **2006**.

105. ISO 5660-1:2002 - Reaction-to-Fire Tests - Heat Release, Smoke Production and Mass Loss Rate - Part 1: Heat Release Rate (Cone Calormeter Method), **2002**.

106. ISO 5660-2:2002 - Reaction-to-Fire Tests - Heat Release, Smoke Production and Mass Loss Rate - Part 2: Smoke Production Rate (Dynamic Measurement), **2002**.

107. ISO 5660-3:2003 - Reaction-to-Fire Tests - Heat Release, Smoke Production and Mass Loss Rate - Part 3: Guidance on Measurement, **2002**.

108. Babrauskas V, Development of the Cone Calorimeter - a Bench-Scale Heat Release Rate Apparatus Based on Oxygen-Consumption, *Fire and Materials*, **1984**, 8, 81-95.

109. Schartel B, Hull TR, Development of Fire-Retarded Materials - Interpretation of Cone Calorimeter Data, *Fire and Materials*, **2007**, 31, 327-354.

110. Schartel B, Bartholmai M, Knoll U, Some Comments on the Use of Cone Calorimeter Data, *Polymer Degradation and Stability*, **2005**, 88, 540-547.

111. Davis A, Golden JH, Thermal Degradation of Polycarbonate, *Journal of the Chemical Society B-Physical Organic*, **1968**, 45-47.

112. Suzuki M, Wilkie CA, The Thermal Degradation of Acrylonitrile-Butadiene-Styrene Terpolymer as Studied by Tga/Ftir, *Polymer Degradation and Stability*, **1995**, 47, 217-221.

113. Politou AS, Morterra C, Low MJD, Infrared Studies of Carbons .12. The Formation of Chars from a Polycarbonate, *Carbon*, **1990**, 28, 529-538.

114. Lee LH, Mechanisms of Thermal Degradation of Phenolic Condensation Polymers .I. Studies on the Thermal Stability of Polycarbonate, *Journal of Polymer Science Part a-General Papers*, **1964**, 2, 2859-2873.

115. Davis A, Golden JH, Competition between Scission and Cross-Linking Processes in Thermal Degradation of a Polycarbonate, *Nature*, **1965**, 206, 397.

116. Davis A, Golden JH, Degradation of Polycarbonates. 3. Viscosimetric Study of Thermally-Induced Chain Scission *Makromolekulare Chemie*, **1964**, 78, 16-23.

117. Montaudo G, Carroccio S, Puglisi C, Thermal and Themoxidative Degradation Processes in Poly(Bisphenol A Carbonate), *Journal of Analytical and Applied Pyrolysis*, **2002**, 64, 229-247.

118. Karrasch A, Wawrzyn E, Schartel B, Jäger C, Solid-State NMR on Thermal and Fire Residues of Bisphenol A Polycarbonate/Silicone Acrylate Rubber/Bisphenol A Bis(Diphenyl-Phosphate)/ (PC/SiR/BDP) and PC/SiR/BDP/Zinc Borate (PC/SiR/DP/ZnB) - Part I: PC Charring and the Impact of BDP and ZnB, *Polymer Degradation and Stability*, **2010**, 95, 2525-2533.

119. Jang BN, Wilkie CA, The Effects of Triphenylphosphate and Recorcinolbis(Diphenylphosphate) on the Thermal Degradation of Polycarbonate in Air, *Thermochimica Acta*, **2005**, 433, 1-12.

120. Täuber K, Hyperbranched Polyphosphates as Novel Flame Retarding Materials [Master Thesis], Free University Berlin, **2014**.

121. Braun U, Schartel B, Fichera MA, Jager C, Flame Retardancy Mechanisms of Aluminium Phosphinate in Combination with Melamine Polyphosphate and Zinc Borate in Glass-Fibre Reinforced Polyamide 6,6, *Polymer Degradation and Stability*, **2007**, 92, 1528-1545.

122. Dittrich B, Wartig KA, Hofmann D, Mulhaupt R, Schartel B, Flame Retardancy through Carbon Nanomaterials: Carbon Black, Multiwall Nanotubes, Expanded Graphite, Multi-Layer Graphene and Graphene in Polypropylene, *Polymer Degradation and Stability*, **2013**, 98, 1495-1505.

123. Seefeldt H, Braun U, Burning Behavior of Wood-Plastic Composite Decking Boards in End-Use Conditions: The Effects of Geometry, Material Composition, and Moisture, *Fire Science*, **2011**.

124. Bel'skii VE, Kinetics of the Hydrolysis of Phosphate Esters, *Russian Chemical Reviews*, **1977**, 46, 828-841.

125. Factor A, The High-Temperature Degradation of Poly(2,6-Dimethyl-1,4-Phenylene Ether), *Journal of Polymer Science Part A-1: Polymer Chemistry*, **1969**, 7, 363-377.

126. Factor A, Finkbein.H, Jerussi RA, White DM, Thermal Rearrangement of Ortho Methyldiaryl Ethers, *Journal of Organic Chemistry*, **1970**, 35, 57-&.

127. Oba K, Ishida Y, Ito Y, Ohtani H, Tsuge S, Characterization of Branching and/or Cross-Linking Structures in Polycarbonate by Reactive Pyrolysis-Gas Chromatography in the Presence of Organic Alkali, *Macromolecules*, **2000**, 33, 8173-8183.

128. Montaudo G, Puglisi C, Thermal Decomposition Processes in Bisphenol A Polycarbonate, *Polymer Degradation and Stability*, **1992**, 37, 91-96.

129. Corbridge DEC, Lowe EJ, The Infra-Red Spectra of Some Inorganic Phosphorus Compounds, *Journal of the Chemical Society (Resumed)*, **1954**, 493-502.

130. Allcock HR, Hartle TJ, Taylor JP, Sunderland NJ, Organic Polymers with Cyclophosphazene Side Groups: Influence of the Phosphazene on Physical Properties and Thermolysis, *Macromolecules*, **2001**, 34, 3896-3904.

131. Allcock HR, Taylor JP, Phosphorylation of Phosphazenes and Its Effects on Thermal Properties and Fire Retardant Behavior, *Polymer Engineering and Science*, **2000**, 40, 1177-1189.

132. Schartel B, Braun U, Pawlowski KH, Phosphorus-Containing Polymeric Materials: The Impact of Pyrolysis on Flame Retardancy, In: Conference Proceedings, ed. *Interflam 2007*, Interscience Communications Limited, Greenwich, **2007**. 71-78.

133. Ballistreri A, Foti S, Lora S, Pezzin G, Electron Impact Mass Spectra of Some Hexa-Aryloxy- and -Arylamino-Cyclotriphosphazenes, *Organic Mass Spectrometry*, **1985**, 20, 165-167.

134. Ballistreri A, Foti S, Montaudo G, Lora S, Pezzin G, Mass Spectrometric Characterization and Thermal Decomposition Mechanism of Some Poly(Organophosphazenes), *Die Makromolekulare Chemie*, **1981**, 182, 1319-1326.

135. Levchik SV, Camino G, Luda MP, Costa L, Lindsay A, Stevenson D, Thermal Decomposition of Cyclotriphosphazenes. I. Alkyl-Aminoaryl Ethers, *Journal of Applied Polymer Science*, **1998**, 67, 461-472.

136. Zhang T, Cai Q, Wu DZ, Jin RG, Phosphazene Cyclomatrix Network Polymers: Some Aspects of the Synthesis, Characterization, and Flame-Retardant Mechanisms of Polymer, *Journal of Applied Polymer Science*, **2005**, 95, 880-889.

137. Carty P, White S, A Synergistic Organoiron Flame-Retarding/Smoke-Suppressing System for ABS, *Applied Organometallic Chemistry*, **1991**, 5, 51-56.

138. Petrella RV, The Assessment of Full-Scale Fire Hazards from Cone Calorimeter Data *Journal of Fire Sciences*, **1994**, 12, 14-43.

LIST OF PUBLICATIONS AND PRESENTATIONS

- Marie-Claire Despinasse, Bernhard Schartel

  "Aryl phosphates and Phosphazene Flame Retardants in Polycarbonate/Acrylonitrile-Butadiene-Styrene Blends"

  13th European Meeting on Fire Retardant Polymers FRPM'11, Alessandria, Italy,26th-30th June **2011**

- Marie-Claire Despinasse, Berhard Schartel

  "Influence of the structure of aryl phosphates on the flame retardancy of polycarbonate/acrylonitrile-butadiene-styrene"

  Polymer Degradation and Stability, **2012**, 97, 2571-2580.

- Marie-Claire Despinasse, Bernhard Schartel

  "Halogen-free flame retardant combinations in Polycarbonate/Acrylonitrile-butadiene-styrene: possible routes towards a P-P synergy?"

  ISFRMT 2012, 2nd International Symposium on Flame-Retardant Materials & Technologies, Chengdu, China, 16th-19th September **2012**.

- Marie-Claire Despinasse, Bernhard Schartel

  "Aryl Phosphate–Aryl Phosphate Synergy in Flame-Retarded Bisphenol A Polycarbonate/Acrylonitrile-Butadiene-Styrene"

  Thermochimica Acta, **2013**, 563, 51-61

APPENDIX

A.1 Preparation of the materials

BDP contains 2.5 wt.% of TPP and had an averaged repeating unit of n=1.1. BBDP had a repeating unit of n=1-5. HDP had a purity of 98%, and n=1-5. BBXP contained 1.8 wt.% of TPP, and the average repeating unit was n=1.0. DPZ contained 99.8% of the tricyclic phenoxy phosphazene, and DPZ-m contained 70% of the tricyclic phenoxyphosphazene, 20% of the cyclic tetramer of phenoxyphosphazene and 10% of linear oligomers.

For the unbranched PC, the solution viscosity in methylene chloride, at 25°C and a concentration of 0.5 g per 100 ml, was 1.28. The ratio for A:B:S was 21:13:66 for ABS and 58:30:12 for ABS 2. For the blends, the ratio PC:ABS was maintained at 4.7:1. All the materials indicated by the subscript PTFE contained 0.45 wt% of polytetrafluoroethylene (PTFE) as anti-dripping agent. An optimal dispersion in the polymer matrix is achieved by using PTFE in the form of a masterbatch with Styrene-acrylonitrile SAN.

The materials were compounded using a twin-screw extruder (ZSK-25, Werner und Pfleiderer) at a rotary speed of 225 rpm and with a throughput of 20 kg h^{-1} at a temperature of 260°C. The test specimens were prepared from the finished granulates by injection molding (Type Arburg 270E, melt temperature 240°C, mould temperature 80°C, melt front speed 240 mm s^{-1}). All materials were provided by Bayer MaterialScience AG (Germany), as powder or liquid for the flame retardants, and as granulate as well as injection molded test specimens for the blends.

The binary system BDP+HDP 60:40 was prepared by hand premixing at room temperature or above the melting temperature of both components (383 K) for 5 minutes in the alumina pan before introduction in the TGA. A mass of around 10 mg of the mixture was prepared (5.973 mg BDP and 4.084 mg HDP. experimental mass ratio 59.4:40.6). For Linkam hot stage measurement of the BDP+HDP system, the melted mixture was applied to a KBr window as a thin film. The binary system BDP+DPZ 40:60 was prepared in the same manner (4.855 mg BDP and 4.914 mg DPZ-m, experimental mass ratio 49.7:50.3, equivalent to the ratio in phosphorus origin 40:60).

A.2 Methods and experimental parameters for pyrolysis and fire behaviour

Thermogravimetry

Thermogravimetric analysis (TGA) was performed using a TG 209 ASC F1 Iris (Netzsch Instrument. Germany) Solid, powder or liquid samples of 10±0.1 mg were heated in alumina pans under nitrogen flow (30 ml min^{-1}. purity 99.999 %) at a heating rate of 10 K min^{-1} up to 1173 K at atmospheric pressure. Values for the residue in TGA were taken at the end of the last decomposition step (between 812 and 816 K). All measurements have been corrected for buoyancy forces and the measurements repeated to insure reproducibility.

Evolved gas analysis

The TG was coupled with a Fourier transformed infrared (FTIR) spectrometer Tensor 27 (Bruker, Germany). The pyrolysis gases produced during the thermal decomposition have been continuously transferred into the analysis cell. The coupling element was a transfer tube (transfer line) with an inner diameter of 1 mm between TG and gas cell. The gas cell of the FTIR and the transfer line were maintained at 503 K to avoid condensation. The FTIR spectrometer was equipped with a liquid nitrogen cooled mercury-cadmium-tellurium LN-MCT detector operating with an optical resolution of 4 cm^{-1} in the wavenumber range 4000-600 cm^{-1}. The spectra were recorded every 14 seconds. A single spectrum was extracted for each decomposition step to identify the evolved gases. The evaluation of the spectra occurred by the attribution of the characteristic vibrational bands and by the comparison with reference spectra from different databases (e.g. Nicolet Vapor Phase).

To confirm the results of the TG-FTIR in case of unambiguity, the TG was coupled with a quadrupole mass spectrometer (TG-MS, Aeolos QMS 403 C, Netzsch, Germany) in multiple ion detection mode (MID) by electron ionization at 70 eV with two iridium cathodes. Nitrogen or helium gas carrier was used to transport the gas species to the spectrometer. A quartz capillary system reduced the pressure continuously from atmospheric pressure down to high vacuum between the TG and the quadrupole. The capillary has a small internal diameter and was kept at 503K. Because of the technical limitation of the apparatus, only species with a mass-to-charge ratio under 150 a.m.u were monitored.

Condensed phase analysis

The change in the condensed phase were analysed by transmission in a FTIR spectrometer (Vertex 70, Bruker, Germany) equipped with a heatable hot stage cell (FTIR 600 Linkam hot stage, Linkam Scientific Instruments Ltd., United Kingdom). The material in powder form was melted on a KBr window to form a thin film, and then let cooled down to room temperature. The KBr window was hold by a clamp in the Linkam cell. The sample was heated up from 298 to 903 K at a heating rate of 10 K min^{-1} under a nitrogen flow of 200 ml min^{-1}. FTIR spectra have been recorded in a wavenumber range of 4000-400 cm^{-1} with an optical resolution of 4 cm^{-1}. A deuterium lanthanide triglycin sulfate (DLaTGS) detector was used.

Attenuated Total reflectance (ATR)-FTIR spectra have been recorded on a FTIR spectrometer (Tensor 27, Bruker, Germany) with a DLaTGS detector in a wavenumber range of 4000-400 cm^{-1} with an optical resolution of 4 cm^{-1}. The samples were solid, liquid or in the form of a powder depending on the physical state. The spectra were acquired with an ATR diamond crystal accessory. Before measurement, the residues from cone calorimeter tests were ground. The measurements were repeated at least two times. The ATR-FTIR spectra were baseline-corrected, but no ATR correction was applied to compare the spectra with transmission spectra.

Flammability tests: UL94 and limiting oxygen index

The flammability of the materials was determined using the UL 94 vertical (V) and horizontal (HB) tests according to IEC 60695-11-10 on samples of 127 mm × 12.7 mm × 3.0 mm or 127 mm × 12.7 mm × 1.6 mm. The oxygen index (LOI) was performed according to ISO 4589-2 on specimens 80 mm × 10 mm × 4 mm in size. All samples were conditioned for a minimum of 48 hours by 50 ± 5% relative humidity and 296 ± 2 K prior to the tests.

Cone calorimeter

Cone calorimeter tests (Fire Testing Technology, UK) were performed according to ISO 5660 with plates of 10 mm × 10 mm × 3 mm. A retainer frame with edges was used and the reduced surface area accounted for. The sample was wrapped in aluminum foil. External heat fluxes of 35, 50 and 70 kW m^{-2} were used and all measurements repeated. The distance

between the bottom of the cone heater and the surface of the sample was 35 mm because of deformations of the sample. It was shown that specimens with deformations of up to 35 mm can be measured accurately in cone calorimeter with a starting distance of 35 mm between cone heater and specimen [109]. The criterion used for flame-out (end of burning) was the time when no more smoke evolved. The measurements have been repeated minimum two times. If the standard deviation of the average of the values of one parameter was higher than 10%, a new measurement was done. All samples were conditioned for a minimum of 48 hours by 50 ± 5% relative humidity and 296 ± 2 K prior to the tests.

Complementary methods

For the quantification of the phosphorus or the nitrogen content of the fire residues, the residues were ground in a mortar. The determination of the elemental composition was mandated to Mikroanalytisches Laboratorium Kolbe (Mühlheim an der Ruhr, Germany).

The measurements of the glass transition temperatures of the blends were performed by differential scanning calorimetry on a Netzsch DSC F1 t-sensor /E (Netzsch, Germany) apparatus. Aluminium pans with a lid pierced two times were used for the sample and for the reference (empty pan). Around 10 mg of the sample in powder form was cooled or heated up between 233 and 523 K, at a heating or cooling rate of 10 K min^{-1}, respectively, under a nitrogen flow of 40 ml min^{-1}. First the sample was cooled down from room temperature to 233 K, heated up a first time to 523 K, cooled back to 233 K and heated up a second time to 523 K. Finally the sample was cooled down to room temperature at a cooling rate of 20 K min^{-1}.The sample was let for 5 min at 233 or 523 K after each ramp, before starting the next step. The T_g given were evaluated on the second heating run, by the tangent method.

Rheology measurements were performed on a Anton Paar MCR501 rheometer (Anton Paar GmbH, Germany), by frequency sweep from 0.1 to 100s^{-1} and at a constant deformation of 0.5% at 503 K, 543 K and 573 K under nitrogen flow. A rheometer in a plate/plate configuration of 25 mm diameter was used. The solid blend of the dimensions 20 x 20 x 3 mm was melted on the lower plate in the heatable rheometer at the desired temperature, then slowly pressed by the upper plate until 1.05 mm gap, the excess of material removed, and finally pressed to 1 mm gap for the measurements. A master curve for the shear stress at 523 K (250°C) was calculated based on the curves of the three temperatures for each material.

A.3 Complementary tables on pyrolysis

Table A.3.1 Thermogravimetric results of ABS and ABS/DPZ blends under nitrogen (10 K min-^{1})

	ABS	ABS/8DPZ$_{PTFE}$	ABS/6ABS2/ 8DPZ	ABS/6ABS2/ 8DPZ$_{PTFE}$
T2% in K	649	624	633	621
Mass Loss I				
ML1 in wt%	98.2	97.7	98.3	97.9
T_{Max} 1 in K	688 (708sh)	700	706	700
Mass Loss II				
ML2 in wt%	-	-	-	-
T_{Max} 2 in K	-	-	-	-
Residue				
Residue in wt%	2.4	2.3	1.7	2.1
Expected residue	-	2.2	2.2	2.2

A.4 Complementary tables on fire behavior

Table A.4.1. Cone calorimeter results of PC/ABS$_{PTFE}$+BDP. PC/ABS$_{PTFE}$+BBDP. PC/ABS$_{PTFE}$+HDP and PC/ABS$_{PTFE}$+BBXP at 35, 50 and 70 kW m^{-2} external heat fluxes.

PC/ABS$_{PTFE}$+	-	BDP	BBDP	BBDP	BBXP
			External heat flux: **35 kW m^{-2}**		
THE in MJ m^{-2}	67 ± 5	56 ± 3	60 ± 3	59 ± 1	61 ± 3
PHRR in kW m^{-2}	281 ± 20	240 ± 35	231 ± 11	216 ± 5	251 ± 25
Residue in wt.%	24.4 ± 4.8	24.8 ± 2.7	27.1 ± 4.2	22.8 ± 1.0	21.1 ± 1.1
Residue/PC content in wt.%/wt.%	30.0 ± 5.9	34.9 ± 3.9	37.8 ± 5.9	30.1 ± 1.4	30.2 ± 1.6
THE/ML in MJ m^{-2} g^{-1}	2.57 ± 0.04	2.12 ± 0.01	2.33 ± 0.02	2.16 ± 0.01	2.22 ± 0.07
Comb. Efficiency χ	0.96 ± 0.01	0.76 ± 0.01	0.84 ± 0.01	0.83 ± 0.02	0.80 ± 0.03
			External heat flux: **50 kW m^{-2}**		
THE in MJ m^{-2}	64.3 ± 0.5	56.4 ± 0.1	56.9 ± 0.6	53.5 ± 1.6	60.0 ± 0.5
PHRR in kW m^{-2}	357 ± 12	285 ± 10	282 ± 11	278 ± 15	276 ± 4
Residue in wt.%	25.1 ± 0.6	20.9 ± 0.4	22.0 ± 1.8	22.5 ± 1.5	20.0 ± 0.1
Residue/PC content in wt.%/wt.%	30.9 ± 0.8	29.4 ± 0.6	30.7 ± 2.6	29.7 ± 2.0	28.6 ± 0.2
THE/ML in MJ m^{-2} g^{-1}	2.50 ± 0.01	2.01 ± 0.01	2.07 ± 0.07	1.95 ± 0.02	2.14 ± 0.01
Comb. Efficiency χ	0.93 ± 0.01	0.72 ± 0.01	0.75 ± 0.03	0.75 ± 0.02	0.78 ± 0.01
			External heat flux: **70 kW m^{-2}**		
THE in MJ m^{-2}	65.0 ± 2.3	56.7 ± 1.6	55.5 ± 1.7	55.4 ± 2.7	58.9 ± 0.3
PHRR in kW m^{-2}	427 ± 20	299 ± 17	304 ± 11	309 ± 12	344 ± 24
Residue in wt.%	20.2 ± 2.3	20.1 ± 1.9	19.4 ± 0.4	19.3 ± 1.5	18.1 ± 0.4
Residue/PC content in wt.%/wt.%	24.8 ± 2.9	28.3 ± 2.7	27.1 ± 0.6	25.5 ± 2.0	25.9 ± 0.6
THE/ML in MJ m^{-2} g^{-1}	2.37 ± 0.05	2.02 ± 0.02	1.95 ± 0.07	1.94 ± 0.09	2.05 ± 0.01
Comb. Efficiency χ	0.89 ± 0.03	0.72 ± 0.01	0.71 ± 0.03	0.74 ± 0.06	0.74 ± 0.01

Table A.4.2 Cone calorimeter results of PC/ABS$_{PTFE}$ and PC/ABS$_{PTFE}$ +BDP:HDP at an external heat flux of 35 kW m^{-2} and 70 kW m^{-2}.

PC/ABS$_{PTFE}$ + BDP:HDP	-	100:0	80:20	60:40	40:60	20:80	0:100	Error or max
External heat flux **35 kW m^{-2}**								
THE in MJ m^{-2}	69.4	53.8	51.5	51.2	54.1	54.2	50.5	± 1.6
THE/ML in MJ m^{-2} g^{-1}	2.55	2.11	2.05	2.05	2.07	2.05	2.00	± 0.09
Residue in wt%	27.8	29.1	30.4	29.6	28.0	25.8	25.7	± 4.0
PHRR in kW m^{-2}	403	325	290	310	313	255	290	± 19
External heat flux **70 kW m^{-2}**								
THE in MJ m^{-2}	70.4	56.1	54.5	54.3	52.7	54.1	55.6	± 1.8
THE/ML in MJ m^{-2} g^{-1}	2.46	1.97	1.94	1.94	1.87	1.90	1.93	± 0.06
Residue in wt%	17.4	19.9	20.0	20.7	20.2	19.5	18.7	± 1.0
PHRR in kW m^{-2}	635	380	383	363	416	385	393	± 18

Table A.4.3 Cone calorimeter results of PC and PC/DPZ blends at 35, 50 and 70 kW m^{-2} and (Reduction) to PC values

PC/..	-	8DPZ	8DPZ$_{PTFE}$
	External heat flux: 35 kW m^{-2}		
THE in MJ m^{-2}	62.2 ± 0.5	58.5 ± 1.1 (-6%)	60.9 ± 0.9 (-2%)
PHRR in kW m^{-2}	476 ± 25	477 ± 23 (-0%)	374 ± 68 (-21%)
Residue in wt.%	24.9 ± 0.4	25.7 ± 0.9 (+4%)	27.0 ± 0.1 (+10%)
THE/ML in MJ m^{-2} g^{-1}	2.39 ± 0.03	2.20 ± 0.06 (-8%)	2.30 ± 0.03 (-4%)
TSR/ML in m^2 m^{-2} g^{-1}	85 ± 2	73 ± 5 (-14%)	76 ± 2 (-11%)
TCOP/ML in g g^{-1}	0.016 ± 0.001	0.028 ± 0.001 (+75%)	0.026 ± 0.001 (+69%)
	External heat flux: 50 kW m^{-2}		
THE in MJ m^{-2}	63.5 ± 0.8	59.1 ± 1.7 (-7%)	61.7 ± 2.1 (-3%)
PHRR in kW m^{-2}	533 ± 27	479 ± 2 (-10%)	407 ± 24 (-23%)
Residue in wt.%	22.1 ± 0.1	24.7 ± 0.1 (+12%)	22.4 ± 0.1 (+1%)
THE/ML in MJ m^{-2} g^{-1}	2.37 ± 0.01.	2.20 ± 0.06 (-7%)	2.22 ± 0.06 (-6%)
TSR/ML in m^2 m^{-2} g^{-1}	88 ± 1	84 ± 1 (-5%)	83 ± 4 (-6%)
TCOP/ML in g g^{-1}	0.016 ± 0.001	0.030 ± 0.002 (+88%)	0.033 ± 0.001 (+106%)
	External heat flux: 70 kW m^{-2}		
THE in MJ m^{-2}	63.4 ± 3.0	55.6 ± 0.4 (-12%)	60.4 ± 2.5 (-5%)
PHRR in kW m^{-2}	720 ± 17	508 ± 14 (-30%)	380 ± 18 (-47%)
Residue in wt.%	20.5 ± 0.3	23.2 ± 0.2 (+13%)	25.3 ± 2.6 (+23%)
THE/ML in MJ m^{-2} g^{-1}	2.29 ± 0.04	2.02 ± 0.02 (-12%)	2.25 ± 0.01 (-2%)
TSR/ML in m^2 m^{-2} g^{-1}	95 ± 2	90 ± 0.1 (-5%)	97 ± 5 (+2%)
TCOP/ML in g g^{-1}	0.016± 0.001	0.029 ± 0.001 (+81%)	0.029 ± 0.001 (+81%)

Table A.4.4 Cone calorimeter results of ABS and ABS/DPZ blends at 35, 50 and 70 kW m^{-2}

ABS/..	-	8DPZ$_{PTFE}$	6ABS2/ 8DPZ	6ABS2/ 8DPZ$_{PTFE}$
External heat flux: 35 kW m^{-2}				
THE in MJ m^{-2}	109.7 ± 2.5	84.7 ± 4.5	85.1 ± 2.5	81.2 ± 0.2
PHRR in kW m^{-2}	680 ± 6	490 ± 14	597 ± 6	416 ± 3
Residue in wt.%	4.2 ± 0.8	3.0 ± 0.2	2.9 ± 0.1	2.0 ± 0.2
THE/ML in MJ m^{-2} g^{-1}	3.66 ± 0.13	2.7 ± 0.1	2.8 ± 0.1	2.6 ± 0.1
TSR/ML in m^2 m^{-2} g^{-1}	113 ± 1	142 ± 4	136 ± 5	131 ± 2
TCOP/ML in g g^{-1}	0.022 ± 0.001	0.034 ± 0.001	0.036 ± 0.001	0.034 ± 0.001
External heat flux: 50 kW m^{-2}				
THE in MJ m^{-2}	103.0 ± 0.2	85.9 ± 1.7	87.1 ± 0.2	86.1 ± 1.3
PHRR in kW m^{-2}	911 ± 11	539 ± 48	755 ± 26	791 ± 42)
Residue in wt.%	3.2 ± 0.8	2.1 ± 0.1	1.6 ± 0.2	2.5 ± 0.6
THE/ML in MJ m^{-2} g^{-1}	3.37 ± 0.01	2.76 ± 0.05	2.81 ± 0.01	2.80 ± 0.06
TSR/ML in m^2 m^{-2} g^{-1}	117 ± 1	144 ± 1	124 ± 2	131 ± 2
TCOP/ML in g g^{-1}	0.022 ± 0.001	0.035 ± 0.001	0.038 ± 0.001	0.038 ± 0.001
External heat flux: 70 kW m^{-2}				
THE in MJ m^{-2}	102.7 ± 1.1	83.3 ± 2.5	86.1 ± 2.8	83.2 ± 1.6
PHRR in kW m^{-2}	1138 ± 35	744 ± 10	1019 ± 63	931 ± 2
Residue in wt.%	1.1 ± 0.8	1.1 ± 0.3	0.3 ± 0.1	0.9 ± 0.1
THE/ML in MJ m^{-2} g^{-1}	3.38 ± 0.09	2.66 ± 0.07	2.74 ± 0.10	2.66 ± 0.05
TSR/ML in m^2 m^{-2} g^{-1}	120 ± 1	140 ± 12	119 ± 2	132 ± 11
TCOP/ML in g g^{-1}	0.023± 0.001	0.036 ± 0.001	0.041 ± 0.002	0.038 ± 0.001

Table A.4.5 Cone calorimeter results of PC/ABS/DPZ$_{PTFE}$ blends at 35, 50 and 70 kW m^{-2} and (Reduction) to PC/ABS$_{PTFE}$ values

PC/ABS$_{PTFE}$/…	-	8DPZ	8DPZ-m
	External heat flux: **35 kW m^{-2}**		
THE in MJ m^{-2}	68.7 ± 1.8	61.4 ± 0.7 (-11%)	60.6 ± 1.7
PHRR in kW m^{-2}	290 ± 19	313 ± 35 (+8%)	244 ± 14
Residue in wt.%	24.4 ± 2.7	22.7 ± 2.7 (-7%)	24 ± 2
THE/ML in MJ m^{-2} g^{-1}	2.61 ± 0.03	2.25 ± 0.01 (-14%)	2.26 ± 0.01
TSR/ML in m^2 m^{-2} g^{-1}	88 ± 4	96 ± 5 (+9%)	110 ± 2
TCOP/ML in g g^{-1}	0.018± 0.001	0.037 ± 0.002 (+112%)	0.028 ± 0.007
	External heat flux: **50 kW m^{-2}**		
THE in MJ m^{-2}	72.5 ± 0.7	62.3 ± 3.2 (-14%)	61 ± 2
PHRR in kW m^{-2}	315 ± 11	354 ± 34 (+12%)	302 ± 35
Residue in wt.%	19.0 ± 0.8	20.3 ± 0.4 (+7%)	18.8 ± 0.5
THE/ML in MJ m^{-2} g^{-1}	2.58 ± 0.05	2.23 ± 0.12 (-14%)	2.16 ± 0.07
TSR/ML	93 ± 3	107 ± 1 (+16%)	119 ± 5
TCOP/ML in g g^{-1}	0.017 ± 0.002	0.038 ± 0.002 (+118%)	0.034 ± 0.002
	External heat flux: **70 kW m^{-2}**		
THE in MJ m^{-2}	71.4 ± 2.0	62.8 ± 0.1 (-12%)	60 ± 2.7
PHRR in kW m^{-2}	419 ± 33	325 ± 30 (-23%)	353 ± 5
Residue in wt.%	17.1 ± 0.5	18.9 ± 1.5 (+10%)	19.4 ± 1.7
THE/ML in MJ m^{-2} g^{-1}	2.50 ± 0.04	2.22 ± 0.03 (-11%)	2.06 ± 0.06
TSR/ML	97 ± 3	117 ± 3 (+21%)	134 ± 6
TCOP/ML in g g^{-1}	0.016 ± 0.001	0.030 ± 0.003 (+90%)	0.029 ± 0.007

Table A.4.6 Cone calorimeter results of PC/ABS$_{PTFE}$+BDP:DPZ at an external heat flux of 35 kW m^{-2} , 50 kW m^{-2} and 70 kW m^{-2}.

PC/ABS$_{PTFE}$	/	+ BDP:DPZ						Error max
		100:0	80:20	60:40	40:60	20:80	0:100	
External heat flux **35 kW m^{-2}**								
THE in MJ m^{-2}	68.7	61.4	60.9	60.2	60.7	64.5	61.4	± 3.4
THE/ML in MJ m^{-2} g^{-1}	2.61	2.24	2.24	2.18	2.23	2.36	2.25	± 0.09
Residue in wt%	24.4	23.4	23.4	22.3	23.2	22.7	22.7	± 2.7
PHRR in kW m^{-2}	290	274	216	259	254	262	313	± 35
External heat flux **50 kW m^{-2}**								
THE in MJ m^{-2}	72.5	60.0	59.0	60.0	63.7	61.2	62.3	± 6
THE/ML in MJ m^{-2} g^{-1}	2.58	2.10	2.12	2.13	2.24	2.16	2.22	± 0.16
Residue in wt%	19.0	19.6	22.4	20.1	19.4	20.2	20.3	± 1.9
PHRR in kW m^{-2}	315	305	288	316	310	344	354	± 40
External heat flux **70 kW m^{-2}**								
THE in MJ m^{-2}	71.4	56.3	59.0	61.5	60.9	59.2	62.8	± 2.4
THE/ML in MJ m^{-2} g^{-1}	2.50	1.96	2.02	2.12	2.11	2.06	2.22	± 0.09
Residue in wt%	17.1	19.6	17.3	18.5	18.4	20.2	18.9	± 0.9
PHRR in kW m^{-2}	419	352	377	343	317	397	325	± 43

A.5 Complementary figure on fire behaviour

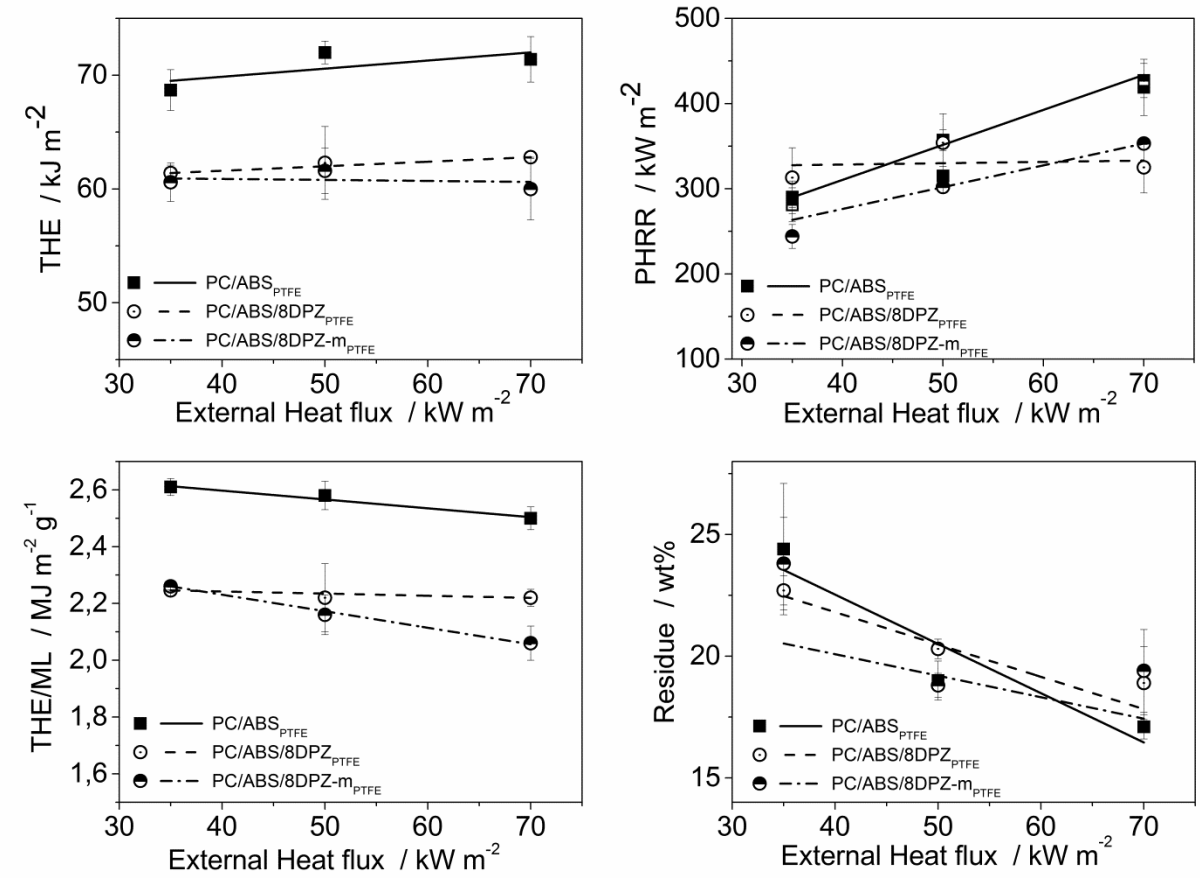

Figure A.5.1 Cone calorimeter results of PC/ABS_{PTFE}, $PC/ABS/DPZ_{PTFE}$ and $PC/ABS/DPZ\text{-}m_{PTFE}$ in dependency of the fire scenario (external heat flux), total heat evolved (top left), peak heat release rate (top right), effective heat of combustion (bottom left) and residue (bottom right).